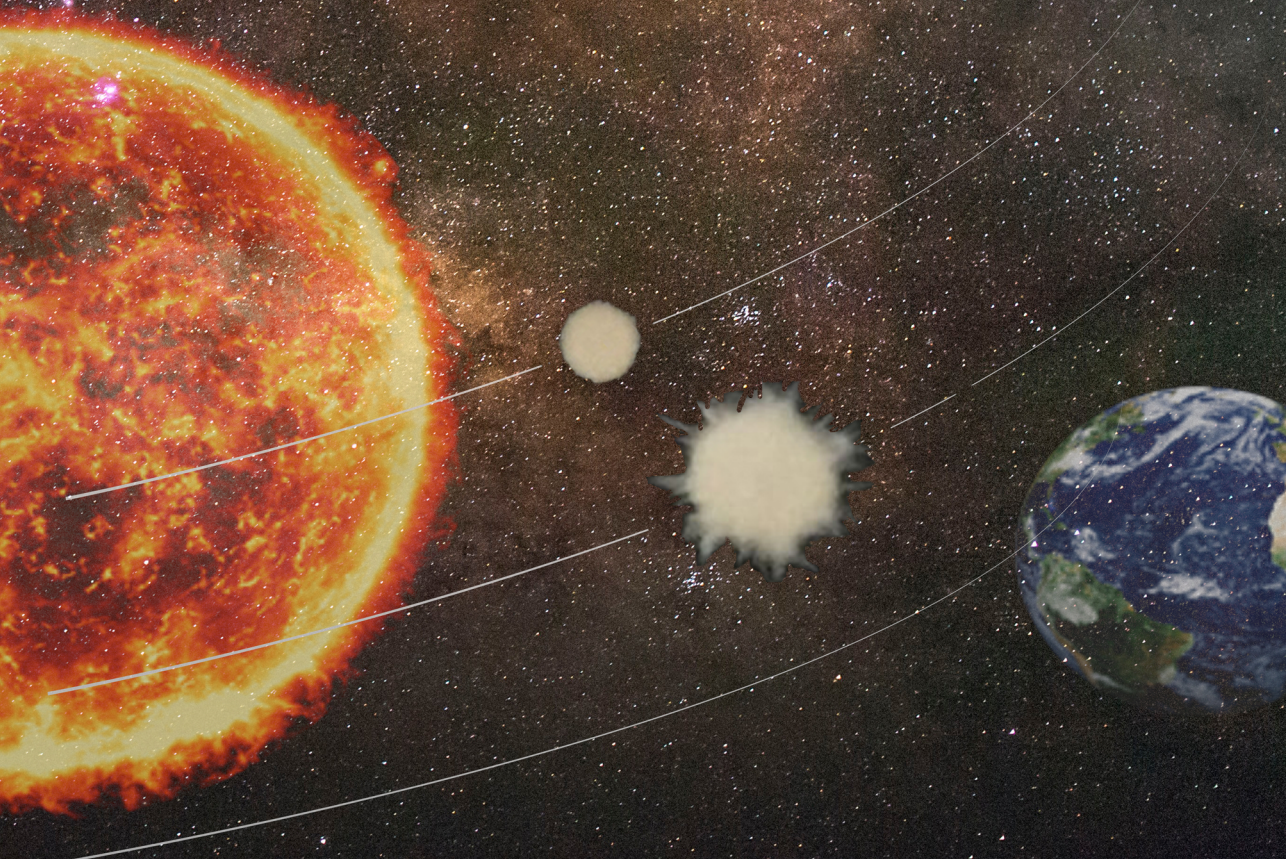


# Functionality of heterogeneity in size of *Aspergillus niger* micro-colonies

Jun Lyu









**Functionality of heterogeneity in size of**  
***Aspergillus niger* micro-colonies**

**Jun Lyu**



PhD thesis Utrecht University, Utrecht, The Netherlands (2022)

The research described in this Thesis was performed within the Microbiology group of Utrecht University, Padualaan 8, 3584 CH Utrecht, The Netherlands.

Copyright © 2022 by J Lyu. All rights reserved.

Cover design: Jun Lyu  
Printed by: ProefschriftMaken | [www.proefschriftmaken.nl](http://www.proefschriftmaken.nl)  
ISBN: 978-94-6423-966-9



# Functionality of heterogeneity in size of *Aspergillus niger* micro-colonies

Functionaliteit van de heterogeniteit in grootte van  
micro-kolonies van *Aspergillus niger*

(met een samenvatting in het Nederlands)

黑曲霉菌丝球异质的功能性研究

(中文论述)

## Proefschrift

ter verkrijging van de graad van doctor aan de Universiteit Utrecht op gezag van  
de rector magnificus, prof. dr. H.R.B.M. Kummeling, ingevolge het besluit van  
het college voor promoties in het openbaar te verdedigen op maandag September  
2022 des ochtends te 16:15 uur

door

Jun Lyu

geboren op 14 Feb 1992

te Anqing, China



Promotor: Prof dr H.A.B. Wösten

Co-promotor: Dr H. de Cock

This thesis was partly accomplished with financial support from China Scholarship Council (No. 201808320441).



4 years ago - *"I want to make a history"*

Now - *"A small step every day"*





# Contents

---

<b>Chapter 1</b>	General introduction	1
<b>Chapter 2</b>	Different sized micro-colonies of the fungus <i>Aspergillus niger</i> help each other to digest food.	19
<b>Chapter 3</b>	Colony size impacts stress survival in <i>Aspergillus niger</i> .	55
<b>Chapter 4</b>	The orotidine 5'-phosphate decarboxylase gene <i>pyrG</i> influences <i>Aspergillus niger</i> pellet formation and secretome in liquid shaken cultures.	67
<b>Chapter 5</b>	The $\alpha$ -(1,3)-glucan synthase gene <i>agsE</i> impacts the secretome of liquid shaken cultures of <i>Aspergillus niger</i> by reducing micro-colony size.	91
<b>Chapter 6</b>	Summary and General Discussion.	121
<b>Appendix</b>	Nederlandse Samenvatting	131
	Chinese Summary	137
	Curriculum vitae	141
	List of Publications	142
	Acknowledgements	143



# **Chapter 1**

## **General Introduction**

*Jun Lyu*



## INTRODUCTION

The Kingdom of Fungi represents diverse eukaryotic organisms such as yeasts and molds, as well as the more familiar mushroom forming fungi. They degrade organic waste such as wood and litter and remainings of animals and other organisms. This makes fungi important in nutrient cycling in nature. Yet, humans also experience severe food spoilage due to the capability of fungi to degrade organic material (Lorenzo et al., 2018). Less known, fungi can also deteriorate inorganic materials like stone and cement by being important components of rock-inhabiting microbial communities (Burgord et al., 2003; Liu et al., 2020). Fungi not only degrade dead (in)organic material, they can also colonize and feed on living organisms. As such, they can balance populations of plants and animals in nature. Yet, they are also responsible for major crop loss, illustrated by the fact that about 30% of all food cannot be harvested due to pathogenic fungi (Avery et al., 2019). For instance, *Ustilago maydis* causes tumor formation in maize leading to severe economic losses (Banuett, 1995; Kamper et al., 2006). In addition, about 1.5 million people die each year due to a fungal infection with *Aspergillus fumigatus* and *Candida albicans* being the main pathogens (Braun et al., 2001; Latgé & Chamilos, 2019).

Fungi have been actively used by mankind. Mushrooms have been consumed for thousands-of years with current sales of up to 40 billion \$ annually (Grimm & Wösten, 2018). In addition, genera like *Aspergillus*, *Penicillium*, *Mucor* and *Monascus* have been widely used for the production of fermented foods, beverages, enzymes and metabolites like organic acids, antibiotics and pigments (Kalra et al., 2020; Keller, 2019; Wösten, 2019; Yang et al., 2017). Recently, fungi have also been used to make sustainable materials that can replace polluting non-sustainable materials such as oil-based plastics (Wösten, 2019).

### *The genus Aspergillus*

The genus *Aspergillus* comprises between 260 and 837 species (Geiser et al., 2007; Hawksworth, 2011; Samson & Varga, 2009; Houbraken et al., 2020) and display significant genetic diversity. For instance, the genomes of *Aspergillus nidulans* and *A. fumigatus* are as related to each other as those of fish and human (Galagan et al., 2005). Aspergilli are dominant fungal species in nature explained by the fact that they are not very selective with respect to growth conditions (Krijgsheld et al., 2013a). For instance, they can grow in a wide range of temperature (6-55 °C), relative humidity (80-100%) and can feed on a large variety of substrates including plant and animal waste. The high number of spores that are dispersed by

*Aspergillus* also explains the success of these fungi. In fact, spores of aspergilli are among the most dominant fungal structures in the air (Bennett, 1998). Aspergilli have both positive and negative impact on human society. This will be illustrated in the next two sections where I will discuss the role of aspergilli, in particular *Aspergillus niger*, as cell factories, pathogens and food spoilage fungi.

### *Aspergilli as a cell factory*

Aspergilli like *A. niger*, *Aspergillus oryzae*, *Aspergillus awamori*, *Aspergillus sojae*, and *Aspergillus terreus* are widely exploited as industrial cell factories (Meyer et al., 2011). James Currie initiated the use of *Aspergillus* as a cell factory more than 100 years ago by publishing the superior properties of *A. niger* to produce citric acid (Cairns et al., 2018). Two years later, the American company Pfizer launched a pilot plant for the production of this organic acid. Notably, sales of citric acid produced by *A. niger* was already higher than that of citrus fruits close to a hundred years ago (Cairns et al., 2018) and the production in industrial bioreactors exceeds nowadays 169 g l<sup>-1</sup> (Hou et al., 2018). The fact that the products of *A. niger* are Generally Regarded As Safe (GRAS) makes that they can be used in food and feed production (products produced under very new culturing conditions are not yet GRAS). Apart from citric acid, *A. niger* is also used to produce gluconic and malic acid for use in food (Iyyappan et al., 2018; Shah & Kothari, 2004). In addition, aspergilli can be used to produce itaconic acid, which is a sustainable alternative to petroleum-based acrylic acid (Bafana & Pandey, 2018). Up to 33.5 g l<sup>-1</sup> of itaconic acid has been produced with recombinant strains of *A. niger* (Hossain et al., 2019), while 129 g l<sup>-1</sup> has been obtained in the natural producer *A. terreus* (Hevekerl et al., 2014). The latter fungus however is not considered a preferred cell factory because it is not very robust and has high production costs (Kuenz & Krull, 2018).

*A. niger* is also a versatile fungal cell factory for the production of industrial enzymes such as lipases, mannanases, peroxidases, xylanases, glucanases and amylases (Li et al., 2020). A production level of 30 g l<sup>-1</sup> glucoamylase has been the highest reported yield of a protein in *A. niger* (Finkelstein, 1987). However, levels obtained by the industry may be much higher (Wösten, 2019). Such production levels combined with the fact that *A. niger* can assimilate a wide range of carbon sources, including low-cost substrates such as wheat bran and rice straw, make this fungus of high interest for upgrading waste streams (Upton et al., 2017). The GRAS status and its high productivity make *A. niger* also attractive for heterologous protein production. However, production levels are still low when compared to endogenous proteins. For instance, production of human erythropoietin was only improved from undetectable to 74

mg l<sup>-1</sup> by inserting introns in the encoding gene and by inactivating genes involved in glycosylation and in production of extracellular proteases (Rojas-Sanchez et al., 2020).

### *Aspergilli as food spoilage fungi and pathogens*

The fact that aspergilli can efficiently degrade plant waste make them effective food and feed spoilage fungi. Food spoilage affects the taste, odor, color, and / or nutritional value of the product (Pitt & Hocking, 2009). Moreover, fungal food spoilage can be accompanied by the production of mycotoxins that are toxic to animals and human. *A. niger* is known to spoil a wide variety of food such as yogurt, cheese, onions, nuts, fresh fruits and sun dried products (Garnier et al., 2017; Gougouli & Koutsoumanis, 2017; Noma & Asakawa, 2010; Saranya et al., 2017). Other aspergilli are also known to spoil food. For instance, *A. flavus* spoils several important agricultural crops such as maize and peanut (Amaike & Keller, 2011). Food spoilage by aspergilli can be accompanied by the production of mycotoxins (Bassetti et al., 2017). For instance, *A. niger* produces fumonisin and ochratoxin (Aerts et al., 2018; Noma & Asakawa, 2010), while *A. flavus* produces aflatoxin (Klich, 2007) and gliotoxin (Kamei & Watanabe, 2005).

Aspergilli are not only known because of their saprobic life style but can be pathogens as well. *A. niger* has been reported to be a pathogen of *Zingiber officinale* plants (Pawar et al., 2008), while *A. flavus* can infect crops like maize (Antiga et al., 2020). Moreover, a wide variety of aspergilli are opportunistic pathogens of animals and humans. They generally do not infect healthy individuals but do infect individuals with a compromised immune system (Brakhage, 2005; Pitt, 1994). Aspergilli (i.e. *A. fumigatus*, and to a lesser extent species such *A. flavus*, *A. niger*, *A. terreus*, and *A. nidulans*) cause invasive aspergillosis (involving several organ systems, particularly pulmonary disease), non-invasive infections like pulmonary aspergilloma, and allergic bronchopulmonary aspergillosis (Denning, 1998; Stevens et al., 2000). Mortality rates of intensive care unit patients with aspergillosis range between 30 and 90% depending on the immune state of the host and the stage of the infection (Taccone et al., 2015). *A. fumigatus* is the second leading cause of invasive fungal diseases worldwide. Its small conidia (2-3 µm in diameter) is one of the reasons why *A. fumigatus* is such a successful pathogen. These conidia are easily spread by wind and can penetrate deep in the lung alveoli (Latgé, 2001). Humans can inhale hundreds of *A. fumigatus* conidia per day (O’Gorman, 2011). Indeed, *Aspergillus* DNA is detected in 37 % of lung biopsies of healthy individuals showing that we are continuously exposed to this fungal genus (Denning et al., 2011).

### *Vegetative growth of Aspergillus*

Germination of a sexual or asexual *Aspergillus* spore results in a mycelium or colony. Germination of conidia starts with isotropic growth, which is accompanied by swelling of the spore. This is followed by polar growth resulting in the formation of a germ tube. This germ tube will extend and form a hypha. As growth continues, septa are formed that partition the extending hyphae into compartments. The apical hyphal zone of *A. niger* ( $\pm 400 \mu\text{m}$ ) is free of septa, but in the sub-apical zone septa can be found every 50-100  $\mu\text{m}$  (de Bekker et al., 2011a). Septa are also formed at positions where branches of hyphae are formed. The fact that septa are porous enables cytosol and even organelles to flow between compartments and branches and the main hypha. However, peroxisome-like organelles can plug these pores (Bleichrodt et al., 2012). These Woronin bodies close  $\sim 50\%$  of the three most apical septa of growing hyphae of *A. niger*, while the more sub-apical septa are almost all closed (Bleichrodt et al., 2015a). Modeling showed that cytoplasm of hyphal compartments are not in physical contact when separated by more than 4 septa. Moreover, apical compartments of growing hyphae behave unicellularly, while older compartments have a multicellular organization. Notably, glucose can be translocated to neighboring hyphal compartments despite Woronin body mediated plugging (Bleichrodt et al., 2015b). This phenomenon would be explained by the presence of glucose transporters that reside in the plasma membrane lining the septal cross-wall. Such transporters would thus facilitate selective transport between compartments and branches.

The branching hyphae resulting from a single spore or a cluster of spores gives rise to a mycelium. Such colonies ultimately have a (sub-)millimeter (micro-colonies) to centimeter (macro-colonies) diameter. Macro-colonies can for instance be formed within a lung, on agar media or in static liquid media. On the other hand, micro-colonies are formed on small substrates like a grain and also in liquid shaken cultures. Micro-colonies in liquid shaken cultures (also known as pellets) have a distinct outer and inner zone (de Bekker et al., 2011b). They result from coagulation of conidia and germlings in the culture medium and thus result from more than one conidium. Mycelium can also grow dispersed or as clumps in liquid shaken cultures. Clumps represent an intermediate state between pelleted and dispersed growth. In the latter case, aggregation of conidia and germlings is minimal or even absent (Krijghsheld et al., 2013a). Aggregation is a two-step process (Grimm et al., 2004). Primary aggregation occurs immediately after introduction of the conidia in the liquid culture, while secondary aggregation takes place when the conidia germinate. Primary aggregation is caused by the hydrophobic nature of the spores due to the presence of the outer hydrophobin and melanin layers. Inactivation of the *A. nidulans* hydrophobin genes *dewA* and *rodA* results in reduced aggregation and, consequently, in smaller micro-colonies (Dynesen & Nielsen, 2003). A

similar effect was obtained by inactivation of the *olvA* pigmentation gene in *A. niger* (van Veluw et al., 2013). Agitation, pH and medium composition also affect aggregation of *A. niger* and *A. oryzae* conidia (Metz & Kossen, 1977; Spohr et al., 1996). These conditions impact the hydrophobic interactions between conidia in the culture medium.

Secondary aggregation shows a linear relationship with the particle growth rate (Grimm et al., 2004) and thus has most impact on micro-colony size. In contrast to non-germinating conidia,  $\alpha$ -(1,3)-glucan forms the outer layer on the germinating spore. This polysaccharide is responsible for the aggregation of germlings in *A. fumigatus* (Fontaine et al., 2010) and *A. nidulans* (He et al., 2014). The  $\alpha$ -glucan synthases AgsA and AgsB and the  $\alpha$ -amylases AmyD and AmyG are involved in  $\alpha$ -(1,3)-glucan synthesis in *A. nidulans*. AgsB is the main  $\alpha$ -(1,3)-glucan synthase in *A. nidulans* (Yoshimi et al., 2013). Inactivation of its encoding gene *agsB* has not an obvious phenotype on agar medium but it shows reduced aggregation of germlings (He et al., 2014; Yoshimi et al., 2013). As a result, the *agsB* deletion strain of *A. nidulans* forms smaller micro-colonies in liquid shaken cultures when compared to the wild-type strain. Overexpression of *agsA* complements  $\alpha$ -glucan synthesis in the  $\Delta$ *agsB* strain but not the phenotypes of this strain in liquid shaken cultures. From this it was concluded that the products of AgsA and AgsB have different roles in the cell wall, which may be related to *agsA* being mainly expressed at conidiation. Inactivation of the  $\alpha$ -amylase gene *amyG*, but not *amyD*, in *A. nidulans* also shows reduced conidial adhesion during germination in liquid shaken cultures (He et al., 2014). The  $\alpha$ -amylases have been proposed to synthesize the primer structure of  $\alpha$ -glucan (Marion et al., 2006). Their absence would thus lead to reduced production of this polysaccharide.

### **Heterogeneity in *Aspergillus***

*Aspergillus* shows notable heterogeneity between micro-colonies, between and within zones of colonies, and even within hyphae and between conidia. This heterogeneity is discussed in the next sections.

#### *Heterogeneity between colonies in a liquid shaken culture*

As described above, *Aspergillus* grows dispersed, as clumps or as micro-colonies in liquid shaken cultures. Dispersed mycelium consists of numerous small networks of hyphae, while micro-colonies are characterized by an inner and outer zone. These types of mycelium show a distinct behavior. Micro-colonies of *A. niger* produce more citric acid when compared to dispersed mycelium (Clark, 1962; Clark et al., 1966), while expression of genes encoding



secreted proteins is higher in dispersed mycelium and small micro-colonies (Tegelaar et al., 2020a). The latter is explained by the fact that these genes are mainly expressed in the outer part of micro-colonies. Modelling predicted that the width of the expression zone was up to 156  $\mu\text{m}$  depending on the growth medium and micro-colony diameter. These data imply that the highest productive micro-colonies are those that have a radius  $\leq$  the width of the peripheral expression zone. This implies that small micro-colonies and dispersed mycelium of *A. niger* produce more secreted proteins per biomass than large micro-colonies. Indeed, inactivation of the  $\alpha$ -glucan synthase genes in *A. oryzae* results in micro-colonies with a 30% reduced diameter in liquid shaken cultures that produce higher levels of a heterologous cutinase when compared to the wild-type (Miyazawa et al., 2016). The fact that large micro-colonies produce less secreted protein may be explained by a limitation of oxygen and nutrient availability in the central parts of the micro-colonies (Hille et al., 2009).

Heterogeneity is even observed within a culture of micro-colonies. Micro-colonies of shaken cultures of *A. niger* are heterogeneous in size and gene expression (de Bekker et al., 2011b). Notably, only a small part of the micro-colonies highly express the glucoamylase gene *glaA*. The reasons for this heterogeneity are not known but it clearly shows its industrial relevance.

### *Heterogeneity within a colony*

Until the end of last century, it was generally believed that hyphae within the vegetative mycelium have a similar composition and function. However, a series of publications from 1991 onwards show that this is actually not the case. It was shown that proteins are produced throughout the mycelium (Wösten et al., 1991). In contrast, growth is restricted to the outer and a central zone of the mycelium (Wösten et al., 1991), while sporulation occurs in the zone immediately behind the periphery of the colony (Krijgsheld et al., 2013b). Moreover, zones secrete different enzymes. For instance, glucoamylase is secreted at the periphery of the colony of *A. niger* (Wösten et al., 1991), while manganese peroxidase is being secreted in the colony center of *Phanerochaete chrysosporium* (Moukha et al., 1993). The differences between hyphae within zones of *A. niger* colonies is also reflected in the mRNA composition of the outer, intermediate and inner zones (Levin et al., 2007). For instance, more than 25% of the active genes are differentially expressed when the inner and outermost zones of the colony are compared. Moreover, 9% of the genes are expressed in only one of the five concentric zones. These differences are explained by reduced nutrient availability in the colony center (about 37% of variation in gene expression) but even more so by differentiation of the hyphae in the

different zones (55% of variation in gene expression) (Levin et al., 2007). These studies used medium with a single carbon source, such as xylose or maltose. Differentiation can be even more pronounced when *A. niger* grows on a heterogeneous medium as occurs in nature. High level of intra-colony differentiation matched the locally available substrate. Zones of the colony exposed to pectin-rich sugar beet pulp show high levels of transcripts and proteins of pectinolytic genes, while zones exposed to xylan-rich wheat bran show high levels of mRNAs and proteins of xylanolytic genes (Daly et al., 2020). Heterogeneity can also be observed between zones of micro-colonies. Hyphae at the outer zone contain 50-fold more RNA than hyphae in the micro-colony center (de Bekker et al., 2011b), which would explain why genes encoding secreted proteins are only expressed in the outer zone (Tegelaar et al., 2020a).

Heterogeneity can even be observed within a zone of macro- and micro-colonies of *A. niger*. Wösten et al. (1991) already showed that only part of the hyphae at the periphery of the *A. niger* colony secrete glucoamylase. GFP expression studies indicate that this is probably caused by regulation at the transcriptional level (Vinck et al., 2005). Hyphae that highly express *glaA* also highly express other genes encoding secreted proteins. Moreover, these hyphae show increased expression of *amyR* (that regulates *glaA* and other amylolytic genes) and the glyceraldehyde-3-phosphate dehydrogenase gene *gpdA* and are characterized by a high 18S rRNA content (Vinck et al., 2011) and increased glucose uptake (Bleichrodt et al., 2015b). From this it was concluded that the outer zone of colonies consists of two types of hyphae; those with a high and those with a low transcriptional and translational activity. The former subpopulation of hyphae secrete enzymes that degrade the substrate resulting in breakdown products that serve as nutrients. On the other hand, the latter subpopulation of hyphae shows increased resistance to stress conditions, in particular heat resistance (Tegelaar et al., 2020b). Possibly, even more types of hyphae exist within the outer zone (and other zones) of the *A. niger* colony as was revealed by the distinct expression profiles of 5 individual neighboring hyphae (de Bekker et al., 2011a).

How can these different expression profiles between neighboring hyphae be explained? Firstly, for this to occur hyphae should have barriers that avoid rapid mixing of the cytosol. As described above, Woronin bodies close septal pores thereby preventing mixing of cytosol. Secondly, hyphae need to differentially express genes despite the fact that they are exposed to identical environmental conditions. Random noise in transcription and translation is the most simple mechanism to create such a heterogeneous expression between hyphae (McAdams & Arkin, 1999). Many inducers or repressing molecules that control gene expression act at a very low intracellular concentration. Fluctuations (noise) in these concentrations but also that of

transcription factors can have high impact because these levels may or may not exceed a critical concentration to induce a differentiation pathway or for instance the expression of genes encoding secreted proteins. To avoid such consequences of noise, cells use redundancy in genes as well as redundancy and extensive feedback in gene regulation. However, noise can also be exploited where variability is advantageous such as at the periphery of a fungal colony. Apart from stochastic processes, epigenetic mechanisms may be involved in differentiation within the colony (Allis & Jenuwein, 2016).

### *Heterogeneity within a hypha*

Compartments of hyphae are different in dimensions and composition of organelles. As mentioned above, the apical and sub-apical compartments of hyphae of *A. niger* are about 400  $\mu\text{m}$  and 50-100  $\mu\text{m}$  in length (de Bekker et al., 2011a). Nuclei are distributed throughout the hypha in *A. niger* except for the region 10 to 20  $\mu\text{m}$  from the tip (de Bekker et al., 2011a), while the tip area of hyphae is most rich in RNA (Vinck et al., 2011). Mitochondria and ER can be found throughout the hyphae in aspergilli but the latter is more abundant at the apex of growing hyphae (Hickey & Read, 2009). In contrast, vacuoles are most abundant in sub-apical zones of the hyphae and in older hyphae.

Apical compartments are self-sustaining in growth (Tegelaar & Wösten, 2017). Growth rate is not affected when this compartment is dissected from the remaining part of the hypha. In contrast, the second compartment has a reduced growth rate when it is separated from the apical compartment and the more sub-apical parts (Tegelaar et al., 2020a). It has also been shown that the first 8 subapical compartments of the wildtype, but not those of the  $\Delta hexA$  strain, act as a backup system for growth by forming new branches when their apical neighbouring compartment is damaged (Tegelaar & Wösten, 2017). Damaging of hyphae is expected to occur often in nature since hyphae at the outer part of the colony continuously explore their surrounding substrate and by this may be exposed to for instance other microorganisms or insects.

### **Heterogeneity in spores**

Formation of conidiophores starts in the colony center and spreads outwards. Only the few most peripheral millimeters of the colony will remain free of conidiophores. This mode of development implies that conidia that have formed within the colony center are older than those at the periphery. At the same time, the spore at the end of a chain of 20 spores is about 1.5 days older than that near the vesicle of the conidiophore (Teertstra et al., 2017). This difference

within the spore chain cannot be eliminated during culturing. Yet, the age differences observed between the center and the periphery of the colony can be eliminated by inoculating spores in a confluent layer on the agar medium. In this way, spores are formed in a more synchronous way on the whole plate. With this culturing technique it was shown that conidia mature on the conidiophore. Maturation involves changes in the RNA profiles, compatible solute composition, melanin extractability, water dispersal efficiency, and germination rate (Teertstra et al., 2017). Two-day-old conidia germinate faster than 5- or 8-day-old conidia. This can not be explained by differences in metabolic activity since conidia in different maturation stages all have metabolic activity (Novodvorska et al., 2016; Teertstra et al., 2017). Although 8-day-old matured conidia are less effectively dispersed by water droplets than younger conidia, no differences are found in dispersal by wind or insect assays (Teertstra et al., 2017). Of importance, only a small part of the conidia are dispersed by each dispersal event. Together, it was concluded that at a given moment conidia of different age are released from a colony and that this heterogeneity could have an ecological advantage. For instance, only part of the conidia will germinate in a micro-environment with sugars or amino acids (Hayer et al., 2013; 2014; Ijadpanahsaravi et al., 2021). Immediate germination will allow rapid colonization of the substrate but germlings will die when environmental conditions become unfavorable for instance due to increased temperature or by evaporation of water. The conidia that do not germinate immediately thus serve as a backup during the dynamic conditions that are encountered in nature. Bleichrodt et al. (2013) showed that conidia have a different composition when produced on a conidiophore in the colony center or at the colony periphery. These differences are probably caused by the different nutritional conditions in these zones of the colony. Heterogeneity in spore composition can even be observed within a spore chain (Bleichrodt et al., 2013). This may be caused by stochastic processes such as expression of regulatory proteins.

## **AIM OF THIS THESIS**

This Thesis studied protein secretion and stress resistance of small and large micro-colonies of *A. niger* and their underlying mechanisms.

In **Chapter 2** it is shown that small and large micro-colonies secrete different enzymes into the culture medium. In fact, these enzymes act synergistically in breakdown of a natural substrate. This synergism is not only of interest for the industry to make blends of enzymes (e.g. for biofuel or bioplastic production) but could also play a role in nature for effective nutrient cycling.

**Chapter 3** describes that large micro-colonies show higher resistance to heat and hydrogen peroxide stress than small micro-colonies. This may be explained by the presence of non-germinated spores in the centre of large micro-colonies as well as a protective shield formed by the outer layer of hyphae of these micro-colonies.

In **Chapter 4** it is shown that the orotidine 5'-phosphate decarboxylase gene *pyrG* is involved in the formation of large micro-colonies, thereby affecting protein secretion and stress resistance in liquid shaken cultures.

**Chapter 5** describes that inactivation of the  $\alpha$ -1-3 glucan synthase gene *agsE* in *A. niger* results in smaller micro-colonies in liquid cultures and in changed protein secretion profiles. Pellet size and protein secretion profiles could be modulated by placing *agsE* under control of an inducible promoter.

Results are summarized and discussed in **Chapter 6**.

## REFERENCES

- Aerts, D., Hauer, E.E., Ohm, R.A., Arentshorst, M., Teertstra, W.R., Phippen, C., Ram, A.F., Frisvad, J.C., Wösten, H.A.B. 2018. The FlbA-regulated predicted transcription factor Fum21 of *Aspergillus niger* is involved in fumonisin production. *Antonie van Leeuwenhoek*, **111**, 311-322.
- Allis, C.D., Jenuwein, T. 2016. The molecular hallmarks of epigenetic control. *Nat Rev Genet*, **17**, 487-500.
- Amaike, S., Keller, N.P. 2011. *Aspergillus flavus*. *Annu Rev Phytopathol*, **49**, 107-133.
- Antiga, L., La Starza, S.R., Miccoli, C., D'Angeli, S., Scala, V., Zaccaria, M., Shu, X., Obrian, G., Beccaccioli, M., Payne, G.A., Reverberi, M. 2020. *Aspergillus flavus* exploits maize kernels using an "orphan" secondary metabolite cluster. *Int J Mol Sci*, **21**, 8213.
- Avery, S.V., Singleton, I., Magan, N., Goldman, G.H. 2019. The fungal threat to global food security. *Fungal Biol*, **123**, 555-557.
- Bafana, R., Pandey, R.A. 2018. New approaches for itaconic acid production: bottlenecks and possible remedies. *Crit Rev Biotechnol*, **38**, 68-82.
- Banuett, F. 1995. Genetics of *Ustilago maydis*, a fungal pathogen that induces tumors in maize. *Annu Rev Genet*, **29**, 179-208
- Bassetti, M., Poulakou, G., Ruppe, E., Bouza, E., van Hal, S.J., Brink, A. 2017. Antimicrobial resistance in the next 30 years, humankind, bugs and drugs: a visionary approach. *Intensive Care Med*, **43**, 1464-1475.



- Bennett, J.W. 1998. Mycotechnology: the role of fungi in biotechnology. *J Biotechnol*, **66**, 101-107.
- Bleichrodt, R.J., van Veluw, G.J., Recter, B., Maruyama, J., Kitamoto, K., Wösten, H.A.B. 2012. Hyphal heterogeneity in *Aspergillus oryzae* is the result of dynamic closure of septa by Woronin bodies. *Mol Microbiol*, **86**, 1334-1344.
- Bleichrodt, R., Vinck, A., Krijgsheld, P., van Leeuwen, M.R., Dijksterhuis, J., Wösten, H.A.B. 2013. Cytosolic streaming in vegetative mycelium and aerial structures of *Aspergillus niger*. *Stud Mycol*, **74**, 31-46.
- Bleichrodt, R.J., Hulsman, M., Wösten, H.A.B., Reinders, M.J. 2015a. Switching from a unicellular to multicellular organization in an *Aspergillus niger* hypha. *mBio*, **6**, e00111-00115.
- Bleichrodt, R.J., Vinck, A., Read, N.D., Wösten, H.A.B. 2015b. Selective transport between heterogeneous hyphal compartments via the plasma membrane lining septal walls of *Aspergillus niger*. *Fungal Genet Biol*, **82**, 193-200.
- Brakhage, A.A. 2005. Systemic fungal infections caused by *Aspergillus* species: epidemiology, infection process and virulence determinants. *Curr Drug Targets*, **6**, 875-886.
- Braun, B.R., Kadosh, D., Johnson, R.I. 2001. NRG1, a repressor of filamentous growth in *C.albicans*, is down-regulated during filament induction. *EMBO J*, **20**, 4753-4761.
- Burgord, E.P., Kierans, M., Gadd, G.M. 2003. Geomycology fungal growth in mineral substrata. *Mycologist*, **17**, 98-107.
- Cairns, T.C., Nai, C., Meyer, V. 2018. How a fungus shapes biotechnology: 100 years of *Aspergillus niger* research. *Fungal Biol Biotechnol*, **5**, 13.
- Clark, D.S. 1962. Submerged citric acid fermentation of ferrocyanide-treated beet molasses: morphology of pellets of *Aspergillus niger*. *Can J Microbiol*, **8**, 133-136.
- Clark, D.S., Ito, K., Horitsu, H. 1966. Effect of manganese and other heavy metals on submerged citric acid fermentation of molasses. *Biotechnol Bioeng*, **8**, 465-471.
- Daly, P., Peng, M., Mitchell, H.D., Kim, Y.M., Ansong, C., Brewer, H., de Gijssel, P., Lipton, M.S., Markillie, L.M., Nicora, C.D., Orr, G., Wiebenga, A., Hilden, K.S., Kabel, M.A., Baker, S.E., Makela, M.R., de Vries, R.P. 2020. Colonies of the fungus *Aspergillus niger* are highly differentiated to adapt to local carbon source variation. *Environ Microbiol*, **22**, 1154-1166.
- de Bekker, C., Bruning, O., Jonker, M.J., Breit, T.M., Wösten, H.A.B. 2011a. Single cell transcriptomics of neighboring hyphae of *Aspergillus niger*. *Genome Biol*, **12**, R71.

- de Bekker, C., van Veluw, G.J., Vinck, A., Wiebenga, L.A., Wösten, H.A.B. 2011b. Heterogeneity of *Aspergillus niger* microcolonies in liquid shaken cultures. *Appl Environ Microbiol*, **77**, 1263-1267.
- Denning, D.W. 1998. Invasive aspergillosis. *Clin Infect Dis*, **26**, 781-805.
- Denning, D.W., Park, S., Lass-Flörl, C., Fraczek, M.G., Kirwan, M., Gore, R., Smith, J., Bueid, A., Moore, C.B., Bowyer, P., Perlin, D.S. 2011. High-frequency triazole resistance found in nonculturable *Aspergillus fumigatus* from lungs of patients with chronic fungal disease. *Clin Infect Dis*, **52**, 1123-1129.
- Dynesen, J., Nielsen, J. 2003. Surface hydrophobicity of *Aspergillus nidulans* conidiospores and its role in pellet formation. *Biotechnol Prog*, **19**, 1049-1052.
- Finkelstein, D.B. 1987. Improvement of enzyme production in *Aspergillus*. *Antonie van Leeuwenhoek*, **53**, 349-352.
- Fontaine, T., Beauvais, A., Loussert, C., Thevenard, B., Fulgsang, C.C., Ohno, N., Clavaud, C., Prevost, M.C., Latge, J.P. 2010. Cell wall  $\alpha$ 1-3glucans induce the aggregation of germinating conidia of *Aspergillus fumigatus*. *Fungal Genet Biol*, **47**, 707-712.
- Galagan, J.E., Calvo, S.E., Cuomo, C., Ma, L.J., Wortman, J.R., Batzoglou, S., Lee, S.I., Basturkmen, M., Spevak, C.C., Clutterbuck, J., Kapitonov, V., Jurka, J., Scaccocchio, C., Farman, M., Butler, J., Purcell, S., Harris, S., Braus, G.H., Draht, O., Busch, S., D'Enfert, C., Bouchier, C., Goldman, G.H., Bell-Pedersen, D., Griffiths-Jones, S., Doonan, J.H., Yu, J., Vienken, K., Pain, A., Freitag, M., Selker, E.U., Archer, D.B., Penalva, M.A., Oakley, B.R., Momany, M., Tanaka, T., Kumagai, T., Asai, K., Machida, M., Nierman, W.C., Denning, D.W., Caddick, M., Hynes, M., Paoletti, M., Fischer, R., Miller, B., Dyer, P., Sachs, M.S., Osmani, S.A., Birren, B.W. 2005. Sequencing of *Aspergillus nidulans* and comparative analysis with *A. fumigatus* and *A. oryzae*. *Nature*, **438**, 1105-1115.
- Garnier, L., Valence, F., Mounier, J. 2017. Diversity and control of spoilage fungi in dairy products: An update. *Microorganisms*, **5**, 33.
- Geiser, D.M., Klich, M.A., Frisvad, J.C., Peterson, S.W., Varga, J., Samson, R.A. 2007. The current status of species recognition and identification in *Aspergillus*. *Stud Mycol*, **59**, 1-10.
- Gougouli, M., Koutsoumanis, K.P. 2017. Risk assessment of fungal spoilage: A case study of *Aspergillus niger* on yogurt. *Food Microbiol*, **65**, 264-273.
- Grimm, D., Wösten, H.A.B. 2018. Mushroom cultivation in the circular economy. *Appl Microbiol Biotechnol*, **102**, 7795-7803.

- Grimm, L.H., Kelly, S., Hengstler, J., Gobel, A., Krull, R., Hempel, D.C. 2004. Kinetic studies on the aggregation of *Aspergillus niger* conidia. *Biotechnol Bioeng*, **87**, 213-218.
- Hawksworth, D.L. 2011. Naming *Aspergillus* species: progress towards one name for each species. *Med Mycol*, **49**, S70-76.
- Hayer, K., Stratford, M., Archer, D.B. 2013. Structural features of sugars that trigger or support conidial germination in the filamentous fungus *Aspergillus niger*. *Appl Environ Microbiol*, **79**, 6924-6931.
- Hayer, K., Stratford, M., Archer, D.B. 2014. Germination of *Aspergillus niger* conidia is triggered by nitrogen compounds related to L-amino acids. *Appl Environ Microbiol*, **79**, 6046-6053.
- He, X., Li, S., Kaminskyj, S.G. 2014. Characterization of *Aspergillus nidulans*  $\alpha$ -glucan synthesis: roles for two synthases and two amylases. *Mol Microbiol*, **91**, 579-595.
- Hevekerl, A., Kuenz, A., Vorlop, K.D. 2014. Influence of the pH on the itaconic acid production with *Aspergillus terreus*. *Appl Microbiol Biotechnol*, **98**, 10005-10012.
- Hickey, P.C., Read, N.D. 2009. Imaging living cells of *Aspergillus* in vitro. *Med Mycol*, **47**, S110-119.
- Hille, A., Neu, T.R., Hempel, D.C., Horn, H. 2009. Effective diffusivities and mass fluxes in fungal biopellets. *Biotechnol Bioeng*, **103**, 1202-1213.
- Hossain, A.H., Ter Beek, A., Punt, P.J. 2019. Itaconic acid degradation in *Aspergillus niger*: the role of unexpected bioconversion pathways. *Fungal Biol Biotechnol*, **6**, 16.
- Hou, L., Liu, L., Zhang, H., Zhang, L., Zhang, L., Zhang, J., Gao, Q., Wang, D. 2018. Functional analysis of the mitochondrial alternative oxidase gene (*aox1*) from *Aspergillus niger* CGMCC 10142 and its effects on citric acid production. *Appl Microbiol Biotechnol*, **102**, 7981-7995.
- Houbraken, J., Kocsubé, S., Visagie, C.M., Yilmaz, N., Wang, X.C., Meijer, M., Kraak, B., Hubka, V., Bensch, K., Samson, R.A., Frisvad, J.C. 2020. Classification of *Aspergillus*, *Penicillium*, *Talaromyces* and related genera (Eurotiales): An overview of families, genera, subgenera, sections, series and species. *Stud Mycol*, **95**, 5-169.
- Ijadpanahsaravi, M., Punt, M., Wösten, H.A.B., Teertstra, W.R. 2021. Minimal nutrient requirements for induction of germination of *Aspergillus niger* conidia. *Fungal Biol*, **125**, 231-238.
- Iyyappan, J., Bharathiraja, B., Baskar, G., Jayamuthunagai, J., Barathkumar, S., Anna Shiny, R. 2018. Malic acid production by chemically induced *Aspergillus niger* MTCC 281 mutant from crude glycerol. *Bioresour Technol*, **251**, 264-267.

- Kalra, R., Conlan, X.A., Goel, M. 2020. Fungi as a potential source of pigments: harnessing filamentous fungi. *Front Chem*, **8**, 369.
- Kamei, K., Watanabe, A. 2005. *Aspergillus* mycotoxins and their effect on the host. *Med Mycol*, **43**, S95-99.
- Kamper, J., Kahmann, R., Bolker, M., Ma, L.J., Brefort, T., Saville, B.J., Banuett, F., Kronstad, J.W., Gold, S.E., Muller, O., Perlin, M.H., Wösten, H.A.B., de Vries, R., Ruiz-Herrera, J., Reynaga-Pena, C.G., Snetselaar, K., McCann, M., Perez-Martin, J., Feldbrugge, M., Basse, C.W., Steinberg, G., Ibeas, J.I., Holloman, W., Guzman, P., Farman, M., Stajich, J.E., Sentandreu, R., Gonzalez-Prieto, J.M., Kennell, J.C., Molina, L., Schirawski, J., Mendoza-Mendoza, A., Greilinger, D., Munch, K., Rossel, N., Scherer, M., Vranes, M., Ladendorf, O., Vincon, V., Fuchs, U., Sandrock, B., Meng, S., Ho, E.C., Cahill, M.J., Boyce, K.J., Klose, J., Klosterman, S.J., Deelstra, H.J., Ortiz-Castellanos, L., Li, W., Sanchez-Alonso, P., Schreier, P.H., Hauser-Hahn, I., Vaupel, M., Koopmann, E., Friedrich, G., Voss, H., Schluter, T., Margolis, J., Platt, D., Swimmer, C., Gnirke, A., Chen, F., Vysotskaia, V., Mannhaupt, G., Guldener, U., Munsterkotter, M., Haase, D., Oesterheld, M., Mewes, H.W., Mauceli, E.W., DeCaprio, D., Wade, C.M., Butler, J., Young, S., Jaffe, D.B., Calvo, S., Nusbaum, C., Galagan, J., Birren, B.W. 2006. Insights from the genome of the biotrophic fungal plant pathogen *Ustilago maydis*. *Nature*, **444**, 97-101.
- Keller, N.P. 2019. Fungal secondary metabolism: regulation, function and drug discovery. *Nat Rev Microbiol*, **17**, 167-180.
- Klich, M.A. 2007. *Aspergillus flavus*: the major producer of aflatoxin. *Mol Plant Pathol*, **8**, 713-722.
- Krijghsheld, P., Bleichrodt, R., van Veluw, G.J., Wang, F., Muller, W.H., Dijksterhuis, J., Wösten, H.A.B. 2013a. Development in *Aspergillus*. *Stud Mycol*, **74**, 1-29.
- Krijghsheld, P., Nitsche, B.M., Post, H., Levin, A.M., Muller, W.H., Heck, A.J., Ram, A.F., Altelaar, A.F., Wösten, H.A.B. 2013b. Deletion of *flbA* results in increased secretome complexity and reduced secretion heterogeneity in colonies of *Aspergillus niger*. *J Proteome Res*, **12**, 1808-1819.
- Kuenz, A., Krull, S. 2018. Biotechnological production of itaconic acid - things you have to know. *Appl Microbiol Biotechnol*, **102**, 3901-3914.
- Latgé, J.P. 2001. The pathobiology of *Aspergillus fumigatus*. *Trends Microbiol*, **9**, 382-389.
- Latgé, J.P., Chamilos, G. 2019. *Aspergillus fumigatus* and Aspergillosis in 2019. *Clin Microbiol Rev*, **33**, e00140-00218.

- Levin, A.M., de Vries, R.P., Conesa, A., de Bekker, C., Talon, M., Menke, H.H., van Peij, N.N., Wösten, H.A.B. 2007. Spatial differentiation in the vegetative mycelium of *Aspergillus niger*. *Eukaryot Cell*, **6**, 2311-2322.
- Li, C., Zhou, J., Du, G., Chen, J., Takahashi, S., Liu, S. 2020. Developing *Aspergillus niger* as a cell factory for food enzyme production. *Biotechnol Adv*, **44**, 107630-107647.
- Liu, X.B., Koestler, R.J., Warscheid, T., Katayama, Y., Gu, J.D. 2020. Microbial deterioration and sustainable conservation of stone monuments and buildings. *Nat Sustain*, **3**, 991-1004.
- Lorenzo, J.M., Munekata, P.E., Dominguez, R., Pateiro, M., Saraiva, J.A., Franco, D. 2018. Main groups of microorganisms of relevance for food safety and stability: general aspects and overall description. in: *Innov Food Sci Emerg Technol*, pp. 53-107.
- Marion, C.L., Rappleye, C.A., Engle, J.T., Goldman, W.E. 2006. An  $\alpha$ -(1,4)-amylase is essential for  $\alpha$ -(1,3)-glucan production and virulence in *Histoplasma capsulatum*. *Mol Microbiol*, **62**, 970-983.
- McAdams, H.H., Arkin, A. 1999. It's a noisy business! Genetic regulation at the nanomolar scale. *Trends Genet*, **15**, 65-69.
- Metz, B., Kossen, N.W.F. 1977. The growth of molds in the form of pellets - a literature review. *Biotechnol Bioeng*, **XIX**, 781-799.
- Meyer, V., Wu, B., Ram, A.F. 2011. *Aspergillus* as a multi-purpose cell factory: current status and perspectives. *Biotechnol Lett*, **33**, 469-476.
- Miyazawa, K., Yoshimi, A., Zhang, S., Sano, M., Nakayama, M., Gomi, K., Abe, K. 2016. Increased enzyme production under liquid culture conditions in the industrial fungus *Aspergillus oryzae* by disruption of the genes encoding cell wall  $\alpha$ -1,3-glucan synthase. *Biosci Biotechnol Biochem*, **80**, 1853-1863.
- Moukha, S.M., Wösten, H.A.B., Asther, M., Wessels, J.G. 1993. In situ localization of the secretion of lignin peroxidases in colonies of *Phanerochaete chrysosporium* using a sandwiched mode of culture. *J Gen Microbiol*, **139**, 969-978.
- Noma, O., Asakawa, Y. 2010. 3.19 - Biotransformation of Monoterpenoids. In: Liu H-W, editor. *Comprehensive Natural Products II*. Mander Oxford L: Elsevier. 669-801.
- Novodvorska, M., Stratford, M., Blythe, M.J., Wilson, R., Beniston, R.G., Archer, D.B. 2016. Metabolic activity in dormant conidia of *Aspergillus niger* and developmental changes during conidial outgrowth. *Fungal Genet Biol*, **94**, 23-31.
- O'Gorman, C.M. 2011. Airborne *Aspergillus fumigatus* conidia: a risk factor for aspergillosis. *Fungal Biol Rev*, **25**, 151-157.

- Pawar, N.V., Patil, V.B., Kamble, S.S., Dixit, G.B. 2008. First report of *Aspergillus niger* as a plant pathogen on *Zingiber officinale* from India. *Plant Dis*, **92**, 1368.
- Pitt, J.I. 1994. The current role of *Aspergillus* and *Penicillium* in human and animal health. *Med Mycol*, **32**, 17-32.
- Pitt, J., Hocking, A.D. 2009. *In fungi and food spoilage (3rd Ed.)*. Springer Science Business Media, LLC, 233 Spring Street, New York, NY 10013.
- Rojas-Sanchez, U., Lopez-Calleja, A.C., Millan-Chiu, B.E., Fernandez, F., Loske, A.M., Gomez-Lim, M.A. 2020. Enhancing the yield of human erythropoietin in *Aspergillus niger* by introns and CRISPR-Cas9. *Protein Expr Purif*, **168**, 105570-105578.
- Samson, R.A., Varga, J. 2009. What is a species in *Aspergillus*? *Med Mycol*, **47**, S13-20.
- Saranya, R., Anadani, V.B., Saranya, R., Vanthana, M., Akbari, L.F. 2017. Management of black mold of onion [*Aspergillus niger* (Van Teigh)] by using various fungicides. *Int J Curr Microbiol Appl Sci*, **6**, 1621-1627.
- Shah, D.N., Kothari, R. 2004. Glucose oxidase-rich *Aspergillus niger* strain, cost-effective protocol and an economical substrate for the preparation of tablet grade calcium gluconate. *Biotechnol Lett*, **15**, 35-40.
- Spohr, A.B., Carlsen, M., Nielsen, J., Villadsen, J. 1996. Morphology and physiology of an  $\alpha$ -amylase producing strain of *Aspergillus oryzae* during batch cultivations. *Biotechnol Bioeng*, **49**, 257-261.
- Stevens, D.A., Kan, V.L., Judson, M.A., Morrison, V.A., S Dummer, S., Denning, D.W., Bennett, J.E., Walsh, T.J., Patterson, T.F., Pankey, G.A. 2000. Practice guidelines for diseasesa caused by *Aspergillus*. *Clin Infect Dis*, **30**, 696-709.
- Taccone, F.S., Van den Abeele, A.M., Bulpa, P., Misset, B., Meersseman, W., Cardoso, T., Paiva, J.A., Blasco-Navalpotro, M., De Laere, E., Dimopoulos, G., Rello, J., Vogelaers, D., Blot, S.I., AspICU. 2015. Epidemiology of invasive aspergillosis in critically ill patients: clinical presentation, underlying conditions, and outcomes. *Crit Care*, **19**, 15.
- Teertstra, W.R., Tegelaar, M., Dijksterhuis, J., Golovina, E.A., Ohm, R.A., Wösten, H.A.B. 2017. Maturation of conidia on conidiophores of *Aspergillus niger*. *Fungal Genet Biol*, **98**, 61-70.
- Tegelaar, M., Wösten, H.A.B. 2017. Functional distinction of hyphal compartments. *Sci Rep*, **7**, 6039.
- Tegelaar, M., Aerts, D., Teertstra, W.R., Wösten, H.A.B. 2020a. Spatial induction of genes encoding secreted proteins in micro-colonies of *Aspergillus niger*. *Sci Rep*, **10**, 1536.



- Tegelaar, M., Bleichrodt, R.J., Nitsche, B., Ram, A.F.J., Wösten, H.A.B. 2020b. Subpopulations of hyphae secrete proteins or resist heat stress in *Aspergillus oryzae* colonies. *Environ Microbiol*, **22**, 447-455.
- Upton, D.J., McQueen-Mason, S.J., Wood, A.J. 2017. An accurate description of *Aspergillus niger* organic acid batch fermentation through dynamic metabolic modelling. *Biotechnol Biofuels*, **10**, 258.
- van Veluw, G.J., Teertstra, W.R., de Bekker, C., Vinck, A., van Beek, N., Muller, W.H., Arentshorst, M., van der Mei, H.C., Ram, A.F., Dijksterhuis, J., Wösten, H.A.B. 2013. Heterogeneity in liquid shaken cultures of *Aspergillus niger* inoculated with melanised conidia or conidia of pigmentation mutants. *Stud Mycol*, **74**, 47-57.
- Vinck, A., Terlouw, M., Pestman, W.R., Martens, E.P., Ram, A.F., van den Hondel, C.A., Wösten, H.A.B. 2005. Hyphal differentiation in the exploring mycelium of *Aspergillus niger*. *Mol Microbiol*, **58**, 693-699.
- Vinck, A., de Bekker, C., Ossin, A., Ohm, R.A., de Vries, R.P., Wösten, H.A.B. 2011. Heterogenic expression of genes encoding secreted proteins at the periphery of *Aspergillus niger* colonies. *Environ Microbiol*, **13**, 216-225.
- Wösten, H.A.B. 2019. Filamentous fungi for the production of enzymes, chemicals and materials. *Curr Opin Biotechnol*, **59**, 65-70.
- Wösten, H.A.B., Moukha, S.M., Sietsma, J.H., Wessels, J.G. 1991. Localization of growth and secretion of proteins in *Aspergillus niger*. *J Gen Microbiol*, **137**, 2017-2023.
- Yang, L., Lübeck, M., Lübeck, P.S. 2017. *Aspergillus* as a versatile cell factory for organic acid production. *Fungal Biol Rev*, **31**, 33-49.
- Yoshimi, A., Sano, M., Inaba, A., Kokubun, Y., Fujioka, T., Mizutani, O., Hagiwara, D., Fujikawa, T., Nishimura, M., Yano, S., Kasahara, S., Shimizu, K., Yamaguchi, M., Kawakami, K., Abe, K. 2013. Functional analysis of the  $\alpha$ -1,3-glucan synthase genes *agsA* and *agsB* in *Aspergillus nidulans*: *agsB* is the major  $\alpha$ -1,3-glucan synthase in this fungus. *PLoS One*, **8**, e54893.

## **Chapter 2**

**Different sized micro-colonies of the fungus**

***Aspergillus niger* help each other to digest food**

*Jun Lyu, Martin Tegelaar, Harm Post, Juan Moran Torres, A. F. Maarten Altelaar, Robert-Jan Bleichrodt, Hans de Cock, Luis G. Lugones and Han A. B. Wösten*

## ABSTRACT

The fungus *Aspergillus niger* secretes a wide variety and high amounts of enzymes to degrade organic material. Its secretion capacity is important for nutrient recycling in nature and is used for industrial protein production. *A. niger* forms micro-colonies of different size when grown in a liquid medium such as in bioreactors. We here describe the secretomes of small (diameter  $285 \pm 8 \mu\text{m}$ ) and large (diameter  $> 1456 \mu\text{m}$ ) *A. niger* micro-colonies that include 21 proteins with a signal sequence for secretion that have not been described before being part of the secretome of this fungus. Notably, the secretomes of the small and large micro-colonies have a different composition and complementary activities. For instance, cellulase activity increased when the culture media of the small and large micro-colonies were mixed. Forming different sized micro-colonies is thus a strategy of *A. niger* to produce a meta-secretome optimally suited to degrade complex substrates not only in bioreactors but potentially also in nature.

## INTRODUCTION

The fungus *Aspergillus niger* is abundantly present in nature colonizing dead and living organic material like fruits and bulbs (Krijgsheld et al., 2013). It is used as a cell factory to produce enzymes and small molecular weight metabolites such as organic acids (Meyer et al., 2011; Wösten, 2019). Germination of *A. niger* conidia results in hyphae that extend at their apices and that branch sub-apically, ultimately resulting in a mycelium. Such a mycelium of *A. niger* can reach a (sub-)millimeter (micro-colonies) to centimeter (macro-colonies) size when grown on a solid substrate. In liquid cultures, *A. niger* grows as micro-colonies. Micro-colonies known as pellets have a distinct central and outer zone, while dispersed mycelium consists of a small network of hyphae (Krijgsheld et al., 2013).

Citric acid production by *A. niger* is higher when grown as pellets when compared to dispersed mycelium (Clark, 1962; Clark et al., 1966). The reason for this is not yet known but it may be due to the difference in viscosity of the culture medium imposed by the different morphologies of the mycelium. Viscosity is high when fungi grow dispersed, while it is lower when fungi grow as pellets (Bhargava et al., 2003). The reduced availability of oxygen and nutrients in the center of pellets may also affect organic acid production (Hille et al., 2009). The impact of morphology of the mycelium on composition and amounts of proteins released into the medium is also not yet clear. Morphology in bioreactors is controlled by changing growth conditions such as the amount and formulation of inoculum and medium composition (Krijgsheld et al., 2013; Lu et al., 2010; Wösten et al., 2013). Therefore, it is not possible to conclude whether the changes in productivity are the result of the changes in mycelium

morphology, the culture conditions, or both. The fact that micro-colony size is often heterogeneous in a liquid shaken culture (de Bekker et al., 2011; van Veluw et al., 2013) also complicates to relate the impact of colony morphology on protein secretion.

Here, the impact of morphology on secretome composition and total protein secretion was studied. To this end, micro-colony size was controlled by germinating spores for different periods within alginate beads, after which the beads were dissolved and the fungal cells were transferred to fresh medium to analyze the secretome. We show that small micro-colonies secrete more protein and have a different secretome composition when compared to large micro-colonies. Notably, the secretomes of small and large micro-colonies are complementary, thus having a synergistic effect on polymer degrading activity.

## MATERIAL AND METHODS

### *Strain and culture conditions*

*Aspergillus niger* strain MA234.1 (transient *kusA::amdS*; *pyrG*<sup>+</sup>) (Park et al., 2016) was grown for 3 days at 30 °C on MM with 1% glucose as carbon source. Conidia were harvested with transformation medium with 25 mM xylose as carbon source (TM-X; Aerts et al., 2019). The spore suspension was filtered through a syringe with cotton to remove hyphae. Conidia were counted using a haemocytometer, after which  $2 \times 10^7$  spores were introduced in 50 ml TM-X in 250 ml Erlenmeyer flasks (free spore cultures also called F-cultures). Alternatively, the same number of spores were introduced that had been immobilized in alginate beads with a diameter of 700  $\mu\text{m}$  (bead spore cultures also called B-cultures). To this end, 4% Na-alginate was dissolved overnight in Milli-Q water and sterilized at 121 °C for 20 min. The spores were mixed with the alginate solution at a final concentration of  $2 \times 10^7$  conidia  $\text{ml}^{-1}$ . The suspension was introduced into a 3% aqueous solution of  $\text{CaCl}_2 \cdot 2\text{H}_2\text{O}$  with a dropping device (Delgado-Ramos et al., 2014) using  $40 \text{ cm}^3 \text{ min}^{-1}$  pressurized air and  $5 \text{ cm h}^{-1}$  pump speed. The suspension was mixed with a magnetic stirrer at 300 rpm. As a control, empty beads were added to the culture medium containing free spores. Alternatively, either 1 ml Na-alginate solution or 11 mg  $\text{CaCl}_2 \cdot 2\text{H}_2\text{O}$  was added to the culture medium. To dissolve the beads at specific time points, 5 ml 1 M sodium citrate buffer, pH 6.0, was added to the 50 ml cultures. The same amount of buffer was added to the cultures with the free spores and the control cultures. After dissolving the beads, the germlings and / or mycelium (from here on collectively called mycelium) were washed twice with 50 ml Milli-Q water with intermittent filtering over a filter with 1  $\mu\text{m}$  pores (PluriSelect, Deutscher, Germany). The mycelium was transferred to 100 ml MM-X (minimal medium; de Vries et al., 2004) with 25 mM xylose as a carbon source). After a total period of

48 h of pre-culturing (TM-X) and culturing (MM-X), the mycelium and culture medium were separated by using a 40 µm cell strainer (Corning, 352340, New York, United States). All experiments were carried out as quadruplicates.

### *Analysing micro-colony diameter*

Bright field images of micro-colonies were converted to binary images by thresholding. Using the particle analysis tool in ImageJ, micro-colonies were automatically segmented using a size > 50,000 square pixel (i.e. 1000 µm<sup>2</sup>), to get rid of small debris, and a circularity between 0 and 1. The diameter of micro-colonies was calculated using the formula  $2 \cdot \sqrt{\frac{area}{\pi}}$  assuming that micro-colonies are circular. Bimodality of micro-colony diameter within treatments was assessed using a custom script (Vinck et al., 2005). Diameter range belonging to the sub-population with a proportion >50% of the total population were analyzed using one-way ANOVA followed by Dunnett's T3 post-hoc test for multiple comparisons. Treatments producing similar micro-colony diameter were assessed by hierarchical clustering. The impact of the presence of empty beads, alginate, and CaCl<sub>2</sub> on the diameter of micro-colonies grown from free spores was assessed by Students' or Welch's t-test.

### *Determination of biomass and protein concentration*

Mycelium was filtered over filter paper and washed twice with distilled water. The mycelium was dried at 60 °C and weighed. Protein concentration in the culture medium was measured using Bradford's method (Bradford, 1976). The relation between biomass and micro-colony size and between protein release into the medium and micro-colony size were assessed by linear regression.

### *SDS-PAGE*

Proteins contained in 400 µl culture medium were precipitated overnight at -20 °C with four volumes pre-cooled acetone. Proteins were pelleted at 4 °C at 20,000 g for 30 min and dissolved in 20 µl loading buffer (20% glycerol, 4% SDS, 100 mM Tris-HCL pH 6.8, 0.01% bromophenol blue). Proteins were separated in 12.5% SDS-polyacrylamide gels using TGS buffer (30 g Tris base, 144 g glycine, and 10 g SDS l<sup>-1</sup>). Gels were stained in 0.02% CBB G-250, 5% Al<sub>2</sub>(SO<sub>4</sub>)<sub>3</sub>(14-18)-hydrate, 10% ethanol and 2% phosphoric acid and destained in 10% ethanol and 2% phosphoric acid (Krijgsheld et al., 2012).

### *S-Trap micro spin column protein digestion*

Samples were digested using a S-Trap micro spin column (Protifi) following the manufactures protocol. Briefly, samples were mixed 1:1 with lysis buffer (10% SDS, 1 tablet cOmplete mini Protease inhibitor 10 ml<sup>-1</sup> (Roche), 100 mM TEAB, pH 8.5) and centrifuged for 8 min at 13,000 g. Proteins in the supernatant were reduced with 4 mM DTT for 30 min at 56° C, alkylated with 8 mM iodoacetamide for 20 min at room temperature and acidified adding a final concentration of 1% phosphoric acid. After a 1:7 dilution with S-Trap binding buffer (90% MeOH, 100 mM TEAB, pH 7.1), samples were loaded onto the spin column and passed through the column at 2,000 g, followed by 3 washes with S-trap binding buffer. Samples were digested with 3 µg trypsin (Promega, Wisconsin, USA) for 1 h at 47 °C, and eluted with 40 µl each of 50 mM TEAB, 0.2% formic acid and 50% acetonitrile in 0.2% formic acid. Samples were dried in a vacuum concentrator and resuspended in 2% formic acid prior to UHPLC-MS/MS.

### *Data acquisition*

Data was acquired using an UHPLC 1290 system coupled to an Orbitrap Q Exactive HF-X mass spectrometer (Thermo Scientific). Peptides were trapped on a column (Dr. Maisch Reprosil C18, 3 µm, 2 cm x 100 µm), after which they were separated on an analytical column (Agilent Poroshell EC-C18, 278 µm, 40 cm x 75 µm) using a gradient of 39 min at a column flow of 300 nl min<sup>-1</sup>. Trapping was performed at 5 µl min<sup>-1</sup> for 5 min in solvent A (0.1% formic acid in water) and eluted using as gradient; 13-40% solvent B (0.1% formic acid in 80% acetonitrile) in 35 min, 40-100% in 3 min and 100% solvent B for 1 min. Full scan MS spectra from m/z 375-1600 were acquired at a resolution of 60,000 at m/z 400 after accumulation to an automatic gain control target value of 3E6 ions. Up to fifteen most intense precursor ions were selected for fragmentation. HCD fragmentation was performed at normalized collision energy of 27% after the accumulation to a target value of 1e5. MS/MS was acquired at a resolution of 30,000.

### *Proteomics data analysis*

Raw data was analyzed with MaxQuant software (version 1.6.8.0) using label-free quantification (Cox et al., 2011). A false discovery rate (FDR) of 0.01 for proteins and peptides and a minimum peptide length of 7 amino acids were required. MS/MS spectra were searched against the database using the Andromeda search engine. Trypsin allowing N-terminal cleavage to proline was selected for enzyme specificity. Cysteine carbamidomethylation was selected as fixed modification, while protein N-terminal acetylation and methionine oxidation

were selected as variable modifications. Up to two missed cleavages were allowed. Initial mass deviation of precursor ion was up to 7 ppm, mass deviation for fragment ions was 0.05 Dalton. Protein identification required one unique peptide to the protein group and match between run was enabled. In all cases, 4 biological replicates and at least 2 technical replicates were used. All correction analyses were carried out with Perseus software Version 1.6.10.0. All biological replicates had an  $R^2 > 0.97$ . Proteins were considered present when they had been identified in at least 3 out of 4 biological replicates. Pfam over-representation and signal peptide analysis were done as described (El-Gebali et al., 2019; Petersen et al., 2011).

#### *cDNA synthesis and quantitative PCR analysis*

cDNA was synthesized from total RNA using the QuantiTect reverse transcription kit (Qiagen, Hilden, Germany). Quantitative PCR (QPCR) was performed by using ABI Prism 7900HT SDS and SYBR green chemistry (Applied Biosystems, Carlsbad, CA) and primers as indicated in Supplemental Table 1. The primer pairs had an amplification efficiency of 91.5% -112.5%. Expression of genes was related to levels of actin mRNA using the  $2^{-\Delta\Delta CT}$  method using QuantStudio™ Real-Time PCR Software (Applied Biosystems, Carlsbad, CA), setting the relative expression of the F12 sample at 1. Data was analyzed by t-test comparing F12 and B12 samples after 12 and 48 hours.

#### *Cellulase activity assay*

Cellulase activity was quantified using the filter paper activity assay (FPase) (Xiao et al., 2004). To this end, 7-mm diameter circles of Whatman No. 1 filter paper were incubated with 60  $\mu$ l culture medium for 24 h at 50 °C. This was followed by a 5 min incubation at 95 °C after adding 120  $\mu$ l DNS (10 g l<sup>-1</sup> 3,5-dinitrosalicylic acid, 400 g l<sup>-1</sup> KNa-tartrate and 16 g NaOH L<sup>-1</sup>). Aliquots of the samples (100  $\mu$ l) were transferred to the wells of a flat-bottom plate and the A<sub>540</sub> was determined using a Synergy HTX Microplate Reader (BioTek, Winooski, VT, USA). Calibration curves were made using different concentrations of glucose. A unit of cellulase activity was defined as 1  $\mu$ mol glucose released in 1 min. Cellulase activity within the culture media of B and F cultures that had been transferred at the same time point (e.g. B6 and F6) were compared to a 1:1 mixture of these media by one-way ANOVA, followed by either a Bonferroni or Dunnett's T3 test for multiple comparisons. Additionally, hypothesized cellulase activity of 1:1 mixed medium, defined as the mean cellulase activity of medium originating from B and F cultures, were compared to the actual cellulase activity in the mixtures by either Students' or Welch's t-test.

## RESULTS

### *Impact of spore encapsulation on morphology*

Alginate-embedded conidia (from now on called bead spore cultures or B-cultures) were grown for 6-16 h in transformation medium with xylose as carbon source (TM-X). The beads were dissolved by adding citrate buffer, after which the germlings and / or mycelium (from now on collectively called mycelium) were transferred to minimal medium with xylose as carbon source (MM-X). Growth of the cultures was continued for a total culturing time of 48 h, resulting in cultures B6-B16. For instance, beads of the B6 culture were dissolved after 6 h of growth in TM-X and growth was continued for 42 h in MM-X. As a control, similar pre-culturing conditions were used but with non-encapsulated spores (from now on called free spore cultures or F cultures; F6-F16). Micro-colony size of the B6-B16 and F6-F16 cultures was assessed. Statistical analysis showed 6 groups with different size (Figure 1B), which in turn were classified in 3 groups by hierarchical clustering. Group 1 consisted of mycelium of B6 cultures and the control cultures F6-F16 that had formed micro-colonies of  $3175 \pm 610 \mu\text{m}$  (mean  $\pm$  SD) (Figure 1). Group 2 consisted of B8 cultures that had formed intermediate sized micro-colonies ( $1559 \pm 69 \mu\text{m}$ ), while group 3 consisted of B10-B16 cultures that had formed small micro-colonies ( $285 \pm 8 \mu\text{m}$ ). Conidia of both B and F cultures had started to germinate after 6 h in the pre-cultures and had developed hyphae after 8 h. Mean biomass of the F6-F16 and B6-B16 cultures was  $1.4 \pm 0.2 \text{ gr l}^{-1}$  after 48 h of growth. Biomass was not significantly affected by micro-colony size or pre-culturing (Figure 2A).

**Table 1.** Proteins with and without a predicted signal sequence for secretion (SignalP) released into the medium of free spore (F) and bead spore (B) cultures. Number following F and B indicates time of transfer of the pre-cultures. Total culturing time was 48 h.

Sample	SignalP	Non-SignalP	Total
F6	155	19	174
B6	126	31	157
F8	158	22	180
B8	173	52	225
F10	149	22	171
B10	258	298	556
F12	170	30	200
B12	257	280	537
F14	124	18	142
B14	250	249	499
F16	179	29	208
B16	225	239	464



In the next set of experiments, cultures were inoculated with the mycelium of 8- or 16-h-old free spore pre-cultures that had either or not been supplemented with either empty beads, alginate or CaCl<sub>2</sub> to confirm that the effect on morphology was due to encapsulation in the alginate beads and not caused by chemical signals from the beads. To this end, B8 and B16 cultures were used as a control. After a total growth period of 48 h, the average diameter of the micro-colonies of the B8 cultures was different compared to that of the F8 culture and the F8 culture supplemented with alginate (Supplemental Figure 1B). These results can be explained by the intermediate size of the B8 micro-colonies. In contrast, the small B16 micro-colonies were distinct in size when compared to the F16 cultures that had either or not been supplemented with empty beads, alginate or CaCl<sub>2</sub>. Together, these results show that the effect of beads on mycelium morphology is due to the embedding and not due to chemical induction caused by alginate and / or CaCl<sub>2</sub>.

#### *Impact of spore encapsulation on the secretome*

Total protein that had been released by the B6-B16 and F6-F16 cultures was plotted against the average micro-colony size of each of the replicates (Figure 2B). Hierarchical clustering showed that the B10-B16 cultures clustered as well as the B6-B8 and F6-F16 cultures. Linear regression demonstrated that smaller colonies secrete more protein than larger micro-colonies. For instance, 270 µm wide micro-colonies released 2-fold more protein in the medium than 2700 µm wide micro-colonies (Figure 2B). The small sized micro-colonies of the B16 cultures had released more protein than the F16 cultures, to which either or not empty beads, alginate or CaCl<sub>2</sub> had been added (Supplemental Figure 1C). This effect was less pronounced when medium of B8 cultures was compared to F8 cultures to which either or not empty beads, alginate or CaCl<sub>2</sub> had been added. This is explained by the fact that the variation in micro-colony size between the F8 and B8 cultures is less distinct when compared to the B16 and F16 cultures. Together, these results show that the effect of embedding spores on protein release is due to its effect on morphology and not due to chemical induction caused by alginate and / or CaCl<sub>2</sub>.

Secretomes of the F6-F16 and B6-B16 cultures (Figure 2C) were analyzed by mass spectrometry (Supplemental Table 2). A set of 93 proteins was shared between all these cultures (Supplemental Figure 2A; Supplemental Table 3A), of which 84 were predicted to have a signal sequence for secretion. The F6-F16 cultures (that all formed large micro-colonies) had secreted 142-208 proteins in the culture medium (Table 1). A set of 118 proteins was shared between these cultures, while 0-15 proteins were unique for each of the cultures (Figure 3A).

In contrast, the B6-B16 cultures had secreted 157-556 proteins (Table 1). A set of 138 proteins was shared between these cultures, while 2-47 proteins were unique to each of these conditions (Figure 3B). The B6 and B8 cultures (forming large and intermediate sized micro-colonies showed the lowest number of proteins (i.e. 157 and 225 proteins, respectively) similar to those of the F6-F16 cultures (forming large micro-colonies) (Table 1). A set of 106 proteins was shared between the F6, F8, B6 and B8 cultures (Figure 3C). On the other hand, the B10-B16 cultures (forming small micro-colonies) shared 388 proteins in their secretome (Figure 3D). Taken together, secretome diversity in cultures is lower when the pellets are larger.

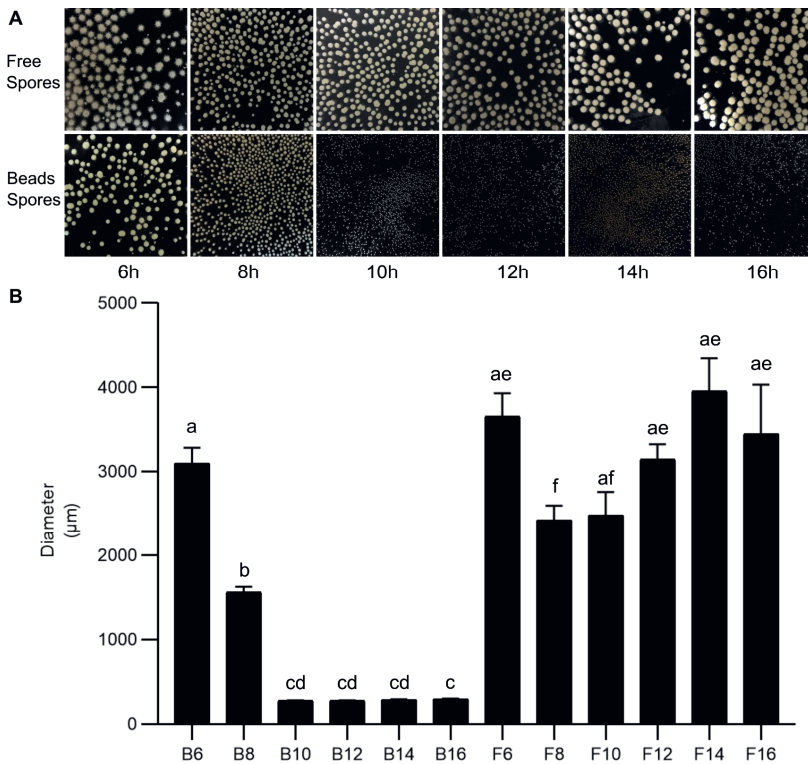


**Figure 1.** (A) Morphology of mycelium from free spore (F) cultures and bead spore (B) cultures. The beads had been dissolved after 6-16 h of pre-culturing and the mycelium was transferred to MM-X for 42-32 h with a total culturing time of 48 h. Similar pre-culturing and culturing conditions were used for the F cultures. (B) Micro-colony diameter as calculated by image analysis. Different letters indicate statistical differences as determined by a one-way ANOVA combined with a Dunnett's T3 post-hoc test. Error bars indicate standard deviation.

**Table 2.** Number of proteins with a Pfam domain identified in free spore (F) and bead spore (B) cultures. Numbers following F and B indicate the time of pre-culturing in hours. Total culturing time was 48 h.

		F 6	F 8	F 10	F 12	F 14	F 16	B 6	B 8	B 10	B 12	B 14	B 16
<b>Proteins with signal sequence for secretion</b>													
PF17678	GH family 92 N-terminal domain	0	0	0	0	0	0	0	0	4	4	4	4
PF12296	Hydrophobic surface binding protein A	0	0	0	0	0	0	0	3	0	0	0	0
PF10342	Ser-Thr-rich glycosyl-phosphatidyl-inositol-anchored membrane family	3	3	3	4	3	3	4	4	5	5	5	5
PF09286	Pro-kumamolisin, activation domain	5	5	5	5	5	5	5	5	5	5	5	4
PF09260	Domain of unknown function (DUF1966)	3	3	3	3	0	3	0	4	4	4	4	4
PF08386	TAP-like protein	0	0	0	0	0	0	0	0	3	3	3	3
PF07983	X8 domain	4	0	0	0	0	3	0	0	3	3	3	0
PF07971	GH family 92	0	0	0	0	0	0	0	0	4	4	4	4
PF07732	Multicopper oxidase	0	0	0	0	0	0	0	0	0	4	4	4
PF07731	Multicopper oxidase	0	0	0	0	0	0	0	0	0	4	4	4
PF04616	GH family 43	4	5	4	5	3	3	3	5	6	6	6	5
PF03663	GH family 76	0	0	0	0	0	0	0	0	0	5	4	0
PF03443	GH family 61	0	4	0	0	0	0	0	3	0	0	3	3
PF03198	Glucanoyltransferase	6	4	4	4	4	5	5	3	6	6	6	5
PF01764	Lipase (class 3)	4	4	3	4	0	3	0	4	4	4	4	0
PF01735	Lysophospholipase catalytic domain	0	3	3	3	3	3	0	0	0	0	0	0
PF01476	LysM domain	0	0	0	0	0	3	0	0	0	0	0	0
PF00734	Fungal cellulose binding domain	0	4	0	0	0	3	0	4	4	0	4	4
PF00450	Serine carboxypeptidase	3	3	0	4	0	4	0	0	7	7	7	6
PF00394	Multicopper oxidase	0	0	0	0	0	0	0	0	0	4	4	4
PF00328	Histidine phosphatase superfamily (branch 2)	0	0	0	0	0	0	0	0	0	4	0	0
PF00150	Cellulase (GH family 5)	5	5	4	5	4	5	3	5	7	7	7	4
PF00085	Thioredoxin	0	0	0	0	0	0	0	0	4	4	0	0
PF00082	Subtilase family	3	4	4	4	3	4	3	4	4	4	4	4
<b>Proteins without signal sequence for secretion</b>													
PF14543	Xylanase inhibitor N-terminal	3	0	3	4	4	5	0	0	5	6	6	4
PF14310	Fibronectin type III-like domain	0	0	0	0	0	0	0	0	5	5	0	0
PF13472	GDSSL-like Lipase/Acylhydrolase family	0	0	0	0	0	0	0	0	0	3	3	0
PF11976	Ubiquitin-2 like Rad60 SUMO-like	0	0	0	0	0	0	0	3	0	3	3	3
PF10584	Proteasome subunit A N-terminal signature	0	0	0	0	0	0	0	0	0	6	0	4
PF08031	Berberine and berberine like	6	5	4	4	0	6	4	7	8	7	0	0
PF07690	Major Facilitator Superfamily	0	0	0	0	0	0	0	0	0	0	1	1
PF06723	MreB/Mbl protein	0	0	0	0	0	0	0	0	4	4	4	3
PF04389	Peptidase family M28	0	0	0	0	0	0	0	0	0	4	0	0
PF04185	Phosphoesterase family	0	0	0	0	0	0	0	3	5	4	5	5
PF01915	GH family 3 C-terminal domain	0	0	0	0	0	0	0	0	5	5	0	0
PF01565	FAD binding domain	9	7	6	7	5	9	6	10	12	10	9	0
PF01328	Peroxidase, family 2	0	0	0	0	0	0	0	0	0	3	0	0
PF01055	GH family 31	0	0	0	0	0	0	3	3	0	3	3	3

PF00933	GH family 3 N terminal domain	0	0	0	0	0	0	0	0	5	5	0	0
PF00722	GH family 16	5	5	5	5	4	5	4	5	6	6	6	6
PF00657	GDSL-like Lipase/Acylhydrolase	3	0	0	3	0	3	3	0	4	4	5	0
PF00557	Metallopeptidase family M24	0	0	0	0	0	0	0	0	0	0	0	4
PF00326	Prolyl oligopeptidase family	0	0	0	0	0	0	0	0	7	7	7	7
PF00240	Ubiquitin family	0	0	0	0	0	0	0	3	0	0	0	0
PF00227	Proteasome subunit	0	0	0	0	0	0	0	0	0	8	0	6
PF00173	Cytochrome b5-like Heme/Steroid binding domain	0	0	0	0	0	0	0	0	6	6	6	6
PF00128	Alpha amylase, catalytic domain	0	0	0	0	0	0	0	4	5	6	5	5
PF00083	Sugar (and other) transporter	0	0	0	0	0	0	0	0	0	0	1	1
PF00076	RNA recognition motif. (a.k.a. RRM, RBD, or RNP domain)	0	0	0	0	0	0	0	0	10	0	0	0
PF00026	Eukaryotic aspartyl protease	5	4	6	7	6	9	4	4	8	10	10	6
PF00012	Hsp70 protein	0	0	0	0	0	0	0	0	4	4	4	0

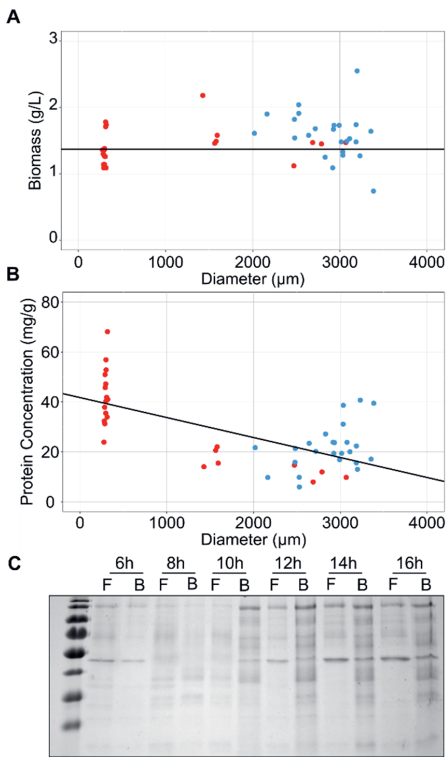


**Figure 2.** Biomass (A) and protein concentration (B) and protein profiles (C) in the culture media related to (A, B) the average micro-colony diameter of bead spore cultures B6-B16 (red dots) and free spore cultures F6-F16 (blue dots). The relation between biomass and micro-colony size and protein concentration in the culture medium and micro-colony size was assessed by linear and quantile regression.

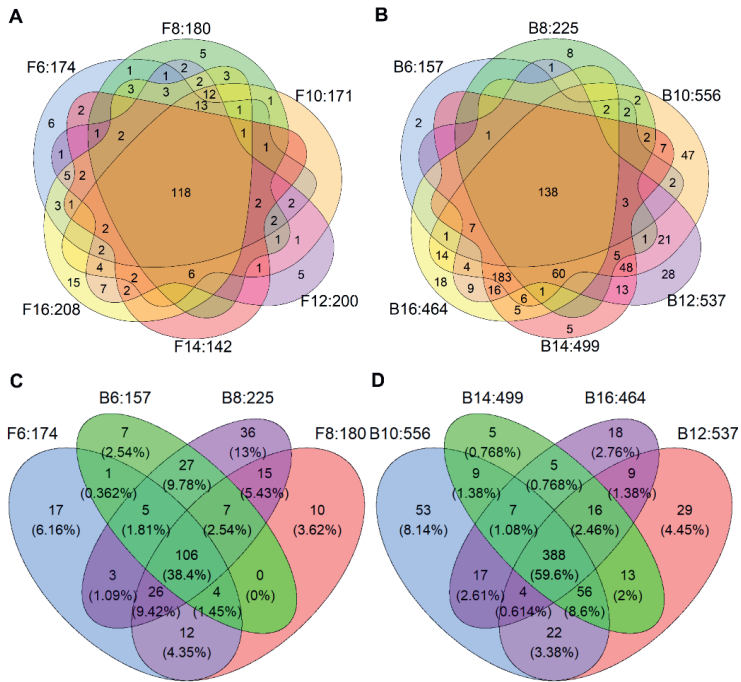


**Figure 3.** Venn diagram of the number of proteins from free spore (F) cultures (**A, C**) and bead spore (B) cultures (**B, C, D**). The beads had been dissolved just before transfer to MM-X and growth was prolonged up to a total culturing time of 48 h. The number following F and B indicate the time of pre-culturing in hours.

Secretomes of the F and B cultures that had been transferred at the same time to fresh medium were pairwise compared (Figure 4; Supplemental Table 4). The number of proteins in the secretomes of the F6 and B6 cultures (both forming large micro-colonies) was similar with 58 and 41 unique proteins in each of the cultures, respectively. From  $t = 8$  h onwards the B cultures secreted a higher variety of proteins (Figure 4). The secretomes of the F8 cultures (forming large micro-colonies) and B8 cultures (forming intermediate sized micro-colonies) had released 26 and 71 unique proteins, respectively. Notably, the B10-B16 cultures (forming small micro-colonies) had released > 300 unique proteins, while 11-46 unique proteins were identified in the media of the F10-F16 cultures (forming large micro-colonies). The number of proteins that were shared between the F and B cultures of the same age was relatively constant with 116-172 proteins (Figure 4).

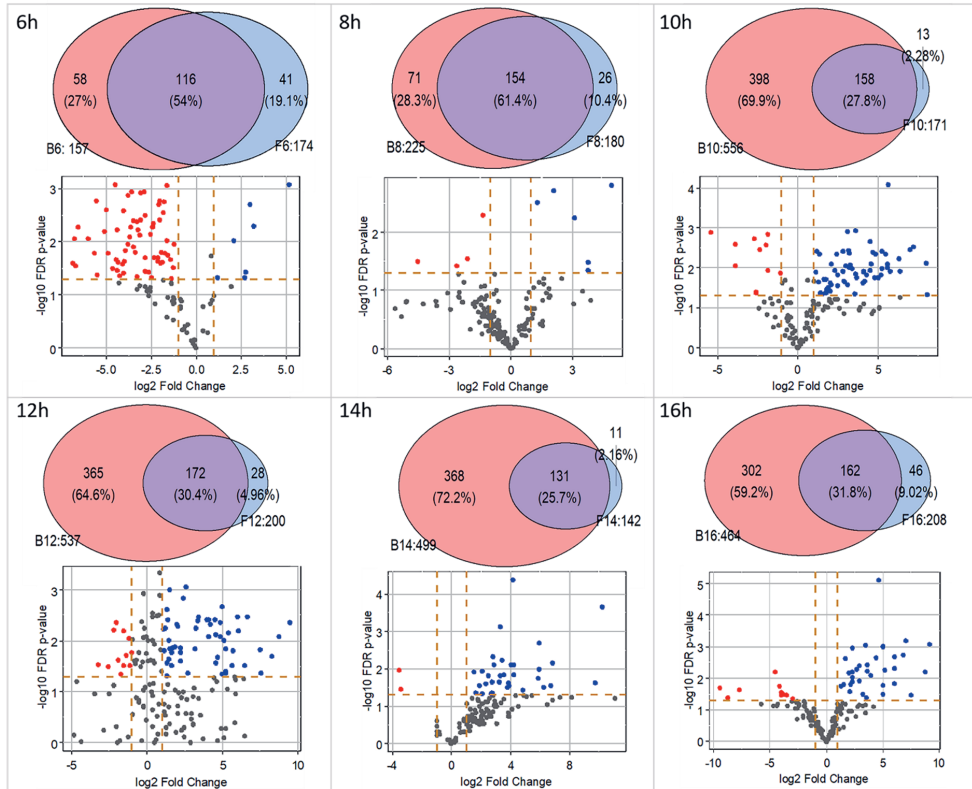


**Figure 4.** Pairwise comparison of number (top) and quantity (bottom) of proteins from liquid shaken free spore (F) and bead spore (B) cultures. Proteins were analyzed after a total culturing time of 48 h. Numbers following F and B indicate the time of pre-culturing in hours. Red and blue dots indicate proteins that were  $\geq 2$  fold down- or up-regulated in B cultures when compared to F cultures, respectively.

Apart from proteins that were uniquely present in one of the cultures in the pair-wise comparison, there were also proteins that had been released in both cultures but at different levels. A set of 7 and 65 proteins was  $> 2$ -fold up- and down-regulated, respectively, in the medium of B6 when compared to the F6 cultures (Figure 4; Supplemental Table 4). Less than 10 proteins were up- or down-regulated in the case of the B8 and F8 cultures. In contrast, a high number of proteins ( $\geq 33$ ) were upregulated in the medium of the B10-B16 cultures when compared to their respective F cultures, while only 2-12 proteins were down-regulated. Similarly, 82-135 proteins were up-regulated in the B8-B16 cultures (forming intermediate or small micro-colonies) when compared to the B6 cultures (forming large micro-colonies)

(Supplemental Figure 2 B,C). Conversely, only 0-3 proteins were upregulated in the B6 cultures when compared to the other B cultures. Together, small micro-colonies do not only produce a higher variety of unique proteins; they also produce more quantity of a set of proteins that are also released in the medium of large micro-colonies.

#### *Type of proteins found in the culture medium*

Presence of predicted signal sequences in the open reading frames of the genes encoding the secretomes was analyzed. 18-30 proteins out of the 142-208 proteins in the secretomes of the F6-F16 cultures (forming large micro-colonies) did not contain a predicted signal sequence for secretion (Table 1). A total of 21 unique proteins with a signal sequence were found in the media of these cultures when compared to the B cultures, while they contained 3 unique proteins without a signal peptide (Supplemental Table 3B). Among the 21 unique proteins with a signal sequence were CAZymes of the GH16, GH18 and GH61 families as well as a cellulase (exocellobiohydrolase II; GH6) (Martinez et al., 2008) that was formed by F16 cultures. A total number of 109 and 333 unique proteins with and without signal sequence, respectively, was found in the B6-B16 cultures (forming large [B6], intermediate [B8] and small micro-colonies [B10-B16]) that were absent in the F-cultures, including proteins of the CAZyme families GH1, GH11, GH20, GH26, GH35, GH47, GH71, GH76, GH88 and GH92, as well as two cellulases (endoglucanase II; GH5) (Martinez et al., 2008) (Supplemental Table 5A). The number of unique proteins in the B10-B16 cultures was 85 and 304 with and without signal sequence, respectively (Supplemental Table 5B). The two B-specific cellulases were produced by the B10-B14 cultures forming small micro-colonies. Together, small and large micro-colonies secrete different cellulases into the culture medium.

Protein family (Pfam) analysis was performed to assess the functions of proteins in the secretomes with (Table 2, Supplemental Table 6A) and without (Table 2, Supplemental Table 6B) predicted signal sequences. The F6-F16 cultures that all formed large micro-colonies showed 7-13 Pfam families in the set of proteins with a signal sequence and 4-6 Pfam families in the set without signal sequences (Table 2, Supplemental Table 6 A,B). Glucanosyltransferase was the Pfam family with most members (i.e. 6 representatives) in a specific culture in the set of proteins with signal sequence. B6 and B8 cultures that formed large and intermediate size micro-colonies showed a similar number of Pfam families in the set of proteins with signal sequence (6 and 11, respectively) and without signal sequence (6 and 9, respectively) when compared to the F6-F16 cultures (Table 2, Supplemental Tables 6 A,B). On the other hand, 15-19 and 15-22 Pfam families were found in the sets of proteins with and without signal sequence,

respectively, in the media of the B10-B16 cultures that form small micro-colonies, which was higher than that found in the F6-F12 cultures. Glucanotransferase and glycosyl hydrolase family GH43 (each 6 proteins) and carboxypeptidase and cellulase (each 7 proteins) were the Pfam families with most members in the set of proteins with signal sequence within specific B10-B16 cultures. Together, cultures with small micro-colonies have more Pfam families in their secretomes when compared to cultures with intermediate or large micro-colonies.

#### *Secretion of proteins encoded by XlnR regulated genes*

XlnR is a transcription factor regulating xylanolytic and cellulolytic encoding genes (de Souza et al., 2013; Hasper et al., 2000). Depending on the carbon source, 38 genes have been found to be regulated solely by XlnR (de Souza et al., 2013). B6-B16 cultures had released 14-23 out of the 38 XlnR regulated proteins (Table 3). The B10-B16 samples (forming small micro-colonies) had released 19-23 of these proteins, while the B6 and B8 samples (forming large and intermediate micro-colonies) had only released 14-16 of these proteins. The latter was similar to that of the F6-F16 cultures (forming large microcolonies) that had released 15-18 xylanolytic proteins. The 6 XlnR-regulated proteins that were exclusively found in the media of small micro-colonies were XarB, EglB, XynB, AgsC, AxlA and FaeA, while the cellulase cellobiohydrolase CBH was exclusively found in the media of large micro-colonies.

#### *Proteins with signal sequences identified in an *A. niger* secretome for the first time*

Within the set of proteins identified in the F6-F16 and B6-B16 cultures, 94 proteins without signal peptide (data not shown) and 21 proteins with signal peptide had not been reported before to be part of the *A. niger* secretome (Table 4). These 21 proteins were all identified in B cultures, while 7 of them were also identified in F cultures. Out of the 21 proteins, 3 were found in all B6-B16 cultures, while 12 were only identified in the B10-B16 cultures that formed small colonies (Table 4). The glycopeptidase PngN, an extracellular carbonic anhydrase and lactonase LctB were among these 21 proteins. The latter is involved in the conversion of glucose into gluconic acid thereby releasing H<sub>2</sub>O<sub>2</sub>.



**Table 3.** XlnR regulated proteins (X) in free spore (F) and bead spore (B) cultures. Numbers following F and B indicate the time of pre-culturing in hours. In all cases, total cultivation time was 48 h.

XlnR	Gene	GH family	Predict function	F6	F8	F10	F12	F14	F16	B6	B8	B10	B12	B14	B16
ATCC64974_109010	BGL/bglA	GH 3	Cellulose	X	X	X	X	X	X	X	X	X	X	X	X
ATCC64974_15350	BXL/xlnD	GH 3	Xylan, pectin	X	X	X	X	X	X	X	X	X	X	X	X
ATCC64974_83150	XLN/xynA	GH 10	Xylan	X	X	X	X	X	X	X	X	X	X	X	X
ATCC64974_2380	XG-EGL	GH 12	Cellulose	X	X	X	X	X	X	X	X	X	X	X	X
ATCC64974_1620	AGL	GH 27	Xyloglucan, xylan	X	X	X	X	X	X	X	X	X	X	X	X
ATCC64974_53780	AGL/aglB	GH 27	Xyloglucan, xylan	X	X	X	X	X	X	X	X	X	X	X	X
ATCC64974_13640	LAC/lacA	GH 35	Xyloglucan, xylan, pectin	X	X	X	X	X	X	X	X	X	X	X	X
ATCC64974_104980	ABF/abfC	GH 51	Xyloglucan, xylan, pectin	X	X	X	X	X	X	X	X	X	X	X	X
ATCC64974_30860	ABF/abfB	GH 54	ABF/abfB	X	X	X	X	X	X	X	X	X	X	X	X
ATCC64974_83160	AXH/axhA	GH 62	Xylan	X	X	X	X	X	X	X	X	X	X	X	X
ATCC64974_4680	AGU/aguA	GH 67	Xylan	X	X	X	X	X	X	X	X	X	X	X	X
ATCC64974_21600	XG-EGL/eglC	GH 74	Cellulose	X	X	X	X	X	X	X	X	X	X	X	X
ATCC64974_37230	AXE/axeA	CE 1	Xylan	X	X	X	X	X	X	X	X	X	X	X	X
ATCC64974_56580	Unknown	GH 3	Unknown	X	X	X	X	X	X	X	X	X	X	X	X
ATCC64974_40800	CBH	GH 6	Cellulose	X	X	X	X				X	X	X	X	X
ATCC64974_75710	PME/pmeA	CE 8	Pectin	X	X	X	X	X	X			X	X	X	X
ATCC64974_64540	BGL	GH 3	Cellulose	X					X		X	X	X	X	X
ATCC64974_87130	BGL	GH 3	Cellulose						X			X	X	X	X
ATCC64974_64370	BXL-BF/xarB	GH 3	Xylan, pectin										X	X	
ATCC64974_49560	EGL/eglB	GH 5	Cellulose									X	X	X	
ATCC64974_104930	CBH	GH 6	Cellulose						X						
ATCC64974_22790	XLN/xynB	GH 11	Xylan												X
ATCC64974_40950	AGS/agsC	GH 13	Cellulose									X	X		
ATCC64974_10330	BXL/axlA	GH 31	Xylan									X	X	X	
ATCC64974_41050	FAE	CE 1	Xylan, pectin										X	X	

**Table 4.** Proteins with a predicted signal sequence that had not been reported before to be part of the *A. niger* secretome. Letters in the samples column refer to free spore (F) and bead spore (B) cultures. Numbers following F and B refer to the time of pre-culturing in hours. In all cases, total cultivation time was 48 h.

ProteinID	Annotation	Location	Samples
ATCC64974_105570	ubiquitin-protein transferase activity (IMP)	Cytoplasm	B10-B16
ATCC64974_10480	PF10342 Ser-Thr-rich glycosyl-phosphatidyl-inositol-anchored membrane family	Integral component of membrane	F6-F16 and B6-B16
ATCC64974_105820	PF05345 Putative Ig domain	Integral component of membrane	B12-B16
ATCC64974_90920	PF03176 MMPL family	Integral component of membrane	B10-B14
ATCC64974_10620	PF00264 Central domain of tyrosinase	Classical secretion pathway: Extracellular	B10-B16
ATCC64974_18030	PF10282 Lactonase, 7-bladed beta-propeller	Classical secretion pathway: Extracellular	B10-B16
ATCC64974_18290	PF16334 Domain of unknown function (DUF4964)	Classical secretion pathway: Extracellular	B6, B10, B12, B16
ATCC64974_25530	PF00194 Eukaryotic-type carbonic anhydrase	Classical secretion pathway: Extracellular	B10-B16
ATCC64974_42730	PF00561 alpha/beta hydrolase fold	Classical secretion pathway: Extracellular	F16, B10-B16
ATCC64974_60000	PF00857 Isochorismatase family	Classical secretion pathway: Extracellular	B10-B12
ATCC64974_74560	C3HC4 type (RING finger) Zinc finger family	Classical secretion pathway: Extracellular	F8-F12, F16, B8-B10, B14-B16
ATCC64974_75850	PF11578 Protein of unknown function (DUF3237)	Classical secretion pathway: Extracellular	B10-B14
ATCC64974_75940	PF00884 Sulfatase	Classical secretion pathway: Extracellular	B12
ATCC64974_78580	PF00328 Histidine phosphatase superfamily (branch 2)	Classical secretion pathway: Extracellular	B12
ATCC64974_84710	PF12222 Peptide N-acetyl-beta-D-glucosaminyl asparaginase amidase A	Classical secretion pathway: Extracellular	B10-B16
ATCC64974_103600	Uncharacterized protein	Unknown	F6-F12, F16, B6-B16

ATCC64974_104760	Uncharacterized protein	Unknown	F16, B10-B16
ATCC64974_18290	PF16334 Domain of unknown function (DUF4964)	Unknown	B6, B10-B16
ATCC64974_53750	PF05630 Necrosis inducing protein (NPP1)	Unknown	F8, B8-B16
ATCC64974_67640	PF10342 Ser-Thr-rich glycosyl-phosphatidyl-inositol-anchored membrane family	Unknown	B10-B16
ATCC64974_89110	PF10342 Ser-Thr-rich glycosyl-phosphatidyl-inositol-anchored membrane family	Unknown	F12, B6-B16

### *Gene expression in micro-colonies of different size*

Expression of 6 genes encoding proteins with a signal sequence for secretion was assessed in micro-colonies to confirm differential protein secretion in micro-colonies of different size. To this end, qPCR was used to quantify expression of genes ATCC64974\_58540, ATCC64974\_96710 and ATCC64974\_67930 that encode proteins that showed higher levels in large micro-colonies (F6-F16, B6-B8) as well as genes ATCC64974\_14700, ATCC64974\_21820 and ATCC64974\_48070 that encode proteins that showed higher quantities in small micro-colonies (B10-B16) (Supplemental Table 7). RNA was extracted after 12 h (at the moment that the culture was transferred to MM-X) and 48 h (at the end of culturing) of the F12 and B12 cultures. The expression levels of these genes was related to the expression of the actin gene (Figure 5). Expression of gene ATCC64974\_48070 at  $t = 48$  h was not in line with the proteomics data. In contrast, expression levels of genes ATCC64974\_14700 and ATCC64974\_21820 were 31.36 and 1.95 fold higher, respectively, after 48 h in the small compared to the large micro-colonies. These differences were not yet observed upon transfer of the mycelium of the pre-cultures to MM-X medium. Genes ATCC64974\_58540, ATCC64974\_67930 and ATCC64974\_96170 also showed the expected gene expression after 48 h of culturing with a 7.73-13.87 times higher expression level in large compared to small pellets. Similar results were observed after 12 h with 1.86-7.10 fold differences in gene expression, although the 1.86-fold difference in gene expression of ATCC64974\_67930 was not statistically significant. Together, 5 out of 6 selected genes showed a similar expression level compared to protein abundance in the culture medium after 48 h of culturing.

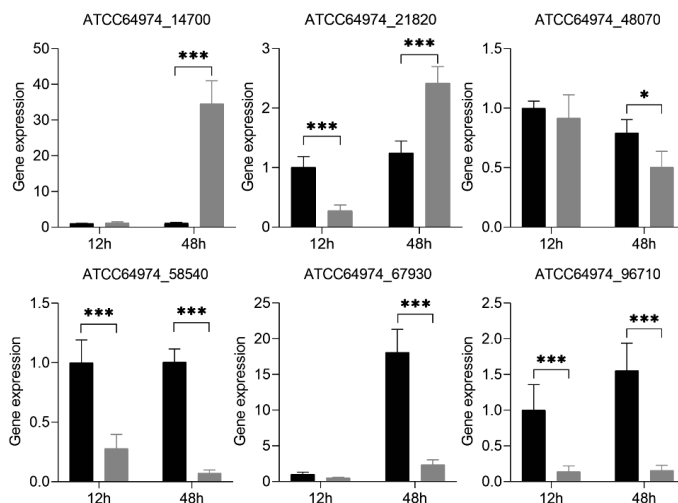


**Figure 5.** Relative gene expression in free spore cultures F12 (black shaded) and bead spore cultures B12 (grey shaded) after 12 h (upon transfer to fresh medium) and 48 h (at the end of culturing). Gene expression in F12 cultures after 12 h was set at 1. \* ( $P < 0.05$ ), \*\* ( $P < 0.01$ ) and \*\*\* ( $P < 0.001$ ) indicate statistical significance. Gene expression was analyzed by t-test. Error bars indicate standard deviations.

### *Cellulase activity in the medium*

Pfam family cellulase was represented by 7 proteins in the set of proteins with a signal sequence in the B6-B16 culture media, while 5 of these proteins were found in the F6-F16 cultures (Table 2). Cellulase activity was compared between the F and B cultures with the same transfer time (e.g. between B6 and F6). Cellulase activity was higher in F6 compared to B6, F8 compared to B8, and F10 compared to B10 (Figure 6A). Next, cellulase activity was measured after mixing culture media of F and B cultures with the same transfer time (i.e. F6 and B6 were mixed, F8 and B8 were mixed, etc) in a 1:1 (v/v) ratio. Notably, the F12/B12 mixture showed higher activity than the activity that was expected from the individual cultures (Figure 6B). The same was observed for the F14/B14 and the F16/B16 mixtures. All these mixtures contained medium of cultures with large and small micro-colonies. In contrast, the B6/F6 and B8/F8 combinations that are made up of media from cultures with large or intermediate micro-colonies only did not show synergistic activity. Together, results show that big and small micro-colonies complement each other's cellulase activity.

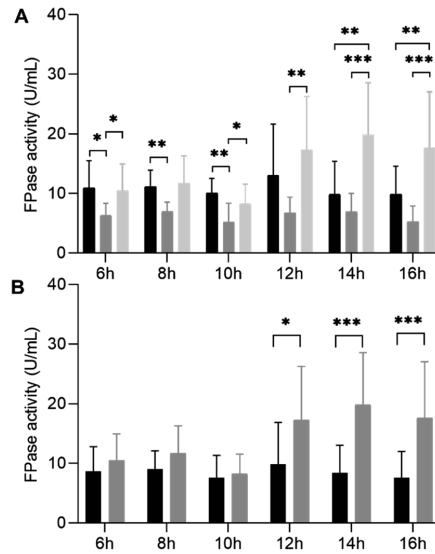


**Figure 6.** Cellulase activity in culture media of free-spore (F) cultures (black shaded bars) and bead-spore (B) cultures (grey shaded bars) or 1:1 mixtures of these culture media after 48 h of culturing (light grey shaded bars) (A). In (B) the predicted cellulase activity in the 1:1 mixed samples (i.e. the average of the free spore and bead spore culture media with the same transfer time) (black shading) is compared with the activity that was actually measured (grey shading). Statistical analysis of cellulase activity was analyzed by a one-way ANOVA, followed by either a Bonferroni or Dunnett's T3 test for multiple comparisons (A) or by either Students' or Welch's t-test (B). \*( $P < 0.05$ ), \*\*( $P < 0.01$ ) and \*\*\*( $P < 0.001$ ) indicate statistical significance. Error bars indicate standard deviations.

## DISCUSSION

Previously, morphology of the mycelium of cell factories like *A. niger* was changed by varying the culture conditions (Cairns et al., 2019). Therefore, changes in yield and secretome composition could have been the result of the changed morphology and / or the changed culture conditions (Krijghsheld et al., 2013; Wösten et al., 2013). Here, we changed the morphology of the mycelium without changing the culture conditions. To this end, conidia were germinated in alginate beads for different periods, after which the beads were dissolved followed by transfer of the mycelium to fresh medium to assess protein secretion. Large micro-colonies ( $\geq 3000 \mu\text{m}$ ) had formed when beads in the pre-cultures had been dissolved after 6 hours (B6 cultures). This size of the micro-colonies was similar to that of the F6-F16 cultures that resulted from spores that had not been embedded in alginate (i.e. free spores). In contrast, pre-culturing

in alginate beads for 10-16 h resulted in small micro-colonies with a diameter of  $285 \pm 8 \mu\text{m}$ . These small micro-colonies had released 556 different proteins in the culture medium, while this number was 208 in the case of the large micro-colonies. In fact, the small micro-colonies did not only release a more diverse palette of proteins, they also secreted higher amounts of a set of proteins that were also released by the large micro-colonies. From this it can be concluded that smaller pellets are more productive with respect to protein secretion. This may be explained by the fact that production of secreted proteins only occurs at the periphery of the micro-colonies in a shell with a relatively constant width (Tegelaar et al., 2020). Of significance, although the large micro-colonies were less effective in protein production, they did release their own unique set of proteins. In fact, cellulase activity of large and small colonies showed synergy when the culture media were combined. We tried to identify regulatory proteins involved in differential protein secretion in large versus small micro-colonies. To this end, cellular proteomics was performed (Supplemental Text 1). This revealed that the carbonic anhydrase protein AacA and the transcription factor ZtfA were higher expressed in large micro-colonies when compared to small micro-colonies. However, inactivation of their encoding genes did not result in changed biomass, micro-colony morphology, or secretome.

About half of the proteins that were released in the medium by the small micro-colonies did not have a signal sequence for secretion, while this was only  $\leq 15\%$  in the case of large micro-colonies. These proteins may be released in the medium by lysis. Aspartyl and serine proteases are regarded as biomarkers of the early stages of autolysis of hyphae (White et al., 2002). These proteins were found in both cultures with large or small micro-colonies. Therefore, these proteases are indicative of a basal level of autolysis that occurs in any liquid shaken culture (McIntyre et al., 2000). The secretomes of the cultures forming small micro-colonies also contained other proteases without signal sequence such as a prolyl oligopeptidase, indicative of a lysis incidence higher than the basal level. It should be noted that microscopy did not reveal lysing hyphae in the cultures. Therefore, proteins without signal sequence may also be released into the medium by a non-classical pathway. Pore-mediated translocation across the plasma membrane (type I), ABC transporter-based secretion (type II) and autophagosome/endosome-based secretion (type III) are non-classical secretion systems in eukaryotes that do not make use of a signal sequence for secretion (Nickel, 2010). It is not known yet whether any of these types is functional in *A. niger*, but evidence has been found for the presence of type III non-classical secretion in yeast (Duran et al., 2010; Manjithaya et al., 2010). Hsp70 is involved in this type of non-classical secretion (Nickel, 2010). Notably, this protein was found in the media of the small micro-colonies. Recently, 51 proteins have

been suggested to be secreted via the non-classical pathway in *A. niger* (Vivek-Ananth et al., 2018), 31 of them were identified in our database (Supplemental Text 2). Of these 31 proteins, 8 proteins did have a signal sequence for secretion. Of the remaining 23 proteins, a total of 13 and 23 were released by large and small micro-colonies, respectively. Together, these data suggest that at least some proteins are released by non-classical secretion.

XlnR is a transcription factor inducing 38 xylanase and cellulase genes (de Souza et al., 2013; Hasper et al., 2000). The cultures with small micro-colonies had released 19-23 of these 38 proteins, while this number was only 15-18 in large micro-colonies. A total of 6 and 1 XlnR-regulated proteins were exclusively found in the media of small and large micro-colonies, respectively. Since the latter micro-colonies exclusively produced a cellobiohydrolase, cellulolytic activity was determined in the culture media. Interestingly, mixing the media of cultures with small micro-colonies and with large micro-colonies resulted in a higher cellulase activity than expected from the activity of the individual cultures. These data are of interest from a biotechnology point of view. If one is interested to highly produce a single protein, one would generally opt to grow small micro-colonies of uniform size, most preferably with a radius  $\leq$  the width of the peripheral expression zone of this particular gene (Tegelaar et al., 2020). Yet, if one is interested in a blend of enzymes, for instance to convert agricultural waste into simple sugars for biofuel or bioplastic production, one would use micro-colonies with heterogeneous size. Such heterogeneity can be obtained by making blends of pre-cultures with micro-colonies of different size. Alternatively, one can use conditions that result in cultures with variable micro-colony size.

The synergy in enzyme activity between small and large micro-colonies as observed in liquid shaken cultures raises the question whether this phenomenon also occurs in nature such as in water droplets on a leaf surface or on rotting fruit (Al-Gashgari et al., 2002). The size of micro-colonies is determined by the extent of spore aggregation. It is tempting to speculate that micro-colonies of different size are formed by stochastic spore aggregation for instance in a water droplet on a leaf surface. In such a case, these micro-colonies would help each other to degrade the plant polymers.

## REFERENCES

- Aerts, D., Bergh, S.G.V.D., Post, H., Altelaar, A.F.M., Arentshorst, M., Ram, A.F.J., Ohm, R.A., Wösten, H.A.B. 2019. FlbA-regulated gene *rpnR* is involved in stress resistance and impacts protein secretion when *Aspergillus niger* is grown on xylose. *Appl Environ Microbiol*, **85**, e02282-18.

- Al-Gashgari, M.G.R., Collage, G. 2002. Occurrence of fungi and pectolytic activity in fruit juices from Saudi Arabia. *Pak J Biol Sci*, **5**, 609-611.
- Bhargava, S., Wenger, K.S., Marten, M.R. 2003. Pulsed addition of limiting-carbon during *Aspergillus oryzae* fermentation leads to improved productivity of a recombinant enzyme. *Biotechnol Bioeng*, **82**, 111-117.
- Bradford, M.M. 1976. A rapid and sensitive method for the quantitation of microgram quantities of protein utilizing the principle of protein-dye binding. *Anal Biochem*, **72**, 248-254.
- Cairns, T.C., Zheng, X., Zheng, P., Sun, J., Meyer, V. 2019. Moulding the mould: understanding and reprogramming filamentous fungal growth and morphogenesis for next generation cell factories. *Biotechnol Biofuels*, **12**, 77.
- Clark, D.S. 1962. Submerged citric acid fermentation of ferrocyanide-treated beet molasses: morphology of pellets of *Aspergillus niger*. *Can J Microbiol*, **8**, 133-136.
- Clark, D.S., Ito, K., Horitsu, H. 1966. Effect of manganese and other heavy metals on submerged citric acid fermentation of molasses. *Biotechnol Bioeng*, **8**, 465-471.
- Cox, J., Neuhauser, N., Michalski, A., Scheltema, R.A., Olsen, J.V., Mann, M. 2011. Andromeda: a peptide search engine integrated into the MaxQuant environment. *J Proteome Res*, **10**, 1794-1805.
- de Bekker, C., van Veluw, G.J., Vinck, A., Wiebenga, L.A., Wösten, H.A.B. 2011. Heterogeneity of *Aspergillus niger* microcolonies in liquid shaken cultures. *Appl Environ Microbiol*, **77**, 1263-1267.
- de Souza, W.R., Maitan-Alfenas, G.P., de Gouvea, P.F., Brown, N.A., Savoldi, M., Battaglia, E., Goldman, M.H., de Vries, R.P., Goldman, G.H. 2013. The influence of *Aspergillus niger* transcription factors AraR and XlnR in the gene expression during growth in D-xylose, L-arabinose and steam-exploded sugarcane bagasse. *Fungal Genet Biol*, **60**, 29-45.
- de Vries, R.P., Burgers, K., van de Vondervoort, P.J., Frisvad, J.C., Samson, R.A., Visser, J. 2004. A new black *Aspergillus* species, *A. vadensis*, is a promising host for homologous and heterologous protein production. *Appl Environ Microbiol*, **70**, 3954-3959.
- Delgado-Ramos, L., Marcos, A.T., Ramos-Guelfo, M.S., Sanchez-Barrionuevo, L., Smet, F., Chavez, S., Canovas, D. 2014. Flow cytometry of microencapsulated colonies for genetics analysis of filamentous fungi. *G3 (Bethesda)*, **4**, 2271-2278.
- Duran, J.M., Anjard, C., Stefan, C., Loomis, W.F., Malhotra, V. 2010. Unconventional secretion of Acb1 is mediated by autophagosomes. *J Cell Biol*, **188**, 527-536.



- El-Gebali, S., Mistry, J., Bateman, A., Eddy, S.R., Luciani, A., Potter, S.C., Qureshi, M., Richardson, L.J., Salazar, G.A., Smart, A., Sonnhammer, E.L.L., Hirsh, L., Paladin, L., Piovesan, D., Tosatto, S.C.E., Finn, R.D. 2019. The Pfam protein families database in 2019. *Nucleic Acids Res*, **47**, D427-D432.
- Hasper, A.A., Visser, J., de Graaff, L.H. 2000. The *Aspergillus niger* transcriptional activator XlnR, which is involved in the degradation of the polysaccharides xylan and cellulose, also regulates D-xylose reductase gene expression. *Mol Microbiol*, **36**, 193-200.
- Hille, A., Neu, T.R., Hempel, D.C., Horn, H. 2009. Effective diffusivities and mass fluxes in fungal biopellets. *Biotechnol Bioeng*, **103**, 1202-1213.
- Krijghsheld, P., Altelaar, A.F., Post, H., Ringrose, J.H., Muller, W.H., Heck, A.J., Wösten, H.A. B. 2012. Spatially resolving the secretome within the mycelium of the cell factory *Aspergillus niger*. *J Proteome Res*, **11**, 2807-2818.
- Krijghsheld, P., Bleichrodt, R., van Veluw, G.J., Wang, F., Muller, W.H., Dijksterhuis, J., Wösten, H.A.B. 2013. Development in *Aspergillus*. *Stud Mycol*, **74**, 1-29.
- Lu, X., Sun, J.B., Nimtz, M., Wissing, J., Zeng, A.P., Rinas, U. 2010. The intra- and extracellular proteome of *Aspergillus niger* growing on defined medium with xylose or maltose as carbon substrate. *Microb Cell Fact*, **9**, 13.
- Manjithaya, R., Anjard, C., Loomis, W.F., Subramani, S. 2010. Unconventional secretion of *Pichia pastoris* Acb1 is dependent on GRASP protein, peroxisomal functions, and autophagosome formation. *J Cell Biol*, **188**, 537-546.
- Martinez, D., Berka, R.M., Henrissat, B., Saloheimo, M., Arvas, M., Baker, S.E., Chapman, J., Chertkov, O., Coutinho, P.M., Cullen, D., Danchin, E.G., Grigoriev, I.V., Harris, P., Jackson, M., Kubicek, C.P., Han, C.S., Ho, I., Larrondo, L.F., de Leon, A.L., Magnuson, J.K., Merino, S., Misra, M., Nelson, B., Putnam, N., Robbertse, B., Salamov, A.A., Schmoll, M., Terry, A., Thayer, N., Westerholm-Parvinen, A., Schoch, C.L., Yao, J., Barabote, R., Nelson, M.A., Detter, C., Bruce, D., Kuske, C.R., Xie, G., Richardson, P., Rokhsar, D.S., Lucas, S.M., Rubin, E.M., Dunn-Coleman, N., Ward, M., Brettin, T.S. 2008. Genome sequencing and analysis of the biomass-degrading fungus *Trichoderma reesei* (*syn. Hypocrea jecorina*). *Nat Biotechnol*, **26**, 553-560.
- McIntyre, M., Berry, D.R., McNeil, B. 2000. Role of proteases in autolysis of *Penicillium chrysogenum* chemostat cultures in response to nutrient depletion. *Appl Microbiol Biotechnol*, **53**, 235-242.
- Meyer, V., Wu, B., Ram, A.F. 2011. *Aspergillus* as a multi-purpose cell factory: current status and perspectives. *Biotechnol Lett*, **33**, 469-476.

- Nickel, W. 2010. Pathways of unconventional protein secretion. *Curr Opin Biotechnol*, **21**, 621-626.
- Park, J., Hulsman, M., Arentshorst, M., Breeman, M., Alazi, E., Lagendijk, E.L., Rocha, M.C., Malavazi, I., Nitsche, B.M., van den Hondel, C.A., Meyer, V., Ram, A.F. 2016. Transcriptomic and molecular genetic analysis of the cell wall salvage response of *Aspergillus niger* to the absence of galactofuranose synthesis. *Cell Microbiol*, **18**, 1268-1284.
- Petersen, T.N., Brunak, S., von Heijne, G., Nielsen, H. 2011. SignalP 4.0: discriminating signal peptides from transmembrane regions. *Nat Methods*, **8**, 785-786.
- Tegelaar, M., Aerts, D., Teertstra, W.R., Wösten, H.A.B. 2020. Spatial induction of genes encoding secreted proteins in micro-colonies of *Aspergillus niger*. *Sci Rep*, **10**, 1536.
- van Veluw, G.J., Teertstra, W.R., de Bekker, C., Vinck, A., van Beek, N., Muller, W.H., Arentshorst, M., van der Mei, H.C., Ram, A.F., Dijksterhuis, J., Wösten, H.A.B. 2013. Heterogeneity in liquid shaken cultures of *Aspergillus niger* inoculated with melanised conidia or conidia of pigmentation mutants. *Stud Mycol*, **74**, 47-57.
- Vinck, A., Terlouw, M., Pestman, W.R., Martens, E.P., Ram, A.F., van den Hondel, C.A., Wösten, H.A.B. 2005. Hyphal differentiation in the exploring mycelium of *Aspergillus niger*. *Mol Microbiol*, **58**, 693-699.
- Vivek-Ananth, R.P., Mohanraj, K., Vandanasree, M., Jhingran, A., Craig, J.P., Samal, A. 2018. Comparative systems analysis of the secretome of the opportunistic pathogen *Aspergillus fumigatus* and other *Aspergillus* species. *Sci Rep*, **8**, 6617.
- White, S., McIntyre, M., Berry, D.R., McNeil, B. 2002. The autolysis of industrial filamentous fungi. *Crit Rev Biotechnol.*, **22**, 1-14.
- Wösten, H.A.B. 2019. Filamentous fungi for the production of enzymes, chemicals and materials. *Curr Opin Biotechnol*, **59**, 65-70.
- Wösten, H.A.B., van Veluw, G.J., de Bekker, C., Krijgsheld, P. 2013. Heterogeneity in the mycelium: implications for the use of fungi as cell factories. *Biotechnol Lett*, **35**, 1155-1164.
- Xiao, Z., Storms, R., Tsang, A. 2004. Microplate-based filter paper assay to measure total cellulase activity. *Biotechnol Bioeng*, **88**, 832-837.

## SUPPLEMENTAL MATERIAL

**Supplemental Table 1.** Primers used in this study.

Primer	Sequence
actFwd	GTTGCTGCTCTCGTCATT
actRev	AACCGGCCTTGACATA
14700Fwd	AGAAGATCCTAAGCAAGCGA
14700Rev	ATTGATGGAAGCCGAAAGTC
21820Fwd	GAGCAAGTCATGTTCCAACC
21820Rev	GAGGTACGAGAAGAGACGG
48070Fwd	CCGTTCCCTCTACCTTCGT
48070Rev	ATCGTGTTCGCCTGACTC
58540Fwd	GTACCACCGTCATCTTCGAG
58540Rev	CGCAGTTGATCTTGGCAC
96170Fwd	CCAAGCTGATCCTCTCCTCC
96170Rev	GCACCGTACCAGTAGACCT
67930Fwd	CGATACCAACAACGAGTACC
67930Rev	TAGTCCAGTCCCAGGCA

**Supplemental Table 2.** Quantity (average and standard deviation) of proteins from free spore (F) and bead spore (B) cultures. Numbers following F and B indicate the time of pre-culturing.

[https://docs.google.com/spreadsheets/d/1R9-wNcnKRDhT0QAOpIF7YZ-n\\_JVYSIPb/edit?usp=sharing&oid=100415537618493008153&rtpof=true&sd=true](https://docs.google.com/spreadsheets/d/1R9-wNcnKRDhT0QAOpIF7YZ-n_JVYSIPb/edit?usp=sharing&oid=100415537618493008153&rtpof=true&sd=true).

**Supplemental Table 3.** Proteins shared in the culture media of free spore cultures F6-F16 and bead spore cultures B6-B16 (A) and proteins found in free spore cultures F6-16 not found in bead cultures B6-B16 (B).

<https://docs.google.com/spreadsheets/d/1grFvZk5EBPC7DHmQFhQTYhPbK2zeqOud/edit?usp=sharing&oid=100415537618493008153&rtpof=true&sd=true>.

**Supplemental Table 4.** Fold changes of proteins found in B cultures when compared to F cultures that had been transferred at the same time point.

<https://docs.google.com/spreadsheets/d/1yb99-LUy8Dg14AY5VkJKouQVYqylb-ovs/edit?usp=sharing&oid=100415537618493008153&rtpof=true&sd=true>.

**Supplemental Table 5.** Proteins found in bead spore cultures B6-B16 not found in free cultures F6-F16 (A) and proteins found in cultures of small micro-colonies (B10-B16) not found in cultures of large micro-colonies (F6-16, B6-8) (B).

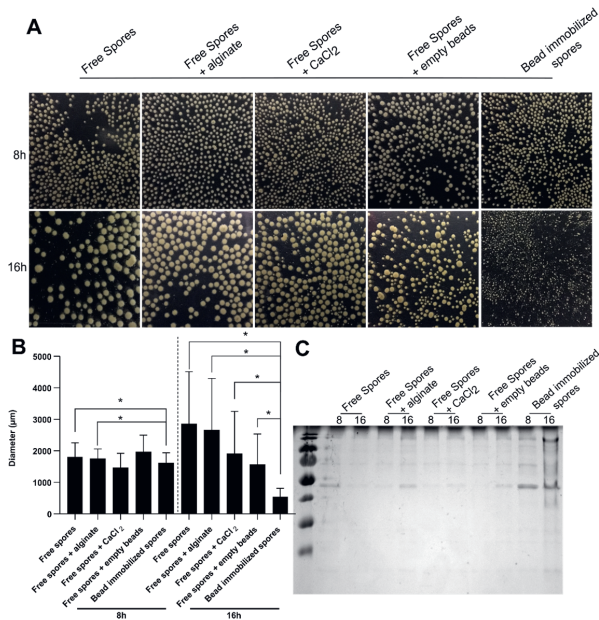
<https://docs.google.com/spreadsheets/d/1JaTUqLOHyq0rIW9BS6Mua2dtO2o0QTVx/edit?usp=sharing&oid=100415537618493008153&rtpof=true&sd=true>.

**Supplemental Table 6.** Proteins with (A) and without (B) signal sequences for secretion identified in liquid shaken cultures that had been inoculated with mycelium of free (F) or bead (B) spores pre-cultures.

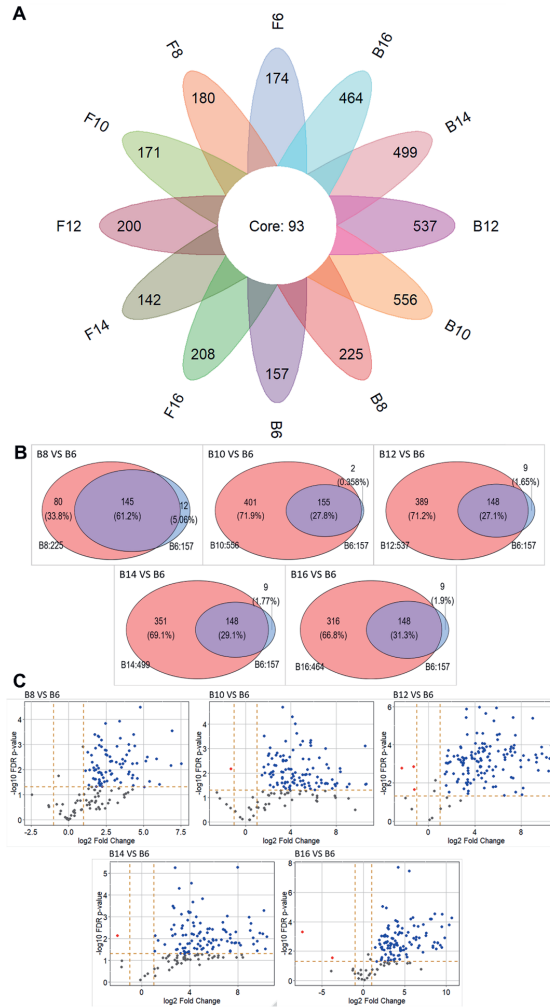
<https://docs.google.com/spreadsheets/d/1o7Gfbw2VU5QFLpt8nB9SdwblOOsU1xAs/edit?usp=sharing&oid=100415537618493008153&rtpof=true&sd=true>.

**Supplemental Table 7.** Proteins that are only highly expressed in cultures with large (B6-8,F6-16) or small micro-colonies (B10-B16).

<https://docs.google.com/spreadsheets/d/1ZJ36cMYJWSM1WwR0Bc4DXJhMytXqZIS7/edit?usp=sharing&oid=100415537618493008153&rtpof=true&sd=true>.



**Supplemental Figure 1.** Morphology of mycelium (A, B) and proteins released in the culture medium (C) from free spore cultures F8 and F16, to which either or not empty beads, alginate or CaCl<sub>2</sub> had been added. Bead spore cultures B8 and B16 served as a control. The beads had been dissolved after 8 h or 16 h of pre-culturing in TM-X and mycelium of the B and F pre-cultures was transferred to MM-X for 40 and 32 h, respectively, for a total culturing time of 48 h. Statistical analysis in B was performed with a t-test or Welch's t-test.



**Supplemental Figure 2.** (A) Flower plot of proteins from free spore (F) and bead spore (B) cultures. The beads had been dissolved after 6-16 h of pre-culturing (indicated by the numbers following B) and culturing was extended for 42-32 h after transfer of the mycelium to have a total culturing time of 48 h. Total number of proteins not being part of the core are indicated in the leaves of the flower plot. (B, C) Pairwise comparison of number (B) and quantity (C) of proteins from bead spore B6 cultures with B8, B10, B12, B14 and B16 cultures. Proteins were analyzed after a total culturing time of 48 h. The number following B indicates the time of pre-culturing in hours. Red and blue dots indicate proteins that were  $\geq 2$  fold up- or down-regulated in B6 cultures when compared to the other B cultures.

**Supplemental Text 1.**

Cellular proteomics was performed to identify proteins that are differentially expressed in large and small micro-colonies. Two genes encoding such proteins were deleted but their phenotype was not different from the wild-type strain.

**Material and Methods***Cellular proteomics*

Cellular proteomics was performed as described in **Chapter 5**. The R package DESeq2 was used to calculate differential protein abundance. The Benjamini-Hochberg correction was used to reduce false positives at p-value  $\leq 0.05$ .

**Suppl Text 1 Table 1.** sgRNA sequences used in this study.

sgRNA	Sequence
Sg25	ATTGCCGACGAGAATCCCA
Sg26	GGGGACAGCAGTGTAGGTG
Sg27	TCTGGTCAGGCACTCCGCG
Sg28	CTCCACCAATCAGCGATGCG

*Gene inactivation*

Genes were inactivated as described in **Chapter 5**. SgRNAs sg25 and sg26 were used for inactivation of the carbonic anhydrase gene *caaA* (ATCC64974\_10520), while sg27 and sg28 were used to inactivate the Zn(2)-C6 fungal-type domain transcription factor gene *ztfA* (ATCC64974\_49970) (Suppl Text 1 Table 1). These sgRNAs produce a double cut 130 and 138 bp before the start codon of *caaA* and *ztfA* and 264 and 74 bp after the stop codon of these genes, respectively. The sgRNAs were expressed under control of the proline tRNA III promoter and terminator in plasmid pMT12.5 (Suppl Text 1 Table 2). This plasmid is a derivative of pFC332 that contains the *cas9* gene, a hygromycin resistance cassette (Nodvig et al., 2018; Suppl Text 1 Table 2), and the GFP gene under control of the proline tRNA promoter and terminator. The sgRNAs (primer pair 1/2 and 3/4 for up- and down-cut sgRNA of *caaA*, 8/9 and 10/11 for up- and down-cut sgRNA of *ztfA*, respectively; Suppl Text 1 Table 3) were cloned in pMT12.5 by digestion with BtsI that removes the *GFP* coding sequence. This resulted in plasmids pJL025, pJL026, pJL027 and pJL028, respectively (Suppl Text 1 Table 2). Plasmid pair pJL025 and pJL026 and pJL027 and pJL028 were introduced in *A. niger* MA234.1 combined with the repair oligos RO001 and RO002 for *caaA* and *ztfA* (Suppl Text 1 Table 3), respectively. Gene deletions were confirmed by PCR using genomic DNA of strain MA234.1 and the transformants as template and the primers described in Suppl Text 1 Table 3. Primer pair 6/7 was designed to give a 2571 bp fragment in the wild-type and a 1024 bp fragment in the *caaA* deletion strain, while primer pair 13/14 was designed to give a 2444 bp fragment in the wild-type and a 937 bp fragment in the *ztfA* deletion strain.

**Suppl Text 1 Table 2.** Plasmids used in this study

Plasmid	Description	Reference
pFC332	contains <i>cas9</i> , a hygromycin resistance cassette and a PacI site for introducing the sgRNA	Nodvig et al., 2018
pMT12.5	Derivative of pFC322 in which the proline tRNA promoter and terminator flank <i>GFP</i>	Unpublished
pJL025	Derivative of pMT12.5 containing the upstream <i>caaA</i> sgRNA	This study
pJL026	Derivative of pMT12.5 containing the downstream <i>caaA</i> sgRNA	This study
pJL027	Derivative of pMT12.5 containing the upstream <i>ztfA</i> sgRNA	This study
pJL028	Derivative of pMT12.5 containing the downstream <i>ztfA</i> sgRNA	This study

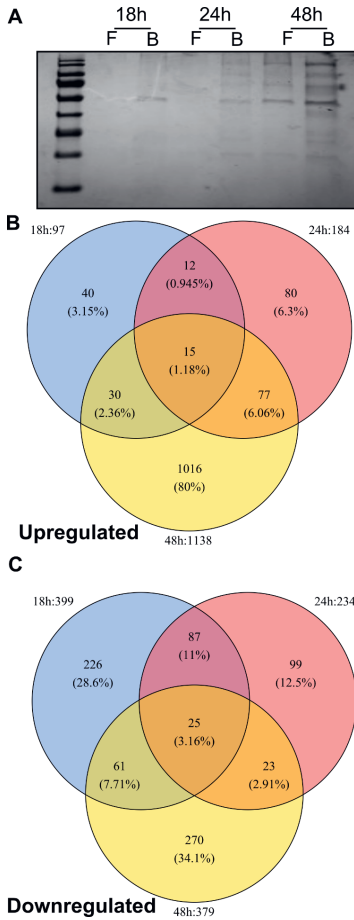
**Suppl Text 1 Table 3.** Primers used in this study

Primer name	Sequence
1. <i>caaA</i> .Uc.Fwd	ATTGCCGACGAGAATCCCCAGT
2. <i>caaA</i> .Uc.Rev	TGGGGATTCTCGTCGGCAATGA
3. <i>caaA</i> .Dc.Fwd	GGGGACAGCAGTGTAGGTGGT
4. <i>caaA</i> .Dc.Rev	CACCTAACACTGCTGTCCCCGA
5. RO001	TGCACTGTTTCATGGTTGGGGGTGAGCATTGCCGACGAGAATCCTAGGGATAACAGGGTAATGG GGGGTGTGGAGTCAAGGAATCAATAGTAGCAGTGAGGAAGAAAGTAGA
6. <i>caaA</i> .Cf.Fwd	CCCTGTGACTTTACAGACTA
7. <i>caaA</i> .Cf.Rev	GAGAGATAGTTGTAGTCGA
8. <i>ztfA</i> .Uc.Fwd	TCTGGTCAGGCACTCCCGCGGT
9. <i>ztfA</i> .Uc.Rev	CGCGGGAGTGCCTGACCAGAGA
10. <i>ztfA</i> .Dc.Fwd	CTCCACCAATCAGCGATGCGGT
11. <i>ztfA</i> . Dc.Rev	CGCATCGCTGATTGGTGAGGA
12. RO002	ATATAGCTGGCTTCCGATTAGGATTAGTCTGGTCAGGCACTCCCTAGGGATAACAGGGTAATGGG GGGCGGGGAACGTAGATGCCTGGATGCTGAGGCCGAGCCTCGTCGTG
13. <i>ztfA</i> .Cf.Fwd	CGATGAATGCTCCTGGACCC
14. <i>ztfA</i> .Cf.Rev	TGGTGCAGGAGCATGGACAG

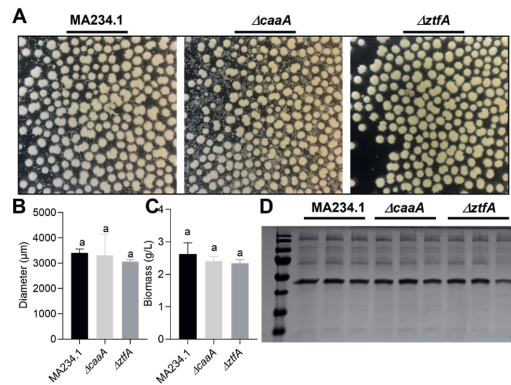
## Results

Cellular proteomics of F12 and B12 cultures was performed to assess which proteins are up- and down-regulated in large and small micro-colonies, respectively. SDS PAGE showed that differences in the secretome started to be visible 18 h after culturing (12 h pre-culturing in TM-X followed by 6 h culturing in MM-X) and became more pronounced in time (Suppl Text 1 Figure 1A). Therefore, it was decided to perform cellular proteomics after 18, 24 and 48 h of culturing. A set of 97 and 399 proteins were significantly up- and down-regulated in small and large micro-colonies, respectively, after 18 h of culturing, while these values were 184 and 234 after 24 h and 1138 and 379 after 48 h of culturing. Among these proteins, 15 and 25 were up- and down-regulated at all three time points in small when compared to large micro-colonies (Suppl Text 1 Figure 1BC, Suppl Text 1 Table 4), respectively. The carbonic anhydrase gene *caaA* (ATCC64974\_10520) was identified as one of the significantly downregulated proteins in small micro-colonies at all three time points. Its encoding protein catalyzes the reversible conversion of CO<sub>2</sub> to HCO<sub>3</sub><sup>-</sup> and as such is involved in the formation of the second messenger cAMP. Also, *caaA* is predicted as co-expressed with the  $\alpha$ -1,3-glucan synthase gene *agsE* (ATCC64974\_10510) with a correlation of 0.85 (fungiDB). Indeed, in **Chapter 5** it is shown that inactivation of *agsE* resulted in small micro-colonies and reduced expression of *caaA*. This raised the question what the effect would be of inactivation of *caaA* on micro-colony morphology and the secretome. In addition, a transcription factor was selected that was differentially expressed at all three time points (this in contrast to all other differentially expressed transcription factors; Suppl Text 1 Table 5). This Zn(2)-C6 fungal-type domain-containing transcription factor protein ZtfA (ATCC64974\_49970) was higher expressed in large micro-colonies (resulting from free spores) at time points 18 h and 24 h, while it was downregulated at timepoint 48 h (only identified in 2 out of 4 replicates in B48, therefore not regarded as expressed at this time point). Both *caaA* and *ztfA* deletion strains did not show any phenotype with respect to biomass, micro-colony morphology and secretome (Suppl Text 1 Figure 2).





**Suppl Text 1 Figure 1.** Protein profiles of the culture media of F12 and B12 cultures that had formed large and small micro-colonies, respectively, 18, 24 and 48 h after transfer to MM-X (A). Venn diagrams showing proteins that are significantly up- (B) and down- (C) regulated in B12 versus F12 cultures at all time points (i.e. after 18, 24, and 48 h of culturing).



**Suppl Text 1 Figure 2.** Morphology (A), diameter (B), biomass (C) and SDS PAGE of proteins in the culture medium (D) of strain MA234.1,  $\Delta caaA$  and  $\Delta ztfA$ . Different letters indicate statistical differences (B,C) as determined by a one-way ANOVA combined with a Dunnett's T3 post-hoc test for diameter and a Games-Howell post-hoc test for biomass. Error bars indicate standard deviation.

**Suppl Text 1 Table 4.** Protein family analysis of the proteins that were up- and down-regulated in cultures of small micro-colonies compared to large micro-colonies at time points 18, 24 and 48 h.

Protein ID	PFAM	Annotation
<b>Significant upregulated proteins</b>		
ATCC64974_104630	PF00248	Aldo/keto reductase family
ATCC64974_109280	PF00107	Zinc-binding dehydrogenase
ATCC64974_109480	PF05362	Lon protease (S16) C-terminal proteolytic domain
ATCC64974_14700	PF01055	Glycosyl hydrolases family 31
ATCC64974_26850	PF13714	Phosphoenolpyruvate phosphomutase
ATCC64974_27560	PF01408	Oxidoreductase family, NAD-binding Rossmann fold
ATCC64974_35130	PF00568	WH1 domain
ATCC64974_47770	PF18404	Glucosyltransferase 24
ATCC64974_63220	PF00106	short chain dehydrogenase
ATCC64974_64650	PF00561	alpha/beta hydrolase fold
ATCC64974_80810	PF12110	Nuclear protein 96
ATCC64974_95010	PF00171	Aldehyde dehydrogenase family
ATCC64974_96990	PF00083	Sugar (and other) transporter
ATCC64974_7980	PF01042	Endoribonuclease L-PSP
ATCC64974_28350	PF01077	Nitrite and sulphite reductase 4Fe-4S domain
<b>Significant downregulated proteins</b>		
ATCC64974_10520	PF00484	Carbonic anhydrase
ATCC64974_108150	PF00203	Ribosomal protein S19
ATCC64974_110190	PF02114	Phosducin
ATCC64974_12930	PF00270	DEAD/DEAH box helicase
ATCC64974_1450	PF00076	RNA recognition motif. (a.k.a. RRM, RBD, or RNP domain)
ATCC64974_17780	PF13344	Haloacid dehalogenase-like hydrolase
ATCC64974_25810	#N/A	#N/A
ATCC64974_26440	PF11563	Protoglobin
ATCC64974_3500	PF13041	PPR repeat family
ATCC64974_37420	PF00962	Adenosine/AMP deaminase
ATCC64974_3930	PF00026	Eukaryotic aspartyl protease
ATCC64974_50990	PF00022	Actin
ATCC64974_51730	PF00735	Septin
ATCC64974_56970	PF05046	Mitochondrial large subunit ribosomal protein (Img2)
ATCC64974_64890	PF01937	Protein of unknown function DUF89
ATCC64974_65560	PF01912	eIF-6 family
ATCC64974_670	PF08611	Fungal protein of unknown function (DUF1774)
ATCC64974_73840	PF08491	Squalene epoxidase
ATCC64974_77310	PF03795	YCII-related domain
ATCC64974_79720	PF06201	PITH domain
ATCC64974_89170	PF02752	Arrestin (or S-antigen), C-terminal domain
ATCC64974_97840	PF00155	Aminotransferase class I and II
ATCC64974_67810	#N/A	#N/A
ATCC64974_35260	PF01849	NAC domain
ATCC64974_32430	PF02826	D-isomer specific 2-hydroxyacid dehydrogenase, NAD binding domain

**Suppl Text 1 Table 5.** Transcription factor analysis of the proteins which identified as significantly up- or downregulated in small micro-colonies compared to large micro-colonies at least in different timepoint. Transcription factors were identified using the Fungal transcription factor database (FTFD, <http://ftfd.snu.ac.kr/intro.php>) (Park et al., 2008).

Protein ID	Annotation
<b>B18vsF18 up</b>	--
<b>B18vsF18 down</b>	
ATCC64974_49970	Fungal Specific TF; Zn(2)-C6 fungal-type domain-containing protein
ATCC64974_69840	CCR4-Not complex component, Not1; regulation of translation
<b>B24vsF24 up</b>	
ATCC64974_96430	Fungal Specific TF; CN hydrolase domain-containing protein
<b>B24vsF24 down</b>	
ATCC64974_49970	Fungal Specific TF; Zn(2)-C6 fungal-type domain-containing protein
ATCC64974_6340	Fungal Specific TF; Zn(2)-C6 fungal-type domain-containing protein
ATCC64974_39350	Zinc finger, CCHC-type
<b>B48vsF48 up</b>	
ATCC64974_100170	Fungal Specific TF; Pyridine nucleotide-disulfide oxidoreductase family protein
ATCC64974_17730	Fungal Specific TF; Zn(2)-C6 fungal-type domain-containing protein
ATCC64974_28300	Fungal Specific TF; Zn(2)-C6 fungal-type domain-containing protein
ATCC64974_3940	Fungal Specific TF; Vps16, N-terminal region family protein
ATCC64974_49970	Fungal Specific TF; Zn(2)-C6 fungal-type domain-containing protein
ATCC64974_54630	Fungal Specific TF; Carboxylesterase family protein
ATCC64974_55290	Zinc finger, PARP-type; PARP-type domain-containing protein
ATCC64974_58300	Histone-like TF; Histone H4
ATCC64974_6340	Fungal Specific TF; Zn(2)-C6 fungal-type domain-containing protein
ATCC64974_80200	UAF complex subunit Rm10
ATCC64974_81740	Homeodomain
ATCC64974_8490	AT-rich interaction region; Nin one binding (NOB1) Zn-ribbon like family protein
ATCC64974_89080	Fungal Specific TF; Zn(2)-C6 fungal-type domain-containing protein
ATCC64974_93520	Fungal Specific TF; Fasciclin domain family protein
ATCC64974_95320	Helix-turn-helix; Transcription elongation factor Spt6
ATCC64974_52880	Helix-turn-helix; Multiprotein-bridging factor 1
ATCC64974_39350	Zinc finger, CCHC-type
<b>B48vsF48 down</b>	
ATCC64974_74060	Helix-loop-helix; BHLH domain-containing protein
ATCC64974_56760	HMG; ARID/BRIGHT DNA binding domain family protein
ATCC64974_93680	Fungal Specific TF; Fungal_trans domain-containing protein
ATCC64974_20230	HMG; HMG box domain-containing protein
ATCC64974_21020	Histone-like +A1:B41TF; CBFD_NFYB_HMF domain-containing protein

## References

- Nodvig, C.S., Hoof, J.B., Kogle, M.E., Jarczynska, Z.D., Lehmbeck, J., Klitgaard, D.K., Mortensen, U.H. 2018. Efficient oligo nucleotide mediated CRISPR-Cas9 gene editing in *Aspergilli*. *Fungal Genet Biol*, **115**, 78-89.

Park, J., Park, J., Jang, S., Kim, S., Kong, S., Choi, J., Ahn, K., Kim, J., Lee, S., Kim, S., Park, B., Jung, K., Kim, S., Kang, S., Lee, Y.H. 2008. FTFD: an informatics pipeline supporting phylogenomic analysis of fungal transcription factors. *Bioinformatics*, **24**, 1024-1025.

### Supplemental Text 2.

The secretome of *A. niger* of the different cultures was compared to the Aspertome database (<https://cb.imsc.res.in/aspertome/home>) (Vivek-Ananth et al., 2018). This database suggests that 31 proteins are secreted by the non-classical pathway (Suppl Text 2 Table 1), of which 23 without a signal sequence for secretion. Of the 31 proteins, 24 were only found in the bead spore cultures, while 13 were only present in cultures with small micro-colonies (i.e.  $\geq 10$  h bead spore cultures).

**Suppl Text 2 Table 1.** Proteins in the bead and free spore cultures that have been described to be secreted by the non-classical pathway in *Aspergilli*.

Protein ID	Gene	Annotation	Identified in
<b>Proteins with signal sequence</b>			
ATCC64974_1620		Alpha galactosidase A	F6-F16, B6-B16
ATCC64974_27940		Eukaryotic aspartyl protease	F6-F16, B6-B16
ATCC64974_67820		Uncharacterized protein	F8-F16, B6-B16
ATCC64974_106110		SMP-30/Gluconolactonase/LRE-like region	F6-F10, F16, B6-B16
ATCC64974_109710	<i>tilA</i>	Multicopper oxidase	B8-B16
ATCC64974_91770		GH family 3 C-terminal domain	B10-B16
ATCC64974_48710		GH family 76	B10-B16
ATCC64974_33160		Uncharacterized protein	B10-B16
<b>Proteins without signal sequence</b>			
ATCC64974_79660	<i>apsA</i>	lysine aminopeptidase ApsA	B6-B16
ATCC64974_100780	<i>aldA</i>	Aldehyde dehydrogenase family	B10-B12, B16
ATCC64974_8440	<i>ndk1</i>	Nucleoside diphosphate kinase	B10-B16
ATCC64974_66140	<i>ssb2</i>	Hsp70 protein	F16, B10-B16
ATCC64974_87920	<i>alrA</i>	Aldo/keto reductase family	B6, B10-B16
ATCC64974_93080		Domain of unknown function (DUF4965)	B10-B14
ATCC64974_79340		Enoyl-(Acyl carrier protein) reductase	B12, B16

ATCC64974_12090	<i>leu2A</i>	Isocitrate/isopropylmalate dehydrogenase	B10-B14
ATCC64974_61280	<i>tpiA</i>	Triosephosphate isomerase	B10-B14
ATCC64974_54170		Arylsulfotransferase (ASST) family protein	B10-B16
ATCC64974_27170		Thioredoxin	B6-B16
ATCC64974_53350		GH family 38 N-terminal domain	B6-B16
ATCC64974_10730		Prolyl oligopeptidase family	B10-B16
ATCC64974_76670		Peptidase family M49	B8-B16
ATCC64974_7620		ERAP1-like C-terminal domain	B8-B16
ATCC64974_105620		Aminotransferase class-V	B6, B10-B16
ATCC64974_84190		TAP-like protein	B10-B16
ATCC64974_23160		Eukaryotic aspartyl protease	F6, F10-F16, B6-B16
ATCC64974_109650		Serine aminopeptidase, S33	F8-F12, F16, B6-B16
ATCC64974_3650		GH family 92	B8-B16
ATCC64974_69070	<i>ssc1</i>	Hsp70 protein	B8-B16
ATCC64974_68870	<i>pgi1</i>	Phosphoglucose isomerase	B8-B16
ATCC64974_85000	<i>glr1</i>	Pyridine nucleotide-disulphide oxidoreductase	B10-B16

## References

- Vivek-Ananth, R.P., Mohanraj, K., Vandanashree, M., Jhingran, A., Craig, J.P., Samal, A. 2018. Comparative systems analysis of the secretome of the opportunistic pathogen *Aspergillus fumigatus* and other *Aspergillus* species. *Sci Rep*, **8**, 6617.

## **Chapter 3**

**Colony size impacts stress survival in**

*Aspergillus niger*

## ABSTRACT

The fungus *Aspergillus niger* forms micro-colonies of different size in nature as well as in industrial bioreactors. These micro-colonies result from germination of spores. Recently, it was reported that small and large micro-colonies secrete different enzymes into the culture medium that act synergistically in breakdown of a natural substrate. This synergism could therefore play an important role in nature in effective nutrient cycling in an aqueous environment. Results also showed that the small micro-colonies secrete a more diverse palette and a higher quantity of proteins. On the other hand, we here show that the large micro-colonies are more resistant to heat and hydrogen peroxide stress. Experimental data indicate that this higher resistance is due to the presence of non-germinated spores in the centre of large micro-colonies (and that are absent in small micro-colonies) and by the protection of these spores and hyphae in the centre by hyphae at the micro-colony periphery. Together, *A. niger* improves its fitness by forming micro-colonies that are heterogeneous in size.

## INTRODUCTION

*Aspergillus niger* is among the most abundant fungi worldwide. It is a saprotrophic fungus that degrades dead organic material but it can also infect plants and immune-compromised animals and humans (Krijgsheld et al., 2013). To this end, *A. niger* secretes a wide variety of metabolites such as organic acids and enzymes. The organic acids reduce the pH of the environment thus inhibiting bacterial growth, while the enzymes degrade the polymers in the substrate into breakdown products that can be taken up by the fungus to serve as nutrients. The high secretion capacity makes *A. niger* one of the main cell factories for industrial protein and organic acid production (Wösten, 2019).

Germination of conidia of *A. niger* results in a network of hyphae. This mycelium can exist as small ( $\pm 300 \mu\text{m}$ ) or large ( $> \pm 1500 \mu\text{m}$ ) microcolonies (**Chapter 2**) even within a single liquid culture (de Bekker et al., 2011; van Veluw et al., 2013). This size difference is due to a different degree of aggregation of conidia and germlings in the culture medium (Metz et al., 1977; Carlsen et al., 1996; Yoshimi et al., 2013). It was recently shown that small micro-colonies produce more protein than large micro-colonies (**Chapter 2**). This can be explained by the fact that genes encoding secreted proteins are expressed in a shell at the outer part of the micro-colony (Tegelaar et al., 2020). As a consequence, highest productivity of a micro-colony is obtained when its radius is  $\leq$  the width of the outer expression zone. Yet, the large micro-colonies produce enzyme activities not secreted by the small micro-colonies. As a

consequence, cellulase activity is higher in a mixture of the culture medium of small and large micro-colonies when compared to the individual culture media (**Chapter 2**). Thus, formation of different-sized micro-colonies is a strategy to produce a meta-secretome optimally suited to degrade complex substrates not only in bioreactors but potentially also in nature, for instance in water droplets on a leaf surface or on rotting fruit (Al-Gashgari et al., 2002). We here show that the large micro-colonies are more resistant to heat and hydrogen peroxide when compared to small micro-colonies. Together, small micro-colonies secrete the bulk of the secreted proteins, while large micro-colonies secrete complementary enzyme activities and are more stress resistant. Formation of different sized micro-colonies thus may have evolved to promote survival of *A. niger* in nature.

## MATERIAL AND METHODS

### *Strains and growth conditions*

*Aspergillus niger* strain MA234.1 (Park et al., 2016) and strain AR9#2 that expresses *GFP* from the *glaA* promoter (Siedenberg et al., 1999) were used in this study. These strains were grown for 72 h on minimal medium (MM) (de Vries et al., 2004) with 1% glucose and 1.5% agarose (MM-GA) at 30 °C. Spores were harvested in 5 ml saline-Tween (0.8% NaCl, 0.005% Tween-80) and filtered through cotton to remove hyphae. Spores were counted using a haemocytometer, diluted and stored at 4 °C for a maximum of 4 weeks.

Micro-colonies were produced from conidia or from mycelium. In the former case *A. niger* was grown in 250 ml Erlenmeyer flasks with 50 ml transformation medium (TM; MM with 5 g l<sup>-1</sup> yeast extract and 2 g l<sup>-1</sup> casamino acids; adjusted to pH 6 with NaOH) using 25 mM xylose as a carbon source (TM-X). To this end, cultures were inoculated with 2.5 10<sup>6</sup> spores ml<sup>-1</sup> that were either or not taken up in 700 µm alginate beads (**Chapter 2**) and grown at 30 °C and 200 rpm. Conidia were embedded in alginate beads by introducing a 4% Na-alginate solution with 2.5 10<sup>6</sup> spores ml<sup>-1</sup> into a 3% aqueous solution of CaCl<sub>2</sub>·2H<sub>2</sub>O by using a dropping device (Delgado-Ramos et al., 2014) using a 40 cm<sup>3</sup> min<sup>-1</sup> air pressure and 5 cm h<sup>-1</sup> pump speed. The suspension was mixed at 200 rpm with a magnetic stirrer. After 16 h incubation, the alginate was dissolved with 5 ml 1 M Na<sub>3</sub>-citrate buffer (pH 6). The buffer was also added to the control cultures that had been inoculated with non-embedded spores. The mycelium of both cultures was separated from the culture medium by using a 40 µm cell strainer, washed with MM (without carbon source) and transferred to 100 ml MM-X in 250 ml Erlenmeyer flasks. Growth was prolonged for 24 h at 30 °C and 200 rpm. To produce micro-colonies from mycelium, the latter culture was homogenized for 1 min in a Waring blender,



after which 2.5 ml of the homogenate was added to 50 ml TM-X in 250 ml Erlenmeyer flasks. After growing for 16 h, the mycelium was harvested, washed with MM and transferred to 100 ml MM-X and growth was prolonged for 24 h.

#### *Biomass and surface area of micro-colonies*

Filter paper discs were dried overnight at 60 °C and weighed. Micro-colonies were collected on the filter, excess of water was removed by using a vacuum pump, after which the filter was dried at 60 °C overnight. Biomass of mycelium was calculated by subtracting the weight of the filter from the weight of the filter and the micro-colonies. Surface area of colonies was calculated with Fiji. To this end, bright field images of micro-colonies that had been taken immediately after harvesting were converted to binary images by thresholding. Using the particle analysis tool in ImageJ, circularity was set between 0.5 to 1 to remove small debris from the data set. The diameter of micro-colonies was calculated using the formula  $2 \cdot \sqrt{\frac{\text{area}}{\pi}}$  assuming that micro-colonies are circular.

#### *Resistance to heat and hydrogen peroxide*

Micro-colonies (up to a total number of 126) or conidia (up to a total number of  $10^6$ ) were taken up in 20 ml or 100  $\mu$ l MM-X, respectively, that was preheated at 60 °C. Heat stress was stopped by adding a similar volume of MM-X that was pre-cooled at 4 °C, after which the micro-colonies and conidia were plated on MM-XA. To this end, conidia were first centrifuged for 1 min at 3000 rpm in an Eppendorf centrifuge, after which they were taken up in 10  $\mu$ l MM-X. To assess H<sub>2</sub>O<sub>2</sub> resistance, micro-colonies (up to a total number of 126) were transferred to 20 ml MM-X containing up to 35 % H<sub>2</sub>O<sub>2</sub>. After 30 min, the pellets were harvested with a 40  $\mu$ m cell strainer (Corning, 352340, New York, United States), washed with 10 ml MM and plated on MM-XA in the case of MA234.1 or MM-MA (MM-A with 25 mM maltose as a carbon source) in the case of AR9#2. In the case of conidia, spores (up to  $10^6$ ) of strain MA234.1 were mixed with 1 ml MM containing 1% H<sub>2</sub>O<sub>2</sub>. After 27 min, the suspension was washed three times with MM with intermittent centrifugation for 1 min at 3000 rpm. Conidia were resuspended in 20  $\mu$ l MM and inoculated in wells of a 12-well-plate filled with MM-XA.

#### *Fluorescence microscopy*

GFP fluorescence was monitored using a Leica MZ16 stereomicroscope equipped with a mercury lamp, a Leica GFP2 filter set and a Leica DFC420 C digital camera.

### *Statistical analysis*

Linear regression was used to assess correlation between colony surface area and survival rate (Prism 8). One-way ANOVA followed by Games-Howell post-hoc test was used to assess differences in biomass formation (SPSS 25.0), while a Dunnett's T3 post-hoc test for multiple comparisons was used to assess differences in micro-colony size.

## **RESULTS**

### *Stress resistance of micro-colonies*

Small ( $\pm 300 \mu\text{m}$ ) microcolonies can be obtained by pre-culturing *A. niger* in alginate beads for  $\geq 10$  hours, while large micro-colonies ( $> \pm 1500 \mu\text{m}$ ) result from preculturing  $\leq 8$  h in alginate beads or by inoculating cultures with non-embedded spores (**Chapter 2**). The disadvantage of the  $300 \mu\text{m}$  micro-colonies is that they are not easily handled individually to assess stress resistance. Therefore, it was decided to reduce the concentration of embedded and non-embedded conidia in the culture medium (see Material and Methods for details). Large ( $3411 \pm 186 \mu\text{m}$ ;  $349.6 \pm 139.4 \mu\text{g}$ ) and small ( $1184 \pm 19 \mu\text{m}$ ;  $30.2 \pm 4.3 \mu\text{g}$ ) micro-colonies were obtained by growing non-embedded or alginate embedded conidia in TM-X pre-cultures for 16 h, followed by growth for 24 h in MM-X (Figure 1). These micro-colonies were exposed individually to heat and  $\text{H}_2\text{O}_2$  stress. All small and large micro-colonies died after exposure to  $60^\circ\text{C}$  for  $\geq 30$  min or to  $\geq 5\%$   $\text{H}_2\text{O}_2$  for 30 min. A total of  $14.3 \pm 2\%$  of the small colonies survived a 10 min-exposure at  $60^\circ\text{C}$ , while  $85.7 \pm 11.6\%$  of the large micro-colonies resisted this treatment. Similarly, only  $9.5 \pm 8.2\%$  of the small colonies survived a 30 min treatment with  $2\%$   $\text{H}_2\text{O}_2$ , while all big colonies survived. Taken together, large micro-colonies showed higher stress resistance than the small ones.

### *Ungerminated spores inside of micro-colonies*

Large (Figure 2AB) but not small (Figure 2C) micro-colonies showed a black core. Dissecting the large micro-colonies revealed the presence of non-germinated conidia in this core. Similar structures were not identified in small pellets. Conidia were also observed in large micro-colonies when they were grown on glucose or maltose instead of xylose (data not shown). Moreover, they were found both at the end of pre-culturing (i.e after 16 h) and after the total culturing time of 40 h. To assess if the non-germinated conidia in the centre of the large micro-colonies were responsible for the higher resistance to environmental stress, a 16 h pre-culture

that had been inoculated with free spores was homogenized in a blender and the resulting mycelium homogenate was used to inoculate a pre-culture. Large micro-colonies ( $4435 \pm 330 \mu\text{m}$ ;  $509.7 \pm 19.2 \mu\text{g}$ ) were formed after transfer of the pre-culture to MM-X (Figure 1).

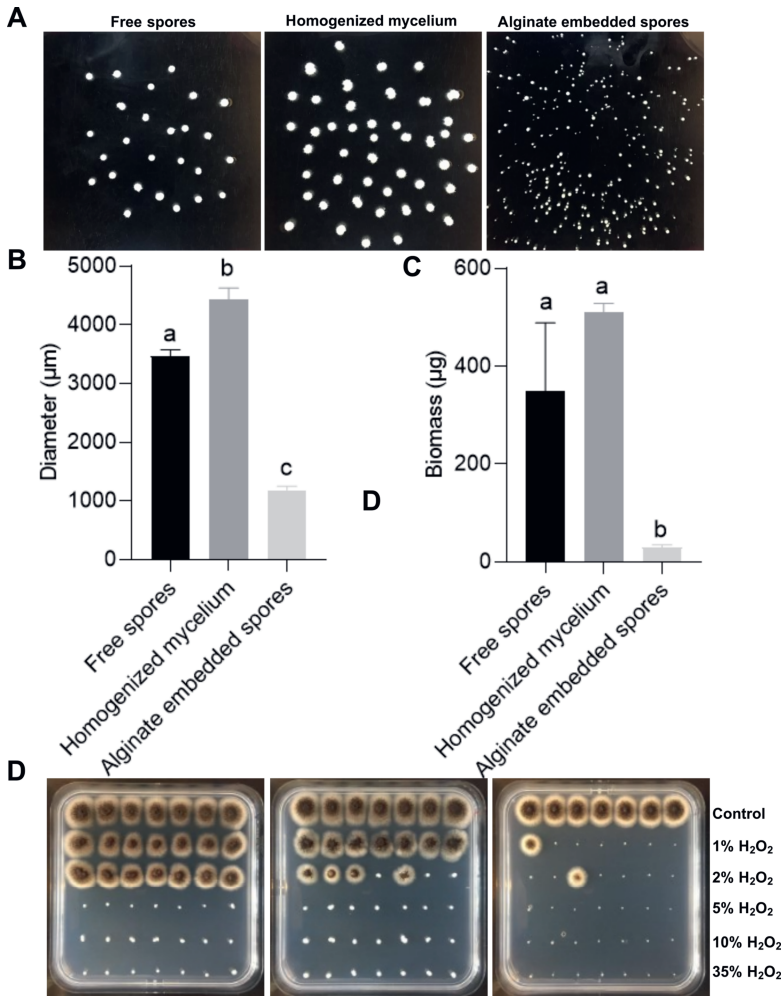


**Figure 1.** Morphology (A), diameter (B), biomass (C) and H<sub>2</sub>O<sub>2</sub> resistance (D) of micro-colonies that had been pre-cultured in TM-X for 16 h and grown for 24 h in MM-X. The pre-cultures had been inoculated with free or alginate-embedded conidia or with homogenized mycelium. Individual colonies were transferred to square MMXA plates after they had been treated for 30 min with 1-35% H<sub>2</sub>O<sub>2</sub>. One-way ANOVA showed statistical significance with Dunnett's T3 post-hoc test for diameter and Games-Howell post-hoc test for biomass ( $P < 0.05$ ).

As expected, these micro-colonies did not contain spores in their centre (Figure 2D). A total of  $38.1 \pm 8.2$  % large micro-colonies without spores inside their centre survived the heat treatment at 60 °C for 10 min, while  $47.6 \pm 8.3$  % survived the 30 min treatment with 2% H<sub>2</sub>O<sub>2</sub>. These data indicate that the large micro-colonies without spores in their centre are less resistant to stress than those with conidia in the colony core. The surface area of micro-colonies that had been exposed to heat stress or H<sub>2</sub>O<sub>2</sub> stress was related to their survival. Linear regression confirmed that both diameter ( $r^2$  0.4553,  $r^2$  0.6572) and biomass ( $r^2$  0.3872,  $r^2$  0.6661) are related with survival rate to H<sub>2</sub>O<sub>2</sub> stress (Figure 3AB) and heat stress (Figure 3CD), respectively. Taken together, more biomass and larger pellet size contribute to stress resistance.

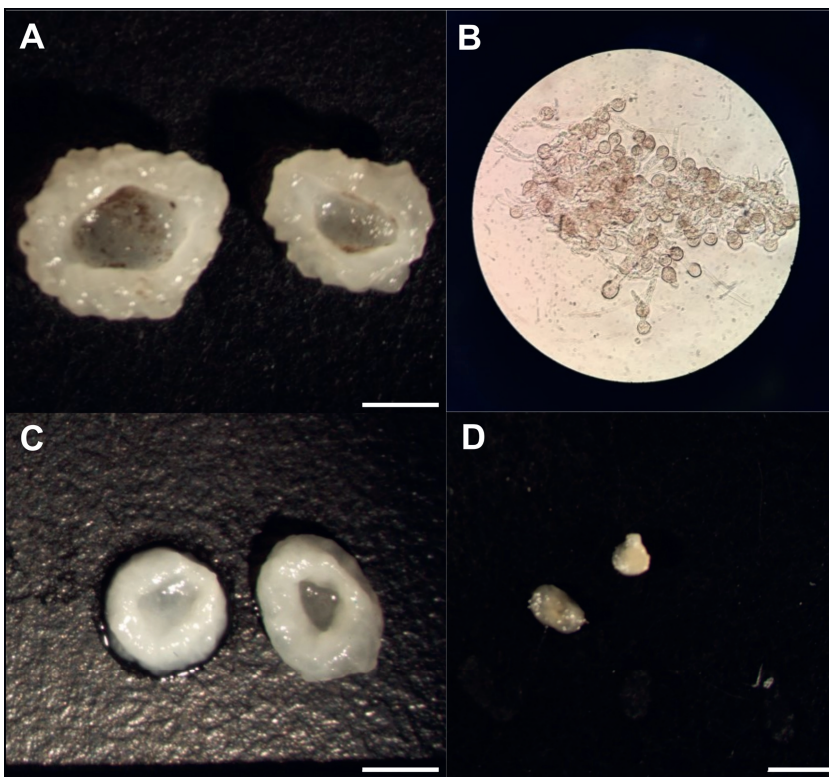


**Figure 2.** Dissection of a 40-h-old large micro-colony resulting from a pre-culture inoculated with free spores revealed conidia in the centre of the pellet as shown by the naked eye (A) and microscopy (B). In contrast, no spores were found in micro-colonies from cultures that had been inoculated with alginate embedded conidia (C) or with homogenized mycelium (D). A, C and D show both halves of the micro-colonies. Bar represents 2000  $\mu$ m.

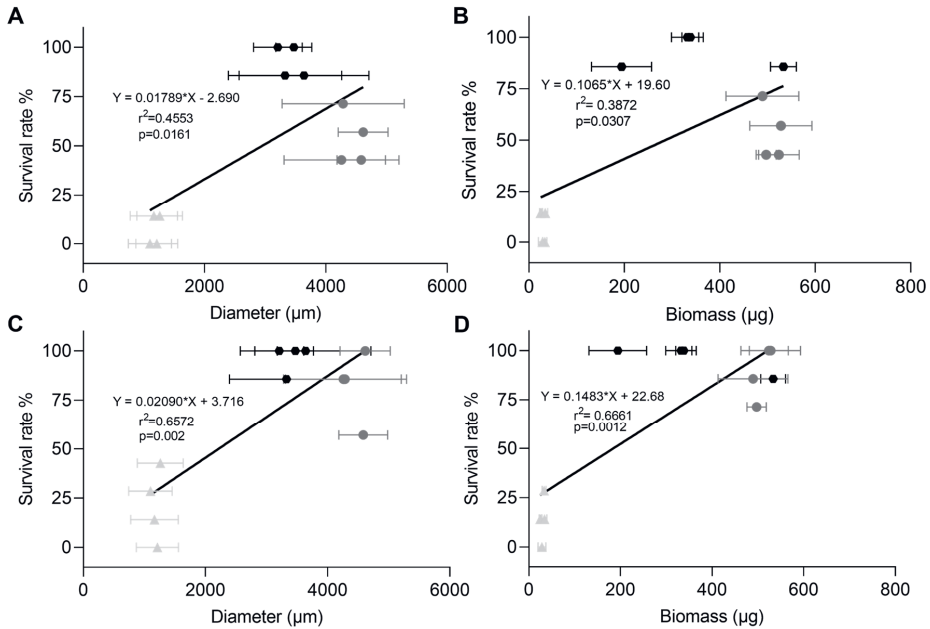


**Figure 3.** Linear regression between survival after 30 min exposure to 2%  $\text{H}_2\text{O}_2$  (A, B) and heat (C, D) and surface area (A, C) and biomass (B, D) of three biological replicates each with seven micro-colonies that resulted from alginate embedded conidia (light grey angle), non-embedded conidia (black hexagons) and homogenized mycelium (dark grey circles). One-way ANOVA showed statistical significance with Tukey post-hoc test between the diameter/biomass of one single micro-colony for each morphology.

#### *Centre micro-colonies are protected*

To study stress resistance in more detail, micro-colonies of strain AR9#2 (that expresses *GFP* from the *glaA* promoter) were exposed to  $\text{H}_2\text{O}_2$  stress. Large micro-colonies with conidia in their core were grown on xylose for a total of 40 h, after which they were exposed to 1-35 %  $\text{H}_2\text{O}_2$  for 10-30 min and plated for 8 h on maltose containing medium to induce the *glaA* promoter. Bright fluorescence was detected at the periphery of the untreated micro-colonies, while low fluorescence was detected in the colony centre (Figure 4). In contrast, the periphery of  $\text{H}_2\text{O}_2$  treated colonies was non-fluorescent, while the colony centre was as fluorescent as the centre of non-treated colonies. These results show that the hyphae in the outer zone are killed upon  $\text{H}_2\text{O}_2$  stress and form a protective layer for the cells in the centre of the micro-colony.

In the next set of experiments it was assessed whether conidia survive the stress conditions that were used for the micro-colonies. Spores from MA.2341 were exposed to heat or H<sub>2</sub>O<sub>2</sub> directly after harvesting or after a 40 h incubation in MM at 4 °C. In both cases, colonies were only obtained after spotting  $\geq 10^4$  spores. Thus, a single big colony is more resistant than  $10^3$  spores.

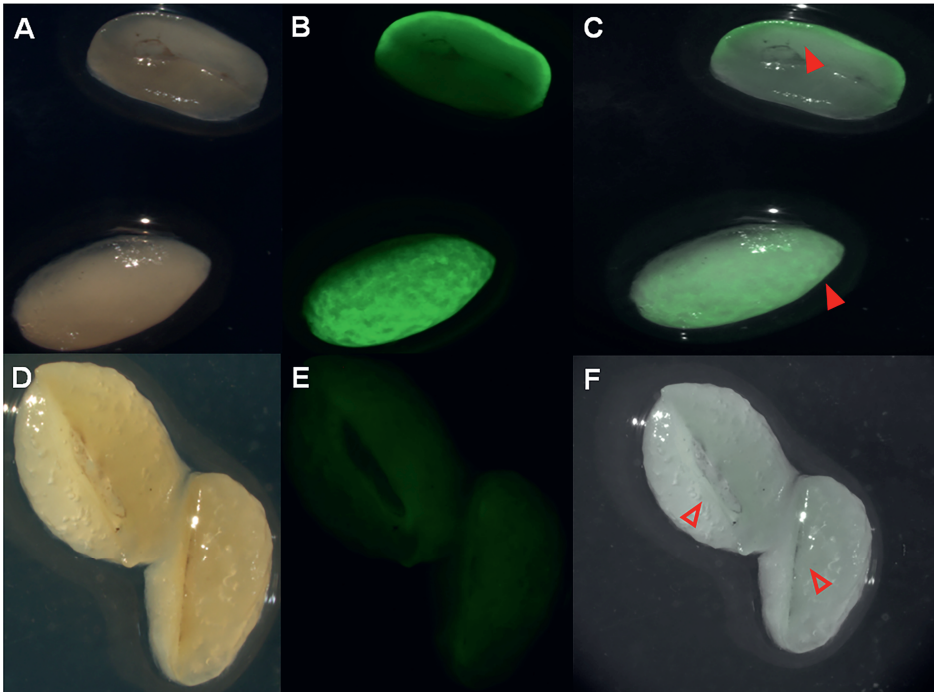


**Figure 4.** Brightfield (A, D) images and GFP fluorescence (B, E) and merged pictures (C, F) of large micro-colonies of strain AR9#2 that were not-exposed (A-C) or exposed (D-F) to 2% H<sub>2</sub>O<sub>2</sub> for 30 min. Non treated micro-colonies show bright and low fluorescence at the colony periphery and centre, respectively. In contrast, treated micro-colonies only show low fluorescence in the colony centre. Closed and open arrows indicate micro-colony periphery and centre, respectively.

## DISCUSSION

*Aspergillus niger* produces micro-colonies in shaking cultures that are heterogeneous in size and in gene expression (de Bekker et al., 2011; van Veluw et al., 2013), while **Chapter 2** showed that small micro-colonies secrete more and a larger diversity of proteins. Yet, the secretomes of large and small micro-colonies have complementary cellulase activity

illustrating that large-micro-colonies do have an important function in protein secretion. Here, it was shown that large micro-colonies are more resistant to heat and H<sub>2</sub>O<sub>2</sub>. In contrast, no difference was observed in sensitivity to pH 2-12 (data not shown).

Conidia were found in the core of large pellets. The fact that conidiophores were absent in the centre of the micro-colonies indicate that the conidia originated from the inoculum. Indeed, conidia were absent in the core of large micro-colonies when liquid shaken cultures were inoculated with mycelium instead of spores. Together, we propose that only part of the conidia that aggregate during the early phase of culturing germinate. These germinating spores form the micro-colony that embeds the non-germinated spores. As far as we know, this is the first report of resting conidia in the core of a micro-colony. Of interest, the resistance of large micro-colonies to heat and H<sub>2</sub>O<sub>2</sub> was shown to partly result from the conidia in the centre of the micro-colony. This was based on the finding that large micro-colonies resulting from a spore inoculum were more stress resistant than large micro-colonies resulting from a mycelium inoculum. It is known that conidia are generally more stress resistant than vegetative hyphae (Dijksterhuis, 2019), which would explain our findings. Yet, the hyphae at the colony periphery also have a protective role by preventing damage of hyphae, and probably spores as well, in the colony centre. H<sub>2</sub>O<sub>2</sub> treatment resulted in hyphae at the periphery of large micro-colonies that no longer could switch on the *glaA* promoter after transfer to an inducing medium, indicating that these hyphae had been damaged. In contrast, non-treated colonies showed very bright *glaA* driven GFP fluorescence at the colony periphery. The centre of treated and non-treated colonies showed both low fluorescence, indicating that heat treatment had not damaged the hyphae in this zone. Nonetheless, we can not conclude from our data whether the conidia and or the hyphae in the centre reinitiate growth of the micro-colony after stress exposure.

The reason why some spores in the centre of large micro-colonies do not germinate is not yet clear. Yet, it is known that conidia of *A. niger* have a very heterogeneous germination response (Ijadpanahsaravi et al., 2021). For instance, only 20% of the spores germinate within 14 h in a defined medium with glucose as a carbon source. Similar responses were observed when amino acids were used as a carbon source in the case of *A. niger* (Ijadpanahsaravi et al., 2021) and *Penicillium roqueforti* (Punt et al., 2022). Thus, the presence of non-germinated conidia in the micro-colony centre is in line with the germination dynamics of these spores and this may have evolved to increase survival capacity of micro-colonies.

## REFERENCES

- Al-Gashgari, M.G.R., Collage, G. 2002. Occurrence of fungi and pectolytic activity in fruit juices from Saudi Arabia. *Pak J Biol Sci*, **5**, 609-611.
- Carlsen, M., Spohr, A.B., Nielsen, J., Villadsen, J. 1996. Morphology and physiology of an  $\alpha$ -amylase producing strain of *Aspergillus oryzae* during batch cultivations. *Biotechnol Bioeng*, **49**, 266-276.
- de Bekker, C., van Veluw, G.J., Vinck, A., Wiebenga, L.A., Wösten, H.A.B. 2011. Heterogeneity of *Aspergillus niger* microcolonies in liquid shaken cultures. *Appl Environ Microbiol*, **77**, 1263-1267.
- de Vries, R.P., Burgers, K., van de Vondervoort, P.J., Frisvad, J.C., Samson, R.A., Visser, J. 2004. A new black *Aspergillus* species, *A. vadensis*, is a promising host for homologous and heterologous protein production. *Appl Environ Microbiol*, **70**, 3954-3959.
- Delgado-Ramos, L., Marcos, A.T., Ramos-Guelfo, M.S., Sanchez-Barrionuevo, L., Smet, F., Chavez, S., Canovas, D. 2014. Flow cytometry of microencapsulated colonies for genetics analysis of filamentous fungi. *G3 (Bethesda)*, **4**, 2271-2278.
- Dijksterhuis, J. 2019. Fungal spores: Highly variable and stress-resistant vehicles for distribution and spoilage. *Food Microbiol*, **81**, 2-11.
- Ijadpanahsaravi, M., Punt, M., Wösten, H.A.B., Teertstra, W.R. 2021. Minimal nutrient requirements for induction of germination of *Aspergillus niger* conidia. *Fungal Biol*, **125**, 231-238.
- Krijgsheld, P., Bleichrodt, R., van Veluw, G.J., Wang, F., Muller, W.H., Dijksterhuis, J., Wösten, H.A.B. 2013. Development in *Aspergillus*. *Stud Mycol*, **74**, 1-29.
- Metz, B., Kossen, N.W.F. 1977. The growth of molds in the form of pellets - a literature review. *Biotechnol Bioeng*, **XIX**, 781-799.
- Park, J., Hulsman, M., Arentshorst, M., Breeman, M., Alazi, E., Lagendijk, E.L. Rocha, M.C., Malavazi, I., Nitsche, B.M., van den Hondel, C.A., Meyer, V., Ram, A.F. 2016. Transcriptomic and molecular genetic analysis of the cell wall salvage response of *Aspergillus niger* to the absence of galactofuranose synthesis. *Cell Microbiol*, **18**, 1268-1284.
- Punt, M., Teertstra, W.R., Wösten, H.A.B. 2022. *Penicillium roqueforti* conidia induced by L-amino acids can germinate without detectable swelling. *Antonie van Leeuwenhoek*, **115**, 103-110
- Siedenberg, D., Mestric, S., Ganzlin, M., Schmidt, M., Punt, P.J., van den Hondel, C., Rinas, U. 1999. GlcA promoter controlled production of a mutant green fluorescent protein



- (S65T) by recombinant *Aspergillus niger* during growth on defined medium in batch and fed-batch cultures. *Biotechnol Prog*, **15**, 43-50.
- Tegelaar, M., Aerts, D., Teertstra, W.R., Wösten, H.A.B. 2020. Spatial induction of genes encoding secreted proteins in micro-colonies of *Aspergillus niger*. *Sci Rep*, **10**, 1536.
- van Veluw, G.J., Teertstra, W.R., de Bekker, C., Vinck, A., van Beek, N., Muller, W.H., Arentshorst, M., van der Mei, H.C., Ram, A.F., Dijksterhuis, J., Wösten, H.A.B. 2013. Heterogeneity in liquid shaken cultures of *Aspergillus niger* inoculated with melanised conidia or conidia of pigmentation mutants. *Stud Mycol*, **74**, 47-57.
- Wösten, H.A.B. 2019. Filamentous fungi for the production of enzymes, chemicals and materials. *Curr Opin Biotechnol*, **59**, 65-70.
- Yoshimi, A., Sano, M., Inaba, A., Kokubun, Y., Fujioka, T., Mizutani, O., Hagiwara, D., Fujikawa, T., Nishimura, M., Yano, S., Kasahara, S., Shimizu, K., Yamaguchi, M., Kawakami, K., Abe, K. 2013. Functional analysis of the  $\alpha$ -1,3-glucan synthase genes *agsA* and *agsB* in *Aspergillus nidulans*: *agsB* is the major  $\alpha$ -1,3-glucan synthase in this fungus. *PLoS One*, **8**, e548.

## Chapter 4

**The orotidine 5'-phosphate decarboxylase gene *pyrG* influences *Aspergillus niger* pellet formation and secretome in liquid shaken cultures**

*Jun Lyu, Juan Pablo Moran Torres, Harm Post, Maarten Punt, A. F. Maarten Altelaar, Hans de Cock and Han A. B. Wösten*

## ABSTRACT

*Aspergillus niger* secretes a wide variety and high amount of enzymes in its culture medium and is therefore widely used by the industry for protein production. To this end, this fungus is grown in bioreactors, where it can form micro-colonies of different size. We here describe that biomass formation, spore swelling and germ tube formation of strains with a less active orotidine 5'-phosphate decarboxylase gene *pyrG* is unaffected when compared to wild-type. In contrast, strains with a less active *pyrG* form smaller micro-colonies, probably due to reduced spore aggregation. Cellular proteomics revealed candidate genes that may be involved in this difference in spore aggregation. This chapter also shows that changed morphology impacts the secretome.

## INTRODUCTION

*Aspergillus niger* colonizes dead and living organic material in nature (Krijgsheld et al., 2013) and is used by the industry to produce enzymes and small molecular weight metabolites (Meyer et al., 2011b; Wösten, 2019). Colonization of a substrate by *A. niger* starts with the germination of conidia, which results in hyphae that grow at their tips and that branch sub-apically. Consequently, a colony (also called mycelium) is formed that consists of a network of hyphae. When grown on a solid substrate, *A. niger* forms macro-colonies (diameter in cm range) or micro-colonies (diameter in (sub-)millimeter range), whose dimensions are restricted by the size of the substrate. In liquid cultures, *A. niger* grows as micro-colonies either as pellets or as dispersed mycelium. Pellets are micro-colonies that have a distinct central and outer zone, while this is not the case for dispersed mycelium (Krijgsheld et al., 2013).

Small micro-colonies release a more diverse palette and higher amount of proteins in liquid shaken cultures when compared to large micro-colonies (**Chapter 2**). Yet, large micro-colonies do secrete proteins that are not secreted by small micro-colonies. In fact, cellulases released by the two types of micro-colonies act synergistically. The fact that genes encoding secreted proteins are (mainly) expressed in a shell at the periphery of the micro-colonies would explain why small micro-colonies secrete more protein (Tegelaar et al., 2020). Yet, other mechanisms would explain the different protein profiles that are secreted by both types of micro-colonies (**Chapter 2**).

So far, presence of small and large micro-colonies in liquid cultures has been explained by differences in aggregation of conidia (Krijgsheld et al., 2013). Aggregation is described as a two-stage process. During the first stage conidia clump together, while in the second stage germlings aggregate (Grimm et al., 2004; Fontaine et al., 2010; He et al., 2014; Yoshimi et al.,

2013). We here describe that strains with a less- or non-active orotidine 5'-phosphate decarboxylase gene *pyrG* form smaller micro-colonies in liquid cultures when compared to wild-type. The changed morphology impacts the secretome and is caused by reduced aggregation of spores.

## MATERIAL AND METHODS

### *Strains and culture conditions*

*Aspergillus niger* strains (Table 1) were grown for 3 days at 30 °C on PDA plates. Conidia were harvested using a cotton swab and suspended in minimal medium with 25 mM glucose (MM-G) (de Vries et al., 2004) or transformation medium (TM-G; MM containing 0.5% yeast extract, 0.2% casamino acids, and 25 mM glucose, pH 6). Spore suspensions were filtered through cotton to remove hyphae and counted using a haemocytometer. A total of  $2 \times 10^7$  spores was used to inoculate 50 ml TM with 25 mM xylose (TM-X) contained in 250 ml Erlenmeyer flasks either or not in the presence of 10 mM uridine and 5-20  $\mu\text{g ml}^{-1}$  doxycycline. After 16 h of growth, mycelium was transferred to 100 ml MM containing 25 mM xylose as a carbon source (MM-X) and growth was prolonged for 32 h. Biomass and culture medium were separated by using a 40  $\mu\text{m}$  cell strainer (Corning, 352340, New York, United States).

**Table 1. *A. niger* strains used in this study.**

Strain	Genotype	Description	Reference
<i>A.niger</i> N400	Wild type		Demirci et al., 2021
<i>A.niger</i> N402	<i>cspA1</i>	UV derivative of N400	Bos et al., 1988
<i>A.niger</i> AB4.1	<i>pyrG</i> <sup>-</sup>	<i>pyrG</i> <sup>378</sup> derivate of N402	van Hartingsveldt et al., 1987
<i>A.niger</i> AB 1.13 <i>pyrG</i> <sup>-</sup>	<i>prtT-13, pyrG</i> <sup>-</sup>	<i>prtT</i> <sup>-</sup> UV mutant of <i>A. niger</i> AB 4.1, <i>pyrG</i> <sup>378</sup>	Mattern et al., 1992
<i>A.niger</i> AB 1.13 <i>pyrG</i> <sup>+</sup>	<i>AB1.13-pyrG</i> <sup>+</sup>	Uridine prototroph of AB 1.13 <i>pyrG</i> <sup>-</sup>	Mattern et al., 1992
<i>A.niger</i> MA169.4	$\Delta$ <i>kusA</i> :DR- <i>amdS</i> -DR, <i>pyrG</i> <sup>-</sup>	<i>ku70</i> disruption in AB4.1, <i>pyrG</i> <sup>378</sup>	Park et al., 2016
<i>A.niger</i> MA234.1	$\Delta$ <i>kusA</i> :DR- <i>amdS</i> -DR, <i>pyrG</i> <sup>+</sup>	3.8 kb <i>XbaI pyrG</i> replacement in MA169.4	Park et al., 2016
<i>A.niger</i> DA001	<i>msnB::pyr4</i>	<i>pyr4</i> from <i>N. crassa</i> replacing <i>msnB</i> in MA169.4	Aerts, 2018
<i>A.niger</i> DA002	<i>pyr4</i>	<i>msnB</i> complementation of DA001	Aerts, 2018
<i>A.niger</i> LZ01	$\Delta$ <i>kusA</i> :DR- <i>amdS</i> -DR, <i>pyr4</i> <sup>+</sup>	Replacement of <i>pyrG</i> for <i>pyr4</i> of <i>N. crassa</i> in MA169.4	this study
<i>A.niger</i> LZ02	$\Delta$ <i>kusA</i> :DR- <i>amdS</i> -DR, <i>Tet-on::pyrG</i>	Replacement of the <i>pyrG</i> promoter for <i>Tet-on promoter</i> in MA234.1	this study
<i>A.niger</i> LZ03	$\Delta$ <i>kusA</i> :DR- <i>amdS</i> -DR, <i>Tet-on::pyr4</i>	Replacement of <i>pyrG</i> for <i>pyr4</i> from <i>Neurospora crassa</i> , under control of the <i>Tet-on promoter</i> in MA169.4	this study

### Plasmid construction

A CRISPR-Cas system (Nodvig et al., 2018) was used to replace the *pyrG* promoter for the *Tet-on* regulatory sequences (Meyer et al., 2011a) or to replace *pyrG* for *pyr4* of *Neurospora crassa* under control of its own promoter or under control of the *Tet-on* regulatory sequences (Figure 1). The sgRNA's sg02 and sg03 were designed by CHOPCHOP (<https://chopchop.cbu.uib.no/>) (Table 2) to produce a double strand break 144 bp upstream of the start codon and 175 bp downstream of the stop codon of *pyrG* in the genomic DNA of *A. niger*, thus effectively removing the entire coding sequence of this gene. These sgRNA's were placed under control of an *A. niger* proline tRNA promoter and terminator (van Leeuwe et al., 2019) in plasmid pFC332 that also contains *cas9*, the AMA1 sequence for replication, and the hygromycin selection marker (Table 3, Figure 1A) (Nodvig et al., 2018). This resulted in vectors pJL002 and pJL003, respectively (Table 3; Figure 1A). For cloning, sgRNA expression units were amplified in two parts using plasmids pTLL108.1 and pTLL109.2 (van Leeuwe et al., 2019) as templates (Figure 1A) to obtain the 5' and 3' overlapping fragments that consist of PtRNA::sgRNA and sgRNA::TtRNA, respectively (van Leeuwe et al., 2019). Primer pairs 1/4 and 2/3 (Table 4) were used to amplify these 5' and 3' fragments followed by Gibson assembly using a PacI-linearized and dephosphorylated pFC332 vector to produce *pyrG* up-cutting sgRNA plasmid pJL002. Similarly, primer pairs 1/6, and 2/5 (Table 4) were used to produce *pyrG* down cutting sgRNA plasmid pJL003.

**Table 2.** sgRNA sequences used in this study.

sgRNA	Sequence	Cutting Site
sg02	TGGTCTTCCTTCAGATTTAA	144 bp before <i>pyrG</i> coding sequence
sg03	GTGTGGCACAAGGATCAATG	175 bp after <i>pyrG</i> stop codon
sg04	CCTGGTAGCTGGACTGAAAGT	768 bp before <i>pyrG</i> coding sequence

**Table 3.** Plasmids used in this study.

Plasmid	Type	Description	Reference
pTLL108.1	/	<i>PtRNA::sgRNA</i>	van Leeuwe et al., 2019
pTLL109.2	/	<i>sgRNA::TtRNA</i>	van Leeuwe et al., 2019
pWR12	<i>pyr4</i>	Gene <i>pyr4</i> was amplified as a 3081 bp fragment with XbaI sites at its ends, which was introduced in the XbaI site of pUC20 resulting in pWR12	Aerts, 2018
pFC332	/	Contains <i>cas9</i> , an AMA1 sequence for replication, hygromycin resistance cassette and a PacI site for introducing sgRNA	Nodvig et al., 2018
pMT4	<i>PfiraA:rtTa2-M2:TcrgA, 7xTetO:Pmin</i>	Reverse activator controlled by <i>A. niger fraA</i> constitutive promoter. Chimeric promoter composed of 7 copies of Tet operator fused to minimal transcribing sequence of <i>A. nidulans gpdA</i> promoter.	unpublished

pJL001	<i>pyr4</i>	<i>pyr4</i> surrounded by 1000 bp flanks up- and downstream of <i>pyrG</i> cutting sites	this study
pJL002	sgRNA	<i>pyrG</i> upstream cut, 143 bp upstream of start codon	this study
pJL003	sgRNA	<i>pyrG</i> downstream cut, 178 bp downstream of stop codon	this study
pJL004	sgRNA	<i>pyrG</i> upstream cut, 770 bp upstream of start codon	this study
pJL007	<i>Tet-on:pyrG</i>	<i>Tet-on</i> promoter surrounded by 1000 bp flank upstream of 5' <i>pyrG</i> cutting site and 1000 bp flank 550 bp downstream of start codon	this study
pJL010	<i>Tet-on:pyr4</i>	<i>pyr4</i> with 1000 bp flank before and after <i>pyrG</i> up- and downstream cutting site	this study

**Table 4.** Primers used in this study.

Primer Name	Primer Sequence
1. pTE1.Fwd	GTTCCGCTGAGGGTTTAATACTCCGCCGAACGTA CTG
2. pTE1.Rev	CTGTCTCGGCTGAGGCTTTAAAAAGCAAAAAGGAAGGTACAAAAAAGC
3. gRNAup.pyrg.Fwd	TTAAATCTGAAGGAAGACCAGTTT TAGAGCTAGAAA TAGCAAG
4. gRNAup.pyrg.Rev	TGGTCTTCCTCAGATTTAAGACGAGCTTACTCGTTTCG
5. gRNA.down.pyrg.Fwd	GTGGACAAGGATCAATGGTTTTAGAGCTAGAAA TAGCAAG
6. gRNAdown.pyrg.Rev	TTGATCCTTGTGCCACACGACGAGCTTACTCGTTTCG
7. gRNASeut.pyrg.Fwd	ACTTCAGTCCAGTACCAGGGTTTTAGAGCTAGAAA TAGCAAG
8. gRNASeut.pyrg.Rev	CCTGGTAGCTGGACTGAAGTGACGAGCTTACTCGTTTCG
9. pJET-pyr4.1000up.Fwd	GATGGCTCGAGTTTTTCAGCAAGATCGAACTACTTTCGGCATCTTC
10. pJET-pyr4.1000up.Rev	CAGTGC GAAGTCTTCTAGAATCTGAAGGAAGACCAAGGACA
11. Pyr4.1000down.Fwd	CCGAAAGCGACGAATGTA TGCGGTACGACGATTTGAT
12. Pyr4.1000down.Rev	GGAGATCTGCTCGAGAGGTGCGGCCCGGGTCAATTTCTCTGTGG
13. pJET.Fwd	ACCTCTCGAGCAGATCTCTAC
14. pJET.Rev	ATCTTGCTGAAAACTCGAGCCATC
15. Tet-on.Fwd	CCCTCGGCTGGTCTGTCTTA
16. Tet-on.Rev	GGTGTGTCTGCTCAAGCG
17. TetpyrG.Up.Homolog.Fwd	GATGGCTCGAGTTTTTCAGCAAGATTACTGGGAAGGTGATAGGCAA
18. TetpyrG.Up.Homolog.Rev	TAAGACAGACCAGCCGAGGGGCTTGCCGGAGTACACATAT
19. TetpyrG.Down.Homolog.Fwd	CGCTTGAGCAGACATCACCATGTCTCCAAGTCGCAATT
20. PyrG.Half.Rev	GTAGGAGATCTGCTCGAGAGGTGCGCAAGATCAACAGACCG
22. Tet-on:pyr4.Fwd	CTACCCCGCTTGAGCAGACATCACCATGTGCAAGTCAGAAACGCAGC
22. Pyr4.CDS.Rev	CTATGCCAGACGCTCCCGCGAT
23. Pyr4.Fwd	TCTAGAAGACTTCGCACTGT
24. Pyr4.CK.Rev	ACATTCGTCGCTTTCGG
25. Tet-on.CK.Fwd	TTCCCACTTCATCGCAGCT
26. Tet-on:pyr4.CK.Rev	ATGTCGGCGTTGGTGTATG

**Replacement of *pyrG* for *pyr4* (Figure 1B).** Gene *pyr4* of *Neurospora crassa* (under control of its own promoter and terminator) was obtained by a XbaI-digestion from plasmid pWR12 (Aerts, 2018). To assist homologous integration, an upstream flank of *pyrG* was obtained by amplifying the 1144-144 bp fragment upstream of the *pyrG* start codon using *A. niger* genomic DNA and primer pair 9/10 (Table 4), while the downstream flank was obtained by amplifying the 175-1175 bp fragment downstream of the *pyrG* stop codon with primer pair 11/12 (Table

4). The *pyr4* gene with the two flanks were introduced into linearized plasmid pJET (commercial pJET template from CloneJET PCR Cloning Kit, ThermoFisher, Massachusetts, US), which was amplified by primer pair 13/14 (Table 4), resulting in repair plasmid pJL001 (Table 3). Primer pair 22/23 (Table 4) was designed to give a 3072 bp band in strains with the introduced *pyr4* gene, while no band would be obtained in the parent strain MA169.4.

Replacement of the *pyrG* and *pyr4* promoters for *Tet-on* regulatory sequences (Figure 1CD). The sgRNA sg04 was designed by CHOPCHOP (<https://chopchop.cbu.uib.no/>) (Table 2) to produce a double strand break 768 bp upstream of the start codon. Plasmid pJL004 was constructed in the same way as pJL002 now using primer pair 1/8 (Table 4) to amplify the PtRNA::sgRNA and primer pair 2/7 (Table 4) to amplify the sgRNA::TtRNA. Vectors pJL002 and pJL004 were used to replace the *pyrG* promoter for the *Tet-on* regulatory sequences in strains MA234.1 and MA169.4, respectively (Figure 1C). These vectors contained sgRNA's that mediate cutting 768 bp (sg04; Table 1) and 144 bp (sg02; Table 1) upstream of the start codon of *pyrG*, respectively, in the genomic DNA of *A. niger*.

Repair plasmid pJL007 contains the upstream *pyrG* flank followed by the *Tet-on* promoter with 500 bp *pyrG* coding sequence. The *Tet-on* promoter consists of a constitutively controlled transactivator CDS followed by a synthetic promoter based on a septuple tetracycline operator and an *Aspergillus* minimal promoter (Wanka et al., 2016). To construct pJL007, the *Tet-on* promoter fragment was amplified from pMT4 (Table 3) using primer pair 15/16 (Table 4) and was cloned in the pJET backbone (CloneJET PCR cloning kit, k1231, ThermoFisher) in between the 1000 bp up- and downstream *pyrG* sequences that were amplified by using primer pairs 17/18 and 19/20, respectively (Table 4). This resulted in plasmid pJL007 (Table 3; Figure 1C). Primer pair 25/20 (Table 4) was designed to give a 615 bp band in strains with a *Tet-on:pyrG* gene, while no band was obtained in the parent strain MA234.1 (forward primer binds to the *Tet-on* promoter and reverse primer binds to coding sequence of *pyrG*). Similarly, plasmid pJL010 was constructed for inducible *Tet-on:pyr4* expression (Figure 1D). To this end, the *Tet-on* promoter and the coding sequence of *pyr4* were amplified by primer pairs 15/16 and 21/22, respectively. Next, these sequences were introduced into the pJET backbone flanked by 1000 bp upstream and downstream sequences of *pyrG*. The pJET backbone was amplified using primer pair 10/11 (Table 4) and pJL001 (Table 3; Figure 1B) as template. Primer pair 25/26 (Table 4) was designed to give a 465 bp band in strains containing *Tet-on:pyr4*, while no band would be obtained in the parent strain MA169.4 (forward primer binds to *Tet-on* promoter and reverse primer binds to coding sequence of *pyr4*).

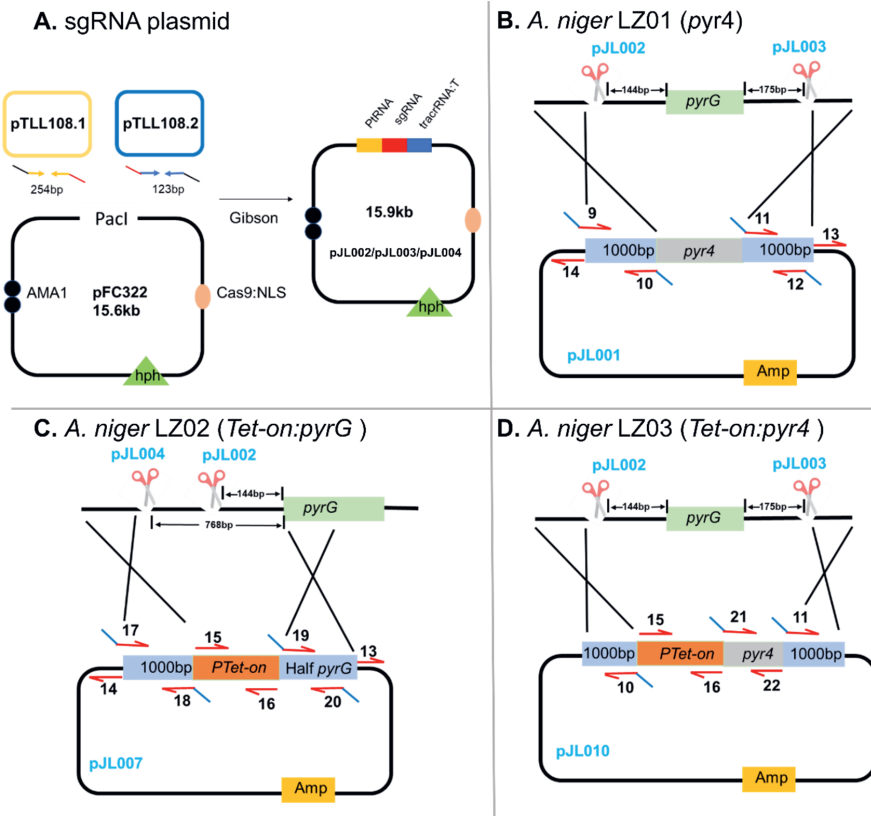


**Figure 1.** Plasmids used for *A.niger* transformation. (A) sgRNA plasmid design. The 254 bp and 123 bp fragments consist of the 5' and 3' fragments encompassing *Pacl*::*Pro*-promoter::sgRNA and sgRNA::Terminator::*Pacl*, respectively. (B-D) Replacement of *pyrG* by *pyr4* (B), replacement of the *pyrG* promoter by the *Tet-on* regulatory sequences (C), and replacement of *pyrG* by *pyr4* under control of the *Tet-on* regulatory sequences (D).

### *Transformation of A. niger*

Protoplasts of strains MA169.4 and MA234.1 were obtained according to de Bekker et al. (2009) and transformed according to Meyer et al. (2010). Transforming DNA was taken up in 20  $\mu$ l STC (50 mM  $\text{CaCl}_2$ , 10 mM Tris/HCl, 1.33 M sorbitol, pH 7.5) and added to 100  $\mu$ l of the same buffer containing  $10^6$  protoplasts. To obtain *pyr4* strains, MA169.4 was co-transformed with 1  $\mu$ g pJL002, 1  $\mu$ g pJL003 and 20  $\mu$ g of *NotI*-digested pJL001. To obtain strains expressing *Tet-on:pyrG* and *Tet-on:pyr4*, MA234.1 and MA169.4 protoplasts were transformed with 1  $\mu$ g pJL002 and 1  $\mu$ g pJL004 or pJL003, respectively, as well as 2  $\mu$ g pJL007



or 20 µg PvuI-linearized pJL010 as donor DNA in the former and latter case, respectively. 50 µl 25% PEG6000 was added and mixed gently before adding 1 ml 25% PEG6000, followed by a 5 min incubation at room temperature. Next, 2 ml STC was added and mixed with 20 ml molten (50 °C) top-agar (MMST; 0.95 M sucrose, 0.6% agar, pH 6), which was spread on top of 12 x 12 cm plates containing 20 ml bottom-agar (MMS: 0.95 M sucrose, 1.2% agar, pH 6). Hygromycin (150 µg ml<sup>-1</sup>) had been added to both MMS and MMST. Transformants were transferred to PDA plates containing 150 µg ml<sup>-1</sup> hygromycin B, followed by two transfers to PDA plates without antibiotic to get rid of the sgRNA plasmid.

### *DNA isolation*

*Escherichia coli* strain NEB® 10-beta was used for cloning purposes and was grown at 37 °C and 200 rpm in LB medium. *E.coli* plasmid DNA was isolated using the NucleoBond PC 100 Plasmid Miniprep Kit (Macherey Nagel). Genomic *A. niger* DNA was isolated as described (Liu et al., 2000) with modifications. Mycelium was grown overnight in MM-X or TM-X at 30 °C and 200 rpm and harvested using a 40 µm cell strainer (Corning, 352340, New York, United States). After excessive water was removed by filter paper, the mycelium was frozen in liquid nitrogen and homogenized with 2 steel beads at 25 Hz for 1 min in a Tissue lyzer II (Qiagen, Hilden, Germany). A total of 500 µl lysis buffer was mixed with 5 - 20 mg mycelium powder and incubated at room temperature for 10 min. This was followed by adding 150 µl 3 M potassium acetate buffer pH 4.8 and centrifugation at 10,000 g for 1 min. The supernatant was centrifuged again at 10,000 g for 2 min after mixing with an equal volume of isopropanol. The pellet was washed with 70% ethanol and dissolved in 50 µl TE Buffer (NucleoBond PC 100 Plasmid Miniprep Kit, Macherey Nagel).

### *Germination and aggregation analysis*

Swelling of conidia and germ tube formation in TM-X was monitored in real time by using an oCelloScope imager (Biosense Solutions, [www.biosensesolutions.dk](http://www.biosensesolutions.dk)) with UniExplorer software version 8.1.0.7682-RL2 (Fredborg et al., 2013; Ijadpanahsaravi et al., 2021). A total of 4 10<sup>4</sup> freshly harvested conidia were added in wells of a 96 wells suspension culture plate (Greiner bio-one, Cellstar 655185) in 150 µl medium. This enabled monitoring of germination of at least 200 spores per well, using 6 wells as technical replicates for each condition and using biological triplicates. Analysis was started after 1 h of incubation to enable settling of the conidia at the bottom of the well. Objects were scanned every hour during the first 10 h and every 2 h during the next 14 h with a scan area length of 405 µm, an object area (min-max) of

70-700 pixels, and a maximum number of objects of 1200. Individual objects were followed over time using oCelloScope XY coordinates and a custom R script. Conidial aggregates and non-conidial objects were manually removed from the data set of  $t = 1$  h. Conidia were followed in time based on their X and Y coordinates using the fast k-nearest neighbor (KNN) searching algorithm from the R package 'FNN' (Beygelzimer et al., 2019). This was done bi-directionally from  $t = x$  to  $t = x+1$  not allowing the neighbour distance of an object to exceed  $27.5 \mu\text{m}$  (i.e. 50 pixels) between 2 adjacent time points. The lineage was discontinued if these conditions were no longer met. The objects were classified based on surface area and circularity. Resting conidia had a surface area  $\leq 39 \mu\text{m}^2$  and a circularity  $> 0.97$ , swollen conidia a surface area  $> 39 \mu\text{m}^2$  and a circularity  $> 0.97$ ; while conidia with germ tubes had a surface area  $> 39 \mu\text{m}^2$  and a circularity  $> 0.75$  and  $\leq 0.97$ . The asymmetric model (Dantigny et al., 2011) was used to describe swelling and germ tube formation (P) as a function of time,  $\tau$  (h) (Eq. 1).

$$P = P_{\max} \left( 1 - \frac{1}{1 + \left(\frac{t}{\tau}\right)^d} \right) \quad (\text{Eq. 1}).$$

$P_{\max}$  is the maximal percentage of swollen conidia or spores that had formed a germ tube (the asymptotic value of P at  $t \rightarrow +\infty$ ),  $\tau$  (h) is the time at which  $P = 0.5 P_{\max}$  and  $d$  is a shape parameter that can be correlated to heterogeneity of the population. A low  $d$  reflects a population where conidia have more variable individual germination times. To estimate the model parameters, the biological triplicates were fitted per tested condition with the R package GrowthRates (Petzold, 2019) using the Levenberg-Marquardt algorithm. Parameters were limited to  $P \geq 0$  and  $\leq 120\%$ ,  $\tau \geq 1$  and  $\leq 18$ ,  $d \geq 1$  and  $\leq 30$  when fitting the model. Confidence intervals (95%) were determined using the standard error of the parameter estimates, where  $\hat{Y}$  represents the estimated P,  $\tau$  or  $d$  value;  $SE_{\hat{y}}$  is the standard error obtained for P,  $\tau$  or  $d$ ;  $\alpha$  is 0.05;  $df$  is the degrees of freedom;  $qt$  represents the Students T distribution function (Eq 2).

$$CI_{\hat{y}} = SE_{\hat{y}} \pm qt\left(1 - \frac{\alpha}{2}, df\right) \quad (\text{Eq. 2})$$

Objects that had an object area  $> 300$  pixels ( $90 \mu\text{m}^2$ ) and that decreased in size were excluded from the data set. Moreover, modelling used the data of the first 17 h because after this time point to many hyphae had formed that obscured other objects.

#### *Analysing micro-colony diameter and biomass*

Bright field images of micro-colonies were converted to binary images by thresholding. Micro-colonies were automatically segmented using the particle analysis tool in Image J with a size  $> 500$  square pixel (i.e.  $100 \mu\text{m}^2$ ), to get rid of small debris, and a circularity between 0.5 and 1.

The diameter of micro-colonies was calculated using the formula  $2 \cdot \sqrt{\frac{area}{\pi}}$  assuming that micro-colonies are circular. More than 120 pellets were analyzed per sample using biological triplicates and analyzed using one-way ANOVA followed by a Dunnett's T3 post-hoc tests for multiple comparisons ( $p \leq 0.05$ ). To determine biomass, mycelium of biological triplicates was filtered over filter paper, washed twice with distilled water, dried at 60 °C, and weighed. Biomass was analyzed using one-way ANOVA followed by Games-Howell post-hoc test for multiple comparisons ( $p \leq 0.05$ ).

### *SDS-PAGE*

Proteins contained in 400 µl culture medium were precipitated overnight at -20 °C with four volumes pre-cooled acetone, pelleted at 4 °C at 20,000 g for 30 min, washed with 400 µl acetone and dissolved in 20 µl loading buffer (20% glycerol, 4% SDS, 100 mM Tris-HCL pH 6.8, 0.01% bromophenol blue). Proteins were separated in 12.5% SDS-polyacrylamide gels using TGS buffer (30 g Tris base, 144 g glycine, and 10 g SDS l<sup>-1</sup>). Gels were stained in 0.02% Coomassie Brilliant Blue G-250 (CBB), 5% Al<sub>2</sub>(SO<sub>4</sub>)<sub>3</sub>(14-18)-hydrate, 10% ethanol and 2% phosphoric acid and destained in 10% ethanol and 2% phosphoric acid (Krijgsheld et al., 2012).

### *Mass spectrometry:RP-nanoLC-MS/MS*

Pellets were harvested and excess water was removed with tissue paper. A total of 50 mg wet weight mycelium was taken up in 100 µl lysis buffer (1 pill cOmplete protease inhibitor [Roche, Switzerland] dissolved in 10 ml 100 mM Tris, 10% SDS, pH 8.47) and centrifuged at 20,000 g for 30 min. 20 µl supernatant was loaded on a SDS PAGE gel (see previous section), separated for 2-3 cm, and stained with colloidal CBB. Gel pieces containing the cellular proteins were reduced, alkylated and digested overnight with trypsin at 37 °C. Peptides were extracted with 100% acetonitrile (ACN) and dried in a vacuum concentrator. Samples were resuspended in 10% (v/v) formic acid and subjected to LC-LC MS/MS using a Thermo Ultimate 3000 coupled to an Orbitrap Exploris 480 mass spectrometer (Thermo Scientific, Bremen, Germany). To this end, peptides were loaded on a C18 PepMAP column (5 µm, 5 mm × 300 µm; Thermo Scientific) using solvent A (0.1% formic acid) before being separated on an analytical column (Agilent Poroshell EC-C18, 2.7 µm, 50 cm × 75 µm). Proteins were eluted during a 104 min run with the following gradient: 9 -13% solvent B (0.1% formic acid in 80% acetonitrile) in 1 min, 13 - 44% solvent B in 95 min, 44 - 99% solvent B in 3 min, 99% solvent B for 4 min and back to 9% solvent B in 1 min. The mass spectrometer was operated in data-

dependent mode. Full-scan MS spectra from  $m/z$  375 - 1600 were acquired at a resolution of 60 000 at  $m/z$  200 after accumulation to the standard target value. Cycle time of 2 sec for the 104 min gradient with standard AGC targets. HCD fragmentation was performed at normalized collision energy of 28.

#### *Proteomics data analysis*

Raw data was analyzed with MaxQuant software (version 1.6.8.0) using label-free quantification (Cox et al., 2011). A false discovery rate (FDR) of 0.01 for peptides and a minimum peptide length of 7 amino acids were required. MS/MS spectra were searched against the database using the Andromeda search engine. Trypsin allowing N-terminal cleavage to proline was selected for enzyme specificity. Cysteine carbamidomethylation was selected as fixed modification, while protein N-terminal acetylation and methionine oxidation were selected as variable modifications. Up to two missing cleavages were allowed. Initial mass deviation of precursor ion was up to 7 ppm, mass deviation for fragment ions was 0.05 Dalton. Protein identification required one unique peptide to the protein group and match between run was enabled. In all cases, 4 biological replicates and at least 2 technical replicates were used. All correction analyses were carried out with Perseus software Version 1.6.10.0. Proteins were considered as present when they had been identified in at least 3 out of 4 biological replicates. Protein expression was calculated using R package “DESeq2” and GO analysis was done as described (Ashburner et al., 2000). The Benjamini-Hochberg was used to reduce false positives at  $p \leq 0.05$ . Signal peptide analysis was done as described (Petersen et al., 2011).

## **RESULTS**

### *Impact of inactivation of *pyrG*/*pyr4* on morphology, biomass and protein secretion of *A. niger**

Genetically related *A. niger* strains (Figure 2) showed different morphologies when grown in liquid shaken cultures according to their *pyrG* genotype. Auxotrophic *pyrG* mutants (MA169.4 or AB1.13 *pyrG*<sup>-</sup>) are hardly grown in MM-X and formed small micro-colonies in the presence of uridine in the medium (Figure 2B). Similarly,  $\Delta$ *pyrG* derivatives (DA001 or DA002) that had been complemented with the *pyr4* gene of *N. crassa* (with its own regulatory sequences) formed small micro-colonies, while wild-type strains (N402) or strains complemented with *pyrG* (MA234.1, AB4.1 *pyrG*<sup>+</sup>) formed large micro-colonies despite the presence of uridine in the medium. This observation led us to systematically assess the role of *pyrG* and its orthologue *pyr4* in colony morphology as well as biomass formation and profiles of secreted

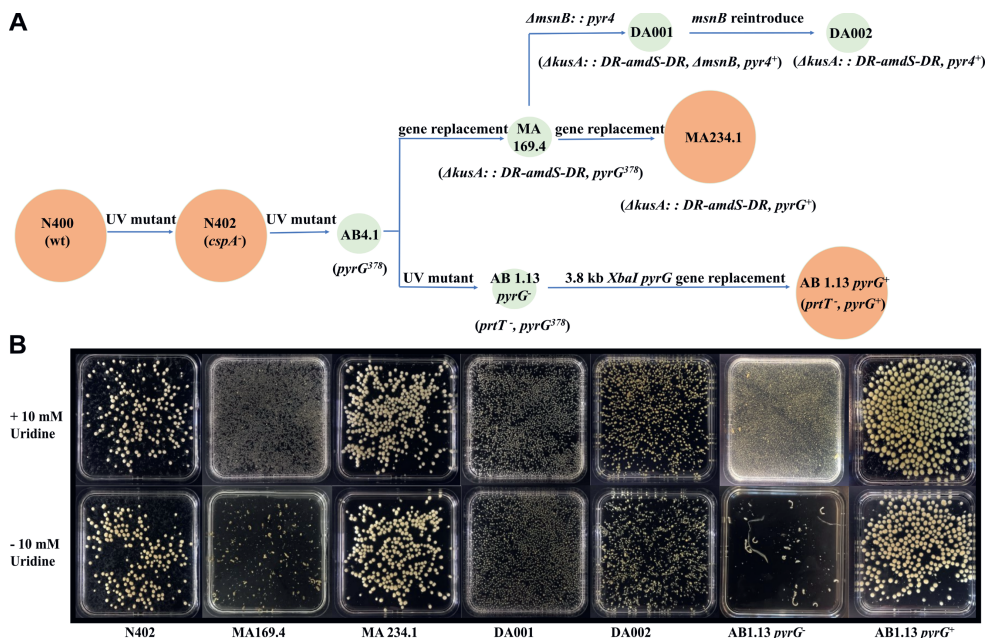


**Figure 2.** Lineage (A) and morphology (B) of *A. niger* strains showing large or small micro-colonies when grown in the absence and presence of uridine. Strains in big orange and small light green circles develop large and small micro-colonies in liquid shaken cultures, respectively.

proteins. To this end, *pyrG*<sup>-</sup> strain MA169.4 was complemented at the *pyrG* locus with the coding and regulatory sequences of *pyr4* of *N. crassa* resulting in strain LZ01. In addition, the locus of *pyrG* in MA234.1 and MA169.4 was replaced by an inducible *Tet-on* promoter that controlled *pyrG* and *pyr4*, respectively, resulting in strains LZ02 and LZ03. Strains MA234.1 and LZ01 are prototrophic for uridine. In contrast, the *Tet-on* strains need uridine in the medium in the absence of the *Tet-on* inducer doxycycline.

Strains MA234.1, LZ01, LZ02, and LZ03 were grown in liquid shaken cultures in the presence or absence of uridine and doxycycline. Cultures were grown for 16 h in complete TM-X medium, after which the mycelium was transferred to defined MM-X prolonging growth for an additional 32 h. Phenotypes (see below) were similar in the doxycycline range 5-20  $\mu\text{g ml}^{-1}$  in the case of LZ02 (*Tet-on:pyrG*), while this range was 10-20  $\mu\text{g ml}^{-1}$  in the case of LZ03 (*Tet-on:pyr4*) (Suppl. Figure 1). Therefore, it was decided to continue with 20  $\mu\text{g ml}^{-1}$  doxycycline as inducer concentration. MA234.1 cultures yielded 1.9  $\text{g l}^{-1}$  biomass irrespective of the presence of uridine and / or doxycycline. Biomass of strain LZ01 (*pyr4*) was not

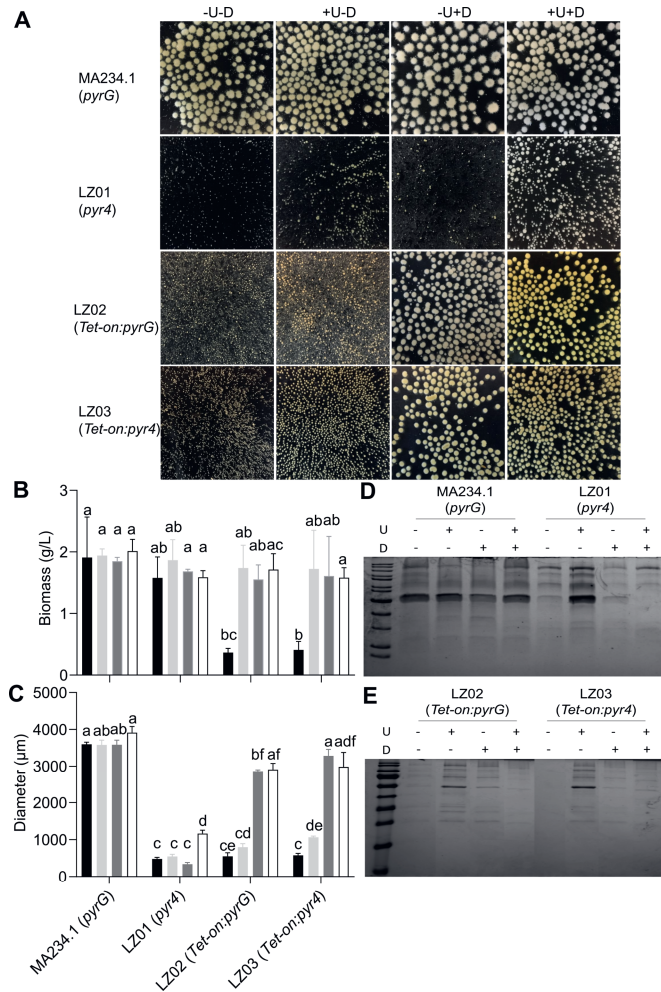


**Figure 3.** Morphology (A), biomass (B), pellet size (C), and protein profiles (D,E) of MA234.1, LZ01 (*pyr4*), LZ02 (*Tet-on:pyrG*) and LZ03 (*Tet-on:pyr4*). (A, D, E) absence and presence of 10 mM uridine (U) and 20  $\mu\text{g ml}^{-1}$  doxycycline (D); (B, C) without uridine and without doxycycline (black bar), with 10 mM uridine but without doxycyclin (light grey bar), with 20  $\mu\text{g ml}^{-1}$  doxycycline but without uridine (dark grey bar), with 10 mM uridine and with 20  $\mu\text{g ml}^{-1}$  doxycycline (white bar). Different letters indicate statistical differences as determined by a one-way ANOVA combined with a Dunnett's T3 post-hoc test for diameter and a Games-Howell post-hoc tests for biomass. Note that lanes of the gel in panel E have been re-ordered to be consistent with panel D.

statistically different from that of MA234.1 under all culture conditions (Figure 3B). Similarly, biomass of strains LZ02 (*Tet-on:pyrG*) and LZ03 (*Tet-on:pyr4*) was not different compared to MA234.1 when the culture medium contained uridine and / or doxycycline. In contrast, biomass was reduced > 5-fold in the absence of these supplements explained by the inability to sustain growth without the presence of uridine.

Pellet size of wild type strain MA234.1 was not affected by the presence of uridine and / or doxycycline in the culture medium with diameters ranging from 3583 to 3914  $\mu\text{m}$  (Figure 3C). In contrast, strain LZ01 (*pyr4*) produced micro-colonies ranging from 338 to 1165  $\mu\text{m}$  in the absence or presence of uridine and / or doxycycline (Figure 3C). Even the largest sized pellets that were obtained when LZ01 was grown in the presence of uridine and doxycycline showed a significant decrease in colony diameter when compared to the reference strain MA234.1. These data are consistent with previous observations that *pyrG*<sup>-</sup> strains produce smaller pellets when complemented with *pyr4*. Pellet sizes of LZ02 (*Tet-on:pyrG*) and LZ03 (*Tet-on:pyr4*) were 552 and 578  $\mu\text{m}$ , respectively, when these strains were grown in the absence of uridine and doxycycline. These sizes are probably explained by some activity of the *Tet-on* promoter in absence of the inducer (Huang et al., 2015). Supplementing the medium with uridine increased colony diameter to 796 and 1063  $\mu\text{m}$ , respectively. When 20  $\mu\text{g ml}^{-1}$  of doxycycline was added instead of uridine, LZ02 and LZ03 developed larger pellets with diameters of 2866 and 3287  $\mu\text{m}$ , respectively. Similar sizes (i.e. 2911 and 2985  $\mu\text{m}$ ) were found when cultures of LZ02 and LZ03, respectively, were grown in the presence of 20  $\mu\text{g ml}^{-1}$  doxycycline and 10 mM uridine. The increased colony size is consistent with the observation that an active *pyrG* results in large-sized micro-colonies. Moreover, results show that *pyr4* can fully complement *pyrG* when controlled by the *Tet-on* promoter.

Secretion profiles of MA234.1 were not affected by the absence or presence of uridine and / or doxycycline in the medium (Figure 3D, E). Strain LZ01 (*pyr4*) secreted more protein in the culture medium when compared to MA234.1 when grown in the absence of doxycycline and uridine and in the presence of uridine. In contrast, for unknown reason, doxycycline reduced secretion levels of LZ01 considerably (i.e. colony size was small but secretion was low). LZ02 (*Tet-on:pyrG*) and LZ03 (*Tet-on:pyr4*) secreted more protein when compared to MA234.1 when supplemented with uridine, correlating with their small micro-colony size. On the other hand, presence of doxycycline reduced levels of secreted protein, which was consistent with the large micro-colony phenotype.



*Germination assessment of strain pyrG and pyr4*

Micro-colony size is mainly determined by aggregation of spores and / germlings. Therefore, swelling and germ tube formation of spores of strains MA234.1, LZ01, LZ02, and LZ03 was monitored in TM-X with or without uridine and doxycycline. The maximum number of spores ( $P_{max}$ ) of MA234.1 that were triggered to swell and to form germ tubes in the 17 h of growth ranged between 77.5-83.96% and 56.97-61.99%, respectively, and was not affected by supplementation with uridine and / or doxycycline (Table 5).  $P_{max}$  of swelling and germination of LZ01 (*pyr4*) was in the same range as MA234.1 with 76.7-85.12% and 55.16-61.2%, respectively. This was also the case for LZ02 (*Tet-on:pyrG*) and LZ03 (*Tet-on:pyr4*). The  $\tau$  (time at which  $P = 0.5 P_{max}$ ) of swelling and germination was similar for MA234.1, LZ01, and LZ03 and ranged between 1-2.49 h and 2.52-4.59 h, respectively with or without supplements. Strain LZ02 showed a slower initiation of swelling with a  $\tau$  of 2.52-4.11 but its  $\tau$  of germination was similar to that of MA234.1 (Table 5). Taken together, swelling and germination of the strains was similar when cultured in TM-X and cannot explain the different morphologies in liquid shaken cultures.

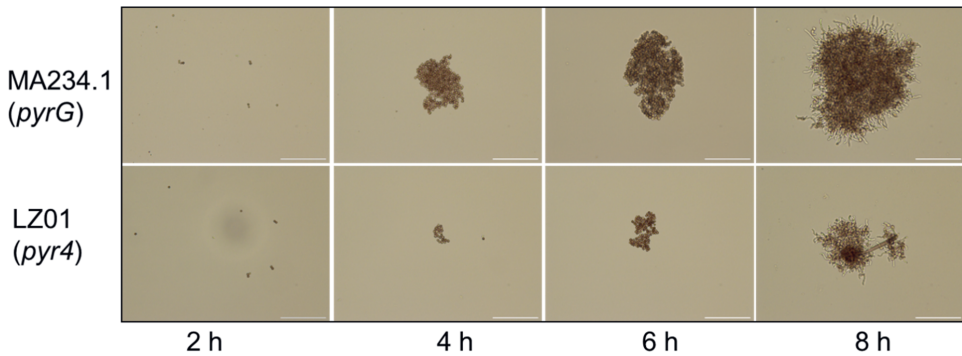


**Figure 4.** Morphology of spores/germlings of strain MA234.1 (*pyrG*) and LZ01 (*pyr4*) in liquid shaken cultures at different time points after inoculation. Bar represents 100  $\mu\text{m}$ .

*Cellular proteomics of strain pyrG and pyr4 during early germination* Aggregation of conidia of MA234.1 and LZ01 was monitored between 2 and 8 h after inoculation of liquid shaken cultures in TM-X. Light microscopy showed that spore clusters formed by LZ01 (*pyr4*) were smaller in size and also more loosely packed after 4 h of inoculation (Figure 4). At this time point, spores were swelling but had not yet formed germlings. The size difference in the spore



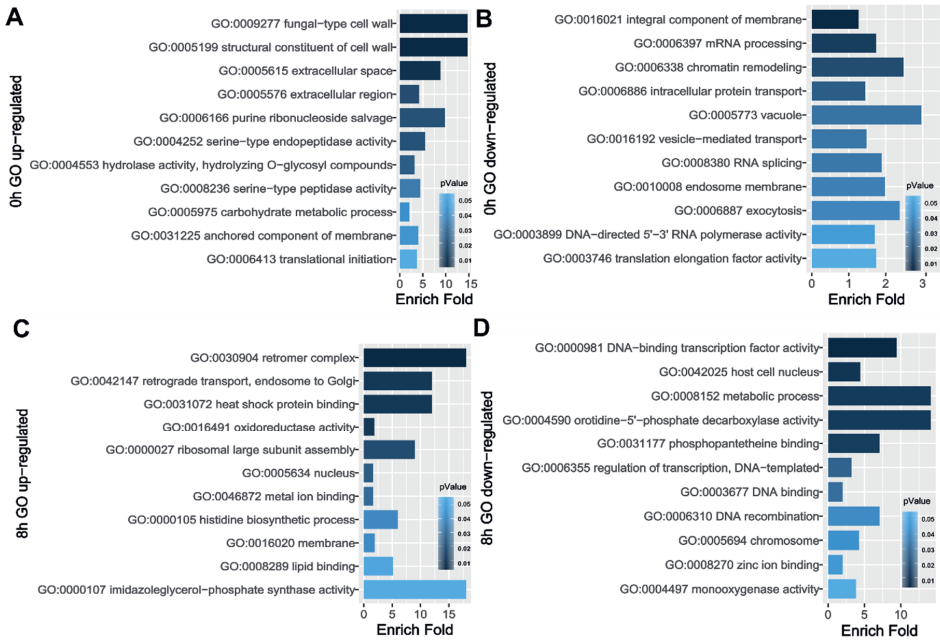


**Figure 5.** GO analysis of proteins up- and down-regulated in TM-X liquid shaken cultures of LZ01 when compared to MA234.1 at t = 0 h (A, B) and t = 8 h (C, D).

clusters between MA234.1 and LZ01 became more pronounced in time up to t = 8 h. At t = 6 h, spores had swollen but germlings had not yet formed, while at t = 8h germlings had formed. Together, data indicate that primary aggregation, and possibly also secondary aggregation, are affected in strain LZ01. To unveil how *pyrG/pyr4* impacts spore aggregation, cellular proteomics was performed for MA234.1 and LZ01 spores from 3-day-old PDA cultures (t = 0) and spores / germlings 8 h after inoculation in TM-X (Supplemental Table 1). GO analysis indicated that GO:0009277 fungal-type cell wall, GO:0005199 structure constituent of cell wall, GO:0005615 extracellular space and GO: 0005576 extracellular region are over-represented in the upregulated proteins, while GO:0016021 integral component membrane and GO:0006397 mRNA processing were most significantly downregulated in LZ01(*pyr4*) compared to MA234.1 (*pyrG*) at t = 0 h (Figure 5AB). A total of 181 and 898 proteins were significantly up- and down-regulated in LZ01 (*pyr4*) compared with MA234.1 (*pyrG*) at this time point (Supplemental Table 2), including 34 and 58 proteins with a predicted signal peptide, respectively.

**Table 5.** Parameter estimates of the asymmetrical model describing swelling and germ tube formation of strain MA234.1 (*pyrG*), LZ01 (*pyr4*), LZ02 (*Tet-on:pyrG*) and LZ03 (*Tet-on:pyr4*). Confidence intervals are indicated between brackets,  $P_{max}$  is the maximal percentage of swollen conidia or spores that had formed a germ tube,  $\tau$  (h) is the time at which  $P = 0.5 P_{max}$ .

Species	Medium	Parameter estimates			
		Pmax(%)		$\tau$ (h)	
<b>Swelling</b>					
MA234.1 ( <i>pyrG</i> )	TM	80.76	[76.86;84.66]	1	[0.77;1.23]
LZ01 ( <i>pyr4</i> )	TM	79.04	[75.74;82.34]	1	[0.8;1.2]
LZ02 ( <i>Tet-on:pyrG</i> )	TM	88.44	[82.73;94.15]	4.11	[3.71;4.5]
LZ03 ( <i>Tet-on:pyr4</i> )	TM	89.39	[83.71;95.06]	1.05	[0.76;1.34]
MA234.1 ( <i>pyrG</i> )	TM-D	80.37	[78.7;82.05]	2.49	[2.36;2.62]
LZ01 ( <i>pyr4</i> )	TM-D	82.95	[81;84.91]	2.14	[1.99;2.28]
LZ02 ( <i>Tet-on:pyrG</i> )	TM-D	80.24	[75.93;84.55]	3.61	[3.26;3.95]
LZ03 ( <i>Tet-on:pyr4</i> )	TM-D	77.42	[75.73;79.12]	2.01	[1.88;2.15]
MA234.1 ( <i>pyrG</i> )	TM-U	83.96	[82.42;85.5]	2.15	[2.05;2.25]
LZ01 ( <i>pyr4</i> )	TM-U	85.12	[83.18;87.06]	1.82	[1.68;1.95]
LZ02 ( <i>Tet-on:pyrG</i> )	TM-U	84.39	[81.26;87.51]	3.5	[3.26;3.73]
LZ03 ( <i>Tet-on:pyr4</i> )	TM-U	83.01	[80.86;85.16]	2.05	[1.89;2.21]
MA234.1 ( <i>pyrG</i> )	TM-UD	77.51	[75.6;79.42]	1.93	[1.78;2.08]
LZ01 ( <i>pyr4</i> )	TM-UD	76.7	[74.82;78.57]	1.66	[1.52;1.81]
LZ02 ( <i>Tet-on:pyrG</i> )	TM-UD	84.58	[79.98;89.18]	2.52	[2.21;2.83]
LZ03 ( <i>Tet-on:pyr4</i> )	TM-UD	76.58	[72.68;80.48]	1.5	[1.26;1.74]
<b>Germ tube formation</b>					
MA234.1 ( <i>pyrG</i> )	TM	61.99	[50.69;73.29]	2.52	[1.58;3.46]
LZ01 ( <i>pyr4</i> )	TM	59.97	[49.33;70.61]	3.45	[2.39;4.52]
LZ02 ( <i>Tet-on:pyrG</i> )	TM	90.44	[84;96.88]	5.5	[4.94;6.07]
LZ03 ( <i>Tet-on:pyr4</i> )	TM	69.25	[56.32;82.18]	3.64	[2.5;4.78]
MA234.1 ( <i>pyrG</i> )	TM-D	57.56	[54.06;61.07]	4.22	[3.83;4.61]
LZ01 ( <i>pyr4</i> )	TM-D	61.12	[56.82;65.41]	4.31	[3.86;4.76]
LZ02 ( <i>Tet-on:pyrG</i> )	TM-D	68.38	[59.56;77.19]	5.03	[4.2;5.85]
LZ03 ( <i>Tet-on:pyr4</i> )	TM-D	57.26	[53.44;61.08]	3.68	[3.28;4.09]
MA234.1 ( <i>pyrG</i> )	TM-U	56.97	[54.15;59.79]	4.38	[4.06;4.7]
LZ01 ( <i>pyr4</i> )	TM-U	55.6	[52.13;59.07]	4.59	[4.18;4.99]
LZ02 ( <i>Tet-on:pyrG</i> )	TM-U	68.4	[60.48;76.31]	5.72	[4.99;6.45]
LZ03 ( <i>Tet-on:pyr4</i> )	TM-U	56.67	[52.89;60.45]	4.43	[4;4.87]
MA234.1 ( <i>pyrG</i> )	TM-UD	57.6	[52.64;62.55]	3.6	[3.08;4.13]
LZ01 ( <i>pyr4</i> )	TM-UD	55.16	[49.84;60.47]	3.72	[3.14;4.31]
LZ02 ( <i>Tet-on:pyrG</i> )	TM-UD	68.48	[54.55;82.4]	4.5	[3.09;5.91]
LZ03 ( <i>Tet-on:pyr4</i> )	TM-UD	57.91	[48.96;66.87]	3.54	[2.62;4.45]



(Supplemental Table 2), including 34 and 58 proteins with a predicted signal peptide, respectively. A total of 11 out of the 34 proteins are related to the cell wall. This protein set consists of three glucanases, one glucan synthase and seven cell wall proteins. The latter set included the hydrophobins HypB, HypC and HypE and the hydrophobic surface binding protein A (Table 6). A total of 5 proteins with signal peptides that are related to the cell wall synthesis were downregulated in LZ01 at  $t = 0$  h, including 2 glucanases, a glucan synthase, and 2 cell wall proteins (Table 6).

At  $t = 8$  h, GO:0030904 retromer complex and GO: retrograde transport, endosome to Golgi were significantly upregulated, while GO:0000981 DNA-binding transcription factor activity and GO:0042025 host cell nucleus were the most significantly downregulated in strain *pyr4* compared to strain *pyrG* (Figure 5CD). Notably, GO:0004590 orotidine-5'-phosphate decarboxylase activity was also significantly downregulated, which is consistent with our data that the *pyr4* promoter is weaker compared to that of *pyrG* (Figure 5CD). 148 and 189 proteins were up- and down-regulated in LZ01 when compared to MA234.1, of which only 6 and 9 proteins are predicted to have a signal peptide for secretion, respectively (Supplemental Table 2). Both these groups contained two cell wall related proteins. Two glucan synthases were up-regulated (one of which was also upregulated at  $t = 0$  h), while two glucanases were down-regulated (one of which was also downregulated at  $t = 0$  h) (Table 6).

**Table 6.** Cell wall related proteins with a predicted signal peptide that are up- or down-regulated in strain LZ01 (*pyr4*) compared to strain MA234.1 (*pyrG*) at  $t = 0$  h and  $t = 8$  h after inoculation in TM-X liquid shaken cultures.

Protein ID	Annotation	GO
<b>0 h upregulated proteins</b>		
ATCC64974_106780	CFEM (common in several fungal extracellular membrane proteins) domain protein	Anchored component of membrane; cell wall; plasma membrane; kinase activity
ATCC64974_67640	Extracellular matrix protein	Integral component of membrane
ATCC64974_84130 ( <i>HypC</i> )	Hydrophobin	Extracellular region; fungal-type cell wall; dioxygenase activity; structural constituent of cell wall
ATCC64974_45620 ( <i>HypE</i> )	Conidial hydrophobin Hyp1 RodA	Extracellular region; fungal-type cell wall; structural constituent of cell wall
ATCC64974_55200	Splits internally a 1,3-beta-glucan molecule and transfers the newly generated reducing end (the donor) to the non-reducing end of another 1,3-beta-glucan molecule (the acceptor) forming a 1,3-beta linkage	Anchored component of membrane; plasma membrane; transferase activity
ATCC64974_8860	Hydrophobic surface binding protein A	
ATCC64974_97830	Cell wall glucanase (Scw4)	

ATCC64974_84110 ( <i>HypB</i> )	Hydrophobin	Fungal-type cell wall; structural constituent of cell wall
ATCC64974_20630	Endo-1,3-beta-glucanase Eng11	Glucan endo-1,3-beta-glucanase activity, C-3 substituted reducing group; glucan endo-1,4-beta-glucanase activity, C-3 substituted reducing group; metabolic process
ATCC64974_77280	GPI-anchored cell wall organization protein Ecm33	Integral component of membrane
ATCC64974_13390	Exo-beta-1,3-glucanase Exg0	extracellular region; transferase activity
<b>0 h downregulated proteins</b>		
ATCC64974_11650	Lactonase, 7-bladed beta-propeller	Protein binding
ATCC64974_48560	Cell wall glucanase (Utr2)	Anchored component of membrane;cell wall;plasma membrane;hydrolase activity, acting on glycosyl bonds;hydrolase activity, hydrolyzing O-glycosyl compounds;carbohydrate metabolic process;cell wall organization
ATCC64974_49190	Allergen asp	Extracellular region;IgE binding
ATCC64974_6440	Splits internally a 1,3-beta-glucan molecule and transfers the newly generated reducing end (the donor) to the non- reducing end of another 1,3-beta-glucan molecule (the acceptor) forming a 1,3-beta linkage	Anchored component of membrane; plasma membrane; dioxygenase activity; transferase activity
ATCC64974_74980	Glucanase that may be involved in beta-glucan degradation and may also function biosynthetically as a transglycosylase	Cell wall; plasma membrane; hydrolase activity, hydrolyzing O-glycosyl compounds; kinase activity; carbohydrate metabolic process; polysaccharide catabolic process
<b>8 h upregulated proteins</b>		
ATCC64974_55200	Splits internally a 1,3-beta-glucan molecule and transfers the newly generated reducing end (the donor) to the non- reducing end of another 1,3-beta-glucan molecule (the acceptor) forming a 1,3-beta linkage	Anchored component of membrane; plasma membrane; transferase activity
ATCC64974_75630	Splits internally a 1,3-beta-glucan molecule and transfers the newly generated reducing end (the donor) to the non- reducing end of another 1,3-beta-glucan molecule (the acceptor) forming a 1,3-beta linkage	Anchored component of membrane; integral component of membrane; plasma membrane; transferase activity
<b>8 h downregulated proteins</b>		
ATCC64974_20630	Endo-1,3-beta-glucanase Eng11	Glucan endo-1,3-beta-glucanase activity, C-3 substituted reducing group; glucan endo-1,4-beta-glucanase activity, C-3 substituted reducing group; metabolic process
ATCC64974_74980	Glucanase that may be involved in beta-glucan degradation and also may also function biosynthetically as a transglycosylase	Cell wall; plasma membrane;hydrolase activity, hydrolyzing O-glycosyl compounds; kinase activity; carbohydrate metabolic process; polysaccharide catabolic process

## DISCUSSION

Here it is shown that also expression of the orotidine 5'-phosphate decarboxylase gene impacts morphology of micro-colonies in liquid shaken cultures. The orotidine 5'-phosphate decarboxylase gene *pyr4* from *N. crassa* is an orthologue of *pyrG* in *A. niger* (Diez et al., 1987), however, complementation of a *pyrG*<sup>-</sup> strain of *A. niger* with *pyr4* and *pyrG* results in different sized micro-colonies without affecting biomass formation. The latter formed large micro-

colonies like a wild type strain ( $\geq 3000 \mu\text{m}$ ), while the former formed micro-colonies with a diameter  $\leq 1000 \mu\text{m}$ . We hypothesized that *pyrG* is a moonlighting protein that is involved in uridine biosynthesis as well as in micro-colony formation. Following this hypothesis, *pyr4* would only rescue the phenotype of uridine biosynthesis. To test this hypothesis both *pyrG* and *pyr4* were expressed from the inducible *Tet-on* promoter system. This resulted in strains forming similar sized micro-colonies, thereby showing that the *pyr4* promoter is probably lower in activity than that of *pyrG* and falsifying the hypothesis of PyrG being a moonlighting protein. The germination of spores expressing *pyr4* from its own regulatory sequences was similar to that of *pyrG* expressing spores. Thus, also germination was not causing different sized micro-colonies. In contrast, primary aggregation (and may be secondary aggregation) of spores was reduced in spores of a *pyr4* expressing strain when compared to a *pyrG* strain (both under control of their own regulatory sequences). So, the former strain is of the non-coagulative type, while the latter is of the coagulative type. The coagulative type spores aggregate fast and subsequently germinate, while spores of the non-coagulative type germinate before pellet formation (Pirt, 1966; Nielsen et al., 1995). We reasoned that differences in spore aggregation between the *pyr4* and *pyrG* strains (both under control of their own regulatory sequences) is due to differences in the cell wall composition and / or cell wall architecture. Cellular proteomics revealed differences in cell wall-related proteins, particularly glucanases, glucan synthases, glycosyltransferases and hydrophobins. Differential expression of one or more of these proteins may explain why the *pyr4* and *pyrG* strains aggregate differently.

## REFERENCES

- Aerts, D. 2018. Regulators controlled by the sporulation gene *flbA* of *Aspergillus niger*. *PhD Thesis, Utrecht University*.
- Ashburner, M., Ball, C.A., Blake, J.A., Botstein, D., Butler, H., Cherry, J.M., Davis, A.P., Dolinski, K., Dwight, S.S., Eppig, J.T., Harris, M.A., Hill, D.P., Issel-Tarver, L., Kasarskis, A., Lewis, S., Matese, J.C., Richardson, J.E., Ringwald, M., Rubin, G.M., Sherlock, G. 2000. Gene ontology: tool for the unification of biology. *Nat Genet*, **25**, 25-29.
- Beygelzimer, A., Kakadet, S., Langford, J., Arya, S., Mount, D., Li, S. 2019. FNN, R package version 1.1.3. <https://cran.r-project.org/packages=FNN>.
- Bos, C.J., Debets, A.J., Swart, K., Huybers, A., Kobus, G., Slakhorst, S.M. 1988. Genetic analysis and the construction of master strains for assignment of genes to six linkage groups in *Aspergillus niger*. *Curr Genet*, **14**, 437-443.

- Cox, J., Neuhauser, N., Michalski, A., Scheltema, R.A., Olsen, J.V., Mann, M. 2011. Andromeda: a peptide search engine integrated into the MaxQuant environment. *J Proteome Res*, **10**, 1794-1805.
- Dantigny, P., Nanguy, S.P.M., Judet-Correia, D., Bensoussan, M. 2011. A new model for germination of fungi. *Int J Food Microbiol*, **146**, 176-181.
- Demirci, E., Arentshorst, M., Yilmaz, B., Swinkels, A., Reid, I.D., Visser, J., Tsang, A., Ram, A.F.J. 2021. Genetic characterization of mutations related to conidiophore stalk length development in *Aspergillus niger* laboratory strain N402. *Front Genet*, **12**, 666684.
- de Bekker, C., Wiebenga, A., Aguilar, G., Wösten, H.A. 2009. An enzyme cocktail for efficient protoplast formation in *Aspergillus niger*. *J Microbiol Methods*, **76**, 305-306.
- de Vries, R.P., Burgers, K., van de Vondervoort, P.J., Frisvad, J.C., Samson, R.A., Visser, J. 2004. A new black *Aspergillus* species, *A. vadensis*, is a promising host for homologous and heterologous protein production. *Appl Environ Microbiol*, **70**, 3954-3959.
- Diez, B., Alvarez, E., Cantoral, J.M., Barredo, J.L., Martin, J.F. 1987. Selection and characterization of *pyrG* mutants of *Penicillium chrysogenum* lacking orotidine-5'-phosphate decarboxylase and complementation by the *pyr4* gene of *Neurospora crassa*. *Curr Genet*, **12**, 277-282.
- Fontaine, T., Beauvais, A., Loussert, C., Thevenard, B., Fulgsang, C.C., Ohno, N., Clavaud, C., Prevost, M.C., Latge, J.P. 2010. Cell wall  $\alpha$ 1-3glucans induce the aggregation of germinating conidia of *Aspergillus fumigatus*. *Fungal Genet Biol*, **47**, 707-712.
- Fredborg, M., Andersen, K.R., Jørgensen, E., Droce, A., Olesen, T., Jensen, B.B., Rosenvinge, F.S., Sondergaard, T.E. 2013. Real-Time optical antimicrobial susceptibility testing. *J Clin Microbiol*, **51**, 2047-2053.
- Grimm, L.H., Kelly, S., Hengstler, J., Gobel, A., Krull, R., Hempel, D.C. 2004. Kinetic studies on the aggregation of *Aspergillus niger* conidia. *Biotechnol Bioeng*, **87**, 213-218.
- He, X., Li, S., Kaminskyj, S.G. 2014. Characterization of *Aspergillus nidulans*  $\alpha$ -glucan synthesis: roles for two synthases and two amylases. *Mol Microbiol*, **91**, 579-595.
- Huang, H.H., Seeger, C., Danielson, U.H., Lindblad, P. 2015. Analysis of the leakage of gene repression by an artificial TetR-regulated promoter in cyanobacteria. *BMC Res Notes*, **8**, 459.
- Ijadpanahsaravi, M., Punt, M., Wösten, H.A.B., Teertstra, W.R. 2021. Minimal nutrient requirements for induction of germination of *Aspergillus niger* conidia. *Fungal Biol*, **125**, 231-238.

- Krijghsheld, P., Altelaar, A.F., Post, H., Ringrose, J.H., Muller, W.H., Heck, A.J., Wösten, H.A.B. 2012. Spatially resolving the secretome within the mycelium of the cell factory *Aspergillus niger*. *J Proteome Res*, **11**, 2807-2818.
- Krijghsheld, P., Bleichrodt, R., van Veluw, G.J., Wang, F., Muller, W.H., Dijksterhuis, J., Wösten, H.A.B. 2013. Development in *Aspergillus*. *Stud Mycol*, **74**, 1-29.
- Liu, D., Coloe, S., Baird, R., Pederson, J. 2000. Rapid mini-preparation of fungal DNA for PCR. *J Clin Microbiol*, **38**, 471.
- Mattern, I.E., van Noort, J.M., van den Berg, P., Archer, D.B., Roberts, I.N., van den Hondel, C.A. 1992. Isolation and characterization of mutants of *Aspergillus niger* deficient in extracellular proteases. *Mol Gen Genet*, **234**, 332-336.
- Meyer, V., Ram, A.F., Punt, P.J. 2010. Genetics, genetic manipulation, and approaches to strain improvement of filamentous fungi. *Manual of Industrial Microbiology and Biotechnology, Third Edition*, 318-329.
- Meyer, V., Wanka, F., van Gent, J., Arentshorst, M., van den Hondel, C.A., Ram, A.F. 2011a. Fungal gene expression on demand: an inducible, tunable, and metabolism-independent expression system for *Aspergillus niger*. *Appl Environ Microbiol*, **77**, 2975-2983.
- Meyer, V., Wu, B., Ram, A.F. 2011b. *Aspergillus* as a multi-purpose cell factory: current status and perspectives. *Biotechnol Lett*, **33**, 469-476.
- Miyazawa, K., Yoshimi, A., Zhang, S., Sano, M., Nakayama, M., Gomi, K., Abe, K. 2016. Increased enzyme production under liquid culture conditions in the industrial fungus *Aspergillus oryzae* by disruption of the genes encoding cell wall  $\alpha$ -1,3-glucan synthase. *Biosci Biotechnol Biochem*, **80**, 1853-1863.
- Nielsen, J., Johansen, C.L., Jacobsen, M., Krabben, P., Villadsen, J. 1995. Pellet formation and fragmentation in submerged cultures of *Penicillium chrysogenum* and its relation to penicillin production. *Biotechnol Prog*, **11**, 93-98.
- Nodvig, C.S., Hoof, J.B., Kogle, M.E., Jarczynska, Z.D., Lehmbeck, J., Klitgaard, D.K., Mortensen, U.H. 2018. Efficient oligo nucleotide mediated CRISPR-Cas9 gene editing in *Aspergilli*. *Fungal Genet Biol*, **115**, 78-89.
- Park, J., Hulsman, M., Arentshorst, M., Breeman, M., Alazi, E., Lagendijk, E.L., Rocha, M.C., Malavazi, I., Nitsche, B.M., van den Hondel, C.A., Meyer, V., Ram, A.F. 2016. Transcriptomic and molecular genetic analysis of the cell wall salvage response of *Aspergillus niger* to the absence of galactofuranose synthesis. *Cell Microbiol*, **18**, 1268-1284.

- Petersen, T.N., Brunak, S., von Heijne, G., Nielsen, H. 2011. SignalP 4.0: discriminating signal peptides from transmembrane regions. *Nat Methods*, **8**, 785-786.
- Petzoldt, T. 2019. GrowthRates, R package version 0.8.1. <https://cran.r-project.org/packages=GrowthRates>.
- Pirt, S.J. 1966. A theory of the mode of growth of fungi in the form of pellets in submerged culture. *Proc R Soc Lond B Biol Sci*, **166**, 369-373.
- Tegelaar, M., Aerts, D., Teertstra, W.R., Wösten, H.A.B. 2020. Spatial induction of genes encoding secreted proteins in micro-colonies of *Aspergillus niger*. *Sci Rep*, **10**, 1536.
- van Hartingsveldt, W., Mattern, I.E., van Zeijl, C.M., Pouwels, P.H., van den Hondel, C.A. 1987. Development of a homologous transformation system for *Aspergillus niger* based on the *pyrG* gene. *Mol Gen Genet*, **206**, 71-75.
- van Leeuwe, T.M., Arentshorst, M., Ernst, T., Alazi, E., Punt, P.J., Ram, A.F.J. 2019. Efficient marker free CRISPR/Cas9 genome editing for functional analysis of gene families in filamentous fungi. *Fungal Biol Biotechnol*, **6**, 13.
- Wanka, F., Arentshorst, M., Cairns, T.C., Jorgensen, T., Ram, A.F., Meyer, V. 2016. Highly active promoters and native secretion signals for protein production during extremely low growth rates in *Aspergillus niger*. *Microb Cell Fact*, **15**, 145.
- Wösten, H.A.B. 2019. Filamentous fungi for the production of enzymes, chemicals and materials. *Curr Opin Biotechnol*, **59**, 65-70.
- Yoshimi, A., Sano, M., Inaba, A., Kokubun, Y., Fujioka, T., Mizutani, O., Hagiwara, D., Fujikawa, T., Nishimura, M., Yano, S., Kasahara, S., Shimizu, K., Yamaguchi, M., Kawakami, K., Abe, K. 2013. Functional analysis of the  $\alpha$ -1,3-glucan synthase genes *agsA* and *agsB* in *Aspergillus nidulans*: *agsB* is the major  $\alpha$ -1,3-glucan synthase in this fungus. *PLoS One*, **8**, e54893.

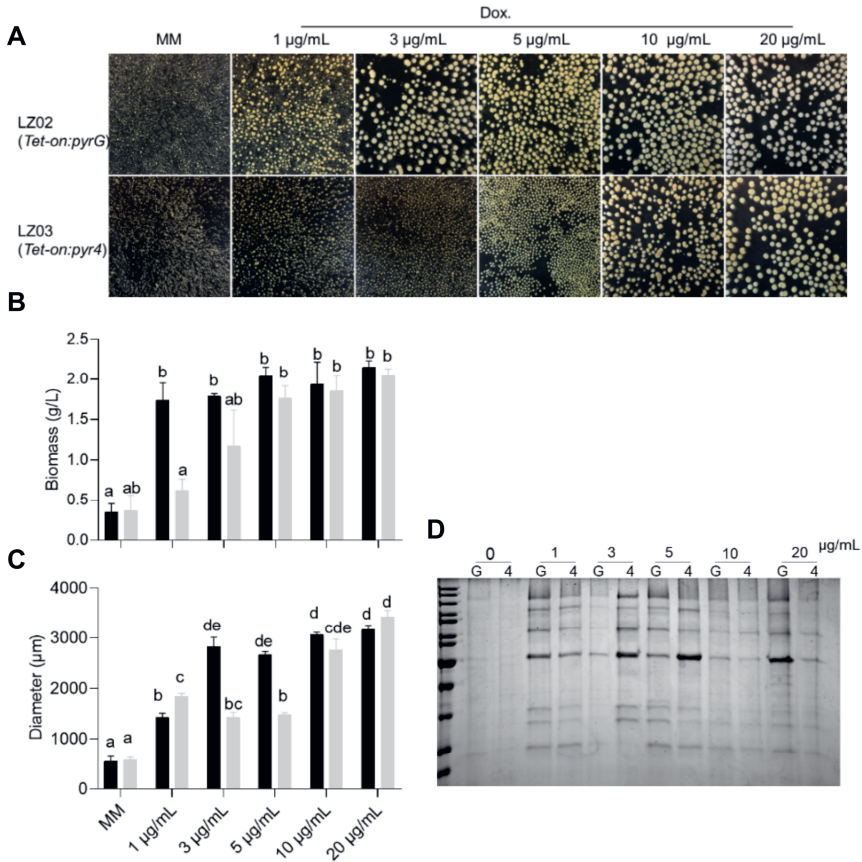
## SUPPLEMENTAL MATERIAL

**Supplemental Table 1.** Proteins identified by cellular proteomics of strains MA234.1 (*pyrG*) and LZ01(*pyr4*) at t = 0 h and t = 8 h of liquid shaken TM-X cultures. All four biological replicates are shown. <https://docs.google.com/spreadsheets/d/169YvxmdmB3uV2lSD0fa0wW9OrcflMxw2t/edit?usp=sharing&ouid=100415537618493008153&rtpof=true&sd=true>.



**Supplemental Table 2.** Significantly up- and downregulated proteins are identified by cellular proteomics of strain LZ01(*pyr4*) TM-X liquid shaken cultures compared to strain MA234.1(*pyrG*) at  $t = 0$  h and  $t = 8$  h ( $p < 0.05$ ).

[https://docs.google.com/spreadsheets/d/1dm7px5ingayN0RY1yzow2DSbyB4to\\_Mj/edit?usp=sharing&ouid=100415537618493008153&rtpof=true&sd=true](https://docs.google.com/spreadsheets/d/1dm7px5ingayN0RY1yzow2DSbyB4to_Mj/edit?usp=sharing&ouid=100415537618493008153&rtpof=true&sd=true).



**Supplemental Figure 1.** Morphology (A), pellet size (B), biomass (C), and protein profile (D) of strains LZ02 (*Tet-on:pyrG*) and LZ03 (*Tet-on:pyr4*) grown with different concentrations of doxycycline. (A-C) LZ02 (black bar), LZ03 (light grey bar); (D) G represents LZ02, while 4 represents LZ03. Different letters indicate statistical differences as determined by a one-way ANOVA combined with a Dunnet's T3 post-hoc test for diameter and a Games-Howell post-hoc tests for biomass.

## Chapter 5

**The  $\alpha$ -(1,3)-glucan synthase gene *agsE* impacts the secretome of liquid shaken cultures of *Aspergillus niger* by reducing micro-colony size**

*Jun Lyu, Costanza Torchia, Harm Post, Juan P. Moran Torres, A. F. Maarten Altelaar, Hans de Cock, and Han A. B. Wösten*

## ABSTRACT

*Aspergillus niger* is widely used as a cell factory for the industrial production of enzymes. Previously, it was shown that morphology of the *Aspergillus* mycelium impacts production of enzymes and that deletion of  $\alpha$ -1-3 glucan synthase genes results in smaller micro-colonies in liquid cultures. However, a direct relation between the secretome and deletion of  $\alpha$ -1-3 glucan synthase genes has not been assessed. Therefore, we here assessed the impact of deletion of the  $\alpha$ -1-3 glucan synthase genes *agsC* and *agsE* on productivity of *A. niger* cultures. Biomass formation was not affected in the deletion strains but pH of the culture medium had changed from 5.2 in the case of the wild-type to 4.6 and 6.4 for  $\Delta$ *agsC* and  $\Delta$ *agsE*, respectively. The diameter of the  $\Delta$ *agsC* micro-colonies was not affected in liquid cultures. In contrast, diameter of the  $\Delta$ *agsE* micro-colonies was reduced from  $3304 \pm 338 \mu\text{m}$  to  $1229 \pm 113 \mu\text{m}$ . Moreover, the  $\Delta$ *agsE* secretome was affected with 54 and 36 unique proteins with a predicted signal peptide in the culture medium of MA234.1 and the  $\Delta$ *agsE*, respectively. Results suggest that these strains have complementary activity on plant biomass degradation.

## INTRODUCTION

Aspergilli like *Aspergillus niger*, *Aspergillus oryzae*, *Aspergillus awamori*, *Aspergillus sojae*, and *Aspergillus terreus* are widely exploited as cell factories for the production of enzymes and metabolites (Meyer et al., 2011; Wösten et al., 2013; 2019). To this end, aspergilli are grown in bioreactors. In such cultures, aspergilli can grow as micro-colonies, also known as pellets, as a dispersed mycelium or in an intermediate state of pelleted and dispersed growth called clumps.

Pellet formation in bioreactors is the result of primary and secondary aggregation. These stages involve the interaction of non-germinated and germinated conidia, respectively (Grimm et al., 2004). Primary aggregation results from the hydrophobic nature of conidia due to the presence of hydrophobin and melanin layers at the outer surface of the spores. Inactivation of the *A. nidulans* hydrophobin genes *dewA* and *rodA* reduces aggregation of conidia and, as a consequence, results in smaller micro-colonies (Dynesen & Nielsen, 2003). Similarly, inactivation of the melanin synthesis gene *olvA* in *A. niger* results in reduced primary aggregation and smaller micro-colonies (van Veluw et al., 2013). Medium composition, agitation, and pH can also affect primary aggregation of *Aspergillus* conidia (Carlsen et al., 1996; Metz & Kossen, 1977) by impacting the hydrophobic interactions between the spores in the culture medium. Secondary aggregation results from the presence of  $\alpha$ -(1,3)-glucan at the surface of germinating conidia of aspergilli (Fontaine et al., 2010; He et al., 2014; Yoshimi et

al., 2013). Synthesis of  $\alpha$ -(1,3)-glucan in *A. nidulans* is mediated by the  $\alpha$ -(1,3)-glucan synthases *AgsA* and *AgsB* and the  $\alpha$ -amylases *AmyD* and *AmyG*. Inactivation of the main  $\alpha$ -(1,3)-glucan synthase gene *agsB* has no obvious phenotype on agar medium but reduces aggregation of germlings and, as a consequence, results in smaller micro-colonies in liquid shaken cultures (He et al., 2014; Yoshimi et al., 2013). Inactivation of the *A. nidulans*  $\alpha$ -amylase gene *amyG*, but not *amyD*, also reduces secondary aggregation (He et al., 2014). This effect has been explained by assuming that this gene is involved in the synthesis of the primer structure of  $\alpha$ -glucan (Marion et al., 2006).

A relation between morphology of the mycelium and yield of secreted enzymes or metabolites has been described. These results were based on studies where the morphology of the mycelium was changed by varying the culture conditions (Krijgsheld et al., 2013). Therefore, changes in yield and secretome composition could also have been the result of the changed culture conditions. Recently, two studies established a direct relation between mycelium morphology and productivity. By sorting large and small micro-colonies from the same liquid shaken culture it was shown that expression of genes encoding secreted proteins mainly occurs in a peripheral shell of the pellet (Tegelaar et al., 2020). Results indicated that pellets with a radius  $\leq$  of the width of the expression shell would be more productive in terms of protein secretion. In **Chapter 2**, mycelium morphology was controlled by different periods of pre-growth in alginate beads. Small micro-colonies secreted a higher amount and diversity of proteins in the culture medium when compared to large micro-colonies. Although the large micro-colonies were less productive, they did release their own unique set of proteins. In fact, cellulases released by large and small micro-colonies showed synergistic activity.

Here, the effects of deleting of *A. niger*  $\alpha$ -(1,3)-glucan synthase genes on biomass formation, morphology, pH of the culture medium and the secretome was assessed. To this end, *agsC* and *agsE* were deleted since these two out of five  $\alpha$ -(1,3)-glucan synthase genes are highly expressed in the first hours of growth in a liquid medium with xylose (Yuan et al., 2008). Inactivation of *agsC* only resulted in a lower pH of the culture medium, whereas deletion of *agsE* impacted micro-colony morphology as well as pH and the protein profiles in the culture medium. Data indicate that the wild-type strain and the  $\Delta$ *agsE* strain have complementary activity on plant substrates.

## MATERIAL AND METHODS

### *Strains and culture conditions*

*Aspergillus niger* strains (Table 1) were grown for 3 days at 30 °C on PDA plates. Conidia were harvested using a cotton swab and suspended in minimal medium (MM) (de Vries et al., 2004) or transformation medium (TM; MM with 0.5% yeast extract and 0.2% casamino acids) with 25 mM xylose (MM-X and TM-X, respectively). Hyphae were removed from the spore suspension by filtering through a syringe with cotton. Conidia were counted using a haemocytometer, after which  $2 \times 10^7$  spores were introduced in 50 ml TM-X in 250 ml Erlenmeyer flasks either or not in the presence of doxycycline. After 16 h of growth, the mycelium was transferred to 100 ml MM-X and growth was prolonged for 32 h. Biomass and culture medium were separated by using a 40 µm cell strainer (Corning, 352340, New York, United States).

**Table 1.** *A. niger* strains used in this study.

Strain	Genotype	Description	Reference
MA234.1	$\Delta$ kusA:DR-amdS-DR, <i>pyrG</i>	3.8 kb <i>XbaI pyrG</i> gene replacement in MA169.4	Park et al., 2016
LZ04	$\Delta$ <i>agsC</i>	Deletion of <i>agsC</i> in MA234.1	this study
LZ05	$\Delta$ <i>agsE</i>	Deletion of <i>agsE</i> in MA234.1	this study
LZ06	<i>Tet-on:agsE</i>	Inducible <i>agsE</i> in MA234.1	this study

### Gene editing in *A. niger*

A CRISPR-Cas system (Nodvig et al., 2018) was used to inactivate *agsC* (ATCC64974\_40950, AspGD) and *agsE* (ATCC64974\_10510, AspGD) of *A. niger* and to replace the promoter of the latter gene for the inducible Tet-on cassette. For gene inactivation, *agsC* sgRNA's sg01 and sg02 and *agsE* sgRNA's sg03 and sg04 (Table 2) were designed using CHOPCHOP (<https://chopchop.cbu.uib.no>) to produce two double strand breaks 254 and 232 bp before the start codon of *agsC* and *agsE* and 252 and 251 bp after the stop codon of these genes, respectively (Figure 1B, C). These sgRNA's were placed under control of an *A. niger* proline tRNA promoter and terminator in plasmid pFC332 (Table 3) that also contains the *cas9* gene and a hygromycin resistance cassette (Nodvig et al., 2018; van Leeuwe et al., 2019)(Figure 1A). The sgRNA expression cassettes were amplified in two parts using plasmids pTLL108.1 and pTLL109.2 (van Leeuwe et al., 2019) (Table 3) as templates for the 5' and 3' fragments consisting of PtRNA::sgRNA and sgRNA::TiRNA, respectively. Primer pairs 1/4 and 2/3 (Table 4) were used to amplify the 5' and 3' fragments followed by Gibson assembly into a PacI-linearized and dephosphorylated pFC332 vector using a Gibson reaction (Nodvig et al., 2018; Seekles et al., 2021) resulting in the *agsC* 5' cutting sgRNA plasmid pCT001 (Table 3). Similarly, primer pairs 1/6 and 2/5 (Table 4) were used to produce the *agsC* 3' cutting sgRNA

plasmid pCT002 (Table 3). Primer pairs 1/8 and 2/7 and 1/10 and 2/9 (Table 4) resulted in the *agsE* 5' and 3' cutting sgRNA plasmids pCT003 and pCT004, respectively (Table 3).

**Table 2.** sgRNA sequences used in this study.

sgRNA	Sequence
sg01	TCGTTTGCATTCTGTTTCTT
sg02	AGCACTTCTTCACCAAACCA
sg03	GTGTTTCTCTCGTTATCTGC
sg04	CCGTGCGATCGTGTCAAAA
sg06	CACCGGAAGCCATTCAGAG

**Table 3.** Plasmids used in this study.

Strain	Type	Description	Reference
pTLL108.1	/	<i>PtRNA::sgRNA</i>	van Leeuwe et al., 2019
pTLL109.2	/	<i>sgRNA::TtRNA</i>	van Leeuwe et al., 2019
pFC332	/	Contains <i>cas9</i> , a hygromycin resistance cassette and a PacI site for introducing a sgRNA	Nodvig et al., 2018; Seekles et al., 2021
pMT4	<i>PfraA::rTa2-M2::TcrgA, 7xTetO::Pmin</i>	Reverse activator controlled by <i>A. niger</i> <i>fraA</i> constitutive promoter. Chimeric promoter composed of 7 copies of Tet operator fused to minimal transcribing sequence of <i>A. nidulans</i> <i>gpdA</i> promoter.	unpublished
pCT001	sgRNA	<i>agsC</i> cut, 254 bp upstream of <i>agsC</i> CDS start codon	this study
pCT002	sgRNA	<i>agsC</i> cut, 252 bp downstream of <i>agsC</i> CDS stop codon	this study
pCT003	sgRNA	<i>agsE</i> cut, 232 bp upstream of <i>agsE</i> CDS start codon	this study
pCT004	sgRNA	<i>agsE</i> cut, 251 bp downstream of <i>agsE</i> CDS stop codon	this study
pJL006	sgRNA	<i>agsE</i> cut, 712 bp upstream of <i>agsE</i> CDS start codon	this study
pJL015	<i>Tet-on::agsE</i>	Tet-on promoter between 1000 bp flanks, the left flank 712-1712 bp upstream of the <i>agsE</i> start codon, while the right flank starts from the start codon	this study

To replace the *agsE* promoter for the inducible Tet-on cassette, sgRNA sg03 (cutting in its start codon; see above) was used combined with sgRNA sg06 (Table 2) that cuts 712 bp upstream in the promoter region (Figure 1D). To this end, the latter sgRNA was introduced in plasmid pFC332 (as described above) resulting in pJL006 (Table 3). The sgRNA expression cassette was amplified in two parts using plasmids pTLL108.1 and pTLL109.2 (van Leeuwe et al., 2019)(Table 3) as templates for the 5' (primer pair 1/14, Table 4) and 3' (primer pair 2/13, Table 4) fragments that consist of the *PtRNA::sgRNA* and *sgRNA::TtRNA*, respectively. The overlapping amplicons were assembled by a Gibson reaction into a PacI-linearized and dephosphorylated pFC332 vector (Nodvig et al., 2018; Seekles et al., 2021). Plasmid pJL015

**Table 4.** Primers used in this study.

Primer name	Primer Sequence
1. pTE1.Fwd	GTTTCCGCTGAGGGTTTAATACTCCGCCGAACGTACTG
2. pTE1.Rev	CTGTCTCGGCTGAGGTCTTAAAAAGCAAAAAGGAAGGTACAAAAAAGC
3. agsC.gRnaUp.Fwd	AAGAAACAGAAATGCAAACGAGTTTTAGAGCTAGAAATAGC
4. agsC.gRnaUp.Rev	TCGTTTGCAATTCTGTTTCTTGACGAGTTACTCGTTTCGT
5. agsC.gRnaDown.Fwd	TGGTTTGGTGAAGAAGTGCTGTTTTAGAGCTAGAAATAGC
6. agsC.gRnaDown.Rev	AGCACTTCTTCCAAACCAGACGAGCTTACTCGTTTCGT
7. agsE.gRnaUp.Fwd	GCAGATAACGAGAGAAACACGTTTTAGAGCTAGAAATAGC
8. agsE.gRnaUp.Rev	GTGTTTCTCTCGTTATCTGCGACGAGTTACTCGTTTCGT
9. agsE.gRnaDown.Fwd	TTTTGAACACGATCGCACGGGTTTTAGAGCTAGAAATAGC
10. agsE.gRnaDown.Rev	CCGTGCGATCGTGTTCAAAAGACGAGTTACTCGTTTCGT
11. agsC Repair Oligo	CCATTCGCAACTGCAGACTTCAGCTGCCAATTGTTTCATCCTTCGTAGGGATAACAG GGTAATGGGGGACTTCTTCCAC CAAACCATTCCCAGTAAGCACCAAGACCATAACAA
12. agsE Repair Oligo	AGATTTCACTCGTTAACGAAGCGTGCCTGTGTTTCTCTCGTTATCTAGGGATAACAG GGTAATGGGGGTGCGATCGTG TTCAAAGGTTTCAATGTAGATGGTATATTGCTA
13. agsE.Tet-on_cut.Fwd	CACCGGGAAGCCATTACAGAGTTTTAGAGCTAGAAATAGC
14. agsE.Tet-on_cut.Rev	CTCTGAATGGCTTCCCGGTGACGAGCTTACTCGTTTCGT
15. agsE.Uflank.Fwd	GAGTTTTTCAGCAAGATGACTACCGGACTACCACCAC
16. Tet-on:agsE.Uflank.Rev	TAAGACAGACCAGCCGAGGGTGAATGGCTTCCCGGTG
17. Tet-on.Fwd	CCCTCGGCTGGTCTGTCTTA
18. Tet-on.Rev	GGTGATGTCTGCTCAAGCG
19. Tet-on:agsE.Dflank.Fwd	CGCTTGAGCAGACATCACCATGAAGTGGGCTATTTCC
20. agsE.Dflank.Rev	TAGGAGATCTGCTCGAGAGGTAGTGCCGGATCAAACGC
21. pJET.Fwd	ACCTCTCGAGCAGATCTCCTAC
22. pJET.Rev	ATCTTGCTGAAAAACTCGAGCCATC
23. agsC.CK.Fwd	CCCACCCTAATCTATTCCGGG
24. agsC.CK.Rev	TGTCGCTGTTATTCCAGTCA
25. agsE.CK.Fwd	AACAATTCATACGAGTGAGCTG
26. agsE.CK.Rev	AGACAGGAGTAGGATGATGAAGAG
27. Tet-on:agsE.CK.Fwd	TTTCCCACTTCATCGCAGCT
28. Tet-on:agsE.CK.Rev	TAGATGGAACCAAAGGTATT

(Table 3) containing the inducible *Tet-on:agsE* cassette was used as repair substrate. The *Tet-on* promoter consists of a constitutively controlled transactivator CDS followed by a synthetic promoter based on a septuple tetracycline operator and an *Aspergillus* minimal promoter (Wanka et al., 2016). To construct pJL015, the *Tet-on* promoter fragment was amplified from pMT4 (Table 3) using primer pair 17/18 (Table 4). The inducible *Tet-on:agsE* cassette was preceded by 1000 bp upstream and downstream flanks of *agsE*. The upstream flank was obtained by amplifying the region upstream of the Cas9 cutting site in the promoter sequence

with primer pair 15/16 (Table 4) and the downstream flank starting in the *agsE* start codon using primer pair 19/20 (Table 4). The Tet-on promoter and the 2 homologous 1000 bp flanks were assembled into the pJET backbone (Figure 1D), which was amplified by using primer pair 21/22 (Table 4) and the commercial pJET template from CloneJET PCR Cloning Kit (ThermoFisher, Massachusetts, US) (Table 2). Primer pair 23/24 was designed to give a 9265 bp fragment in the wild-type and a 1098 bp band in the  $\Delta$ *agsC* strain, while primer pair 25/26 was designed to give a 9075 bp fragment in the wild-type and a 1082 bp band in the  $\Delta$ *agsE* strain. Primer pair 27/28 was designed to give a 1136 bp fragment in *Tet-on:agsE* strain while no band should be obtained in the wild type (forward primer binds to the Tet-on promoter).

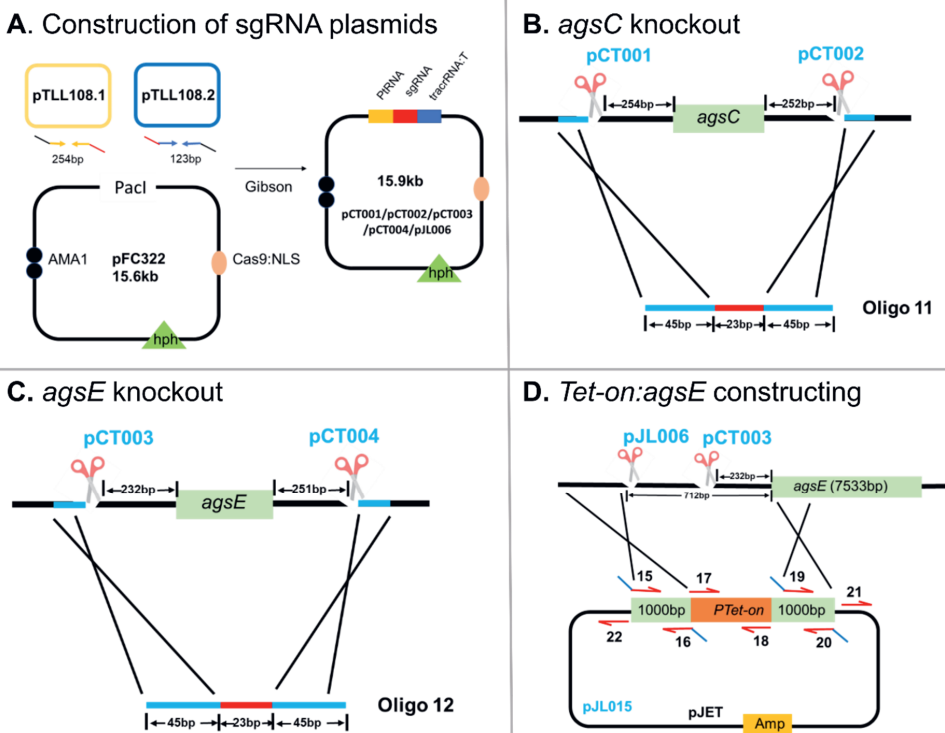


**Figure 1.** Construction of sgRNA plasmids (A) to delete *agsC* (B) and *agsE* (C) and to replace the *agsE* promoter for that of the inducible Tet-on system (D).

### Transformation of *A. niger*

The  $\Delta$ *kusA* strain MA234.1 (Park et al., 2016) (Table 1) was used to promote homologous recombination. Protoplasts were prepared according to de Bekker et al. (2009) and transformation was done as described (Meyer et al., 2010). Transforming DNA was taken up



in 20  $\mu\text{l}$  STC (50 mM  $\text{CaCl}_2$ , 10 mM Tris/HCl, 1.33 M sorbitol, pH 7.5) and added to 100  $\mu\text{l}$  of the same buffer containing  $10^6$  protoplasts. To obtain strain  $\Delta\text{agsC}$ , protoplasts of MA234.1 were co-transformed with 1  $\mu\text{g}$  pCT001, 1  $\mu\text{g}$  pCT002 and 10  $\mu\text{l}$  repair oligo 11 (Biolegio, Nijmegen, Netherlands; Table 4). Similarly, 1  $\mu\text{g}$  pCT003, 1  $\mu\text{g}$  pCT004 and 10  $\mu\text{l}$  repair oligo 12 (Biolegio, Nijmegen, Netherlands; Table 4) were used to co-transform MA234.1 to obtain  $\Delta\text{agsE}$ . To obtain strain MA234.1 *Tet-on:agsE*, protoplasts were transformed with 1  $\mu\text{g}$  pCT003, 1  $\mu\text{g}$  pJL006 and 2  $\mu\text{g}$  pJL015 as donor DNA. 50  $\mu\text{l}$  60% PEG4000 was added and mixed gently before adding 1 ml 60% PEG4000 followed by incubation at room temperature for 5 min. This was followed by adding 2 ml STC, mixing the transformation mixture with 30 ml molten (50  $^\circ\text{C}$ ) MM-ST (0.95 M sucrose, 0.6% agar, pH 6), and spreading it onto two square plates containing MM-S (0.95 M sucrose, 1.2% agar, pH 6). Transformants were selected using 150  $\mu\text{g ml}^{-1}$  hygromycin B both in the top and bottom layer. Single transformants were selected on PDA plates containing 150  $\mu\text{g ml}^{-1}$  hygromycin B followed by two purifications on PDA without antibiotic to get rid of the sgRNA plasmids.

#### *DNA isolation*

*Escherichia coli* strain NEB® 10-beta was grown at 37  $^\circ\text{C}$  and 200 rpm in LB medium. *E.coli* plasmid DNA was isolated with the NucleoBond PC 100 Plasmid Miniprep Kit (Macherey Nagel, Düren, Germany), while genomic DNA of *A. niger* was isolated as described (Liu et al., 2000) with modifications. Mycelium was grown overnight at 30  $^\circ\text{C}$  and 200 rpm and harvested by using a 40  $\mu\text{m}$  cell strainer (Corning, 352340, New York, United States). After removing excess of water using filter paper, the mycelium was frozen in liquid nitrogen and homogenized with 2 steel beads at 25 Hz for 1 min in a Tissue lyzer II (Qiagen, Hilden, Germany). A total of 500  $\mu\text{l}$  lysis buffer was added to 5-20 mg mycelium powder and incubated at room temperature for 10 min. This was followed by mixing with 150  $\mu\text{l}$  3 M potassium acetate buffer (pH 4.8) and centrifugation at 10,000 g for 1 min. The supernatant was centrifuged again at 10,000 g for 2 min after mixing with an equal volume of isopropanol. The pellet was washed with 70 % ethanol and dissolved in 50  $\mu\text{l}$  TE Buffer (NucleoBond PC 100 Plasmid Miniprep Kit, Macherey Nagel).

#### *Analysing micro-colony diameter and biomass*

Bright field images of micro-colonies were converted to binary images by thresholding. The particle analysis tool in ImageJ was used to segment the micro-colonies using a size > 50 square

pixel (i.e.  $>100 \mu\text{m}^2$ ), to get rid of small debris, and a circularity between 0 and 1. The diameter of micro-colonies was calculated using the formula  $2 \cdot \sqrt{\frac{\text{area}}{\pi}}$  assuming that micro-colonies were circular. Analysis was done using biological triplicates with a total of  $> 100$  pellets. Data was analyzed using Levene's Test for equality of variance detection and one-way ANOVA followed by a Dunnett's T3 post-hoc test for multiple comparisons ( $p \leq 0.05$ ). Photo of spore aggregates were made using an Olympus AX70 microscope. To determine biomass, mycelium of biological triplicates was filtered over filter paper, washed twice with distilled water, dried at  $60^\circ\text{C}$ , and weighed. Biomass was analyzed using one-way ANOVA followed by Games-Howell post-hoc test for multiple comparisons ( $p \leq 0.05$ ).

### SDS-PAGE

Protein contained in  $400 \mu\text{l}$  culture medium was precipitated overnight at  $-20^\circ\text{C}$  with four volumes pre-cooled acetone, pelleted at  $4^\circ\text{C}$  at  $20,000 \text{ g}$  for 30 min, and dissolved in  $20 \mu\text{l}$  loading buffer (20 % glycerol, 4 % SDS, 100 mM Tris-HCL pH 6.8, 0.01 % bromophenol blue). Proteins were separated in 12.5 % SDS-poly acrylamide gels using TGS buffer (30 g Tris base, 144 g glycine, and  $10 \text{ g SDS l}^{-1}$ ). Gels were stained in 0.02 % CBB G-250, 5 %  $\text{Al}_2(\text{SO}_4)_3(14-18)$ -hydrate, 10 % ethanol and 2 % phosphoric acid and destained in 10 % ethanol and 2 % phosphoric acid (Krijgsheld et al., 2012).

### Massspectrometry:RP-nanoLC-MS/MS

Pellets were harvested and excess water was removed with tissue paper. A total of 50 mg wet weight mycelium was taken up in  $100 \mu\text{l}$  lysis buffer (1 pill cOmplete protease inhibitor, [Roche, Switzerland] dissolved in 10 ml 100 mM Tris, 10% SDS, pH 8.47) and centrifuged at  $20,000 \text{ g}$  for 30 min.  $20 \mu\text{l}$  supernatant was loaded on a SDS PAGE gel (see previous section), ran for 2-3 cm, and stained with colloidal coomassie dye G-250 (Thermo Fisher Scientific, cat# 24590). Similarly, proteins in the culture medium were separated by SDS PAGE and stained. Gel pieces containing the cellular or extracellular proteins were reduced, alkylated and digested overnight with trypsin at  $37^\circ\text{C}$ . Peptides were extracted with 100% acetonitrile and dried in a vacuum concentrator. Samples were resuspended in 10% (v/v) formic acid for UHPLC-MS/MS analysis.

Resuspended peptides were subjected to LC-LC MS/MS using a Thermo Ultimate 3000 coupled to an Orbitrap Exploris 480 mass spectrometer (Thermo Scientific, Bremen, Germany). To this end, peptides were loaded on a C18 PepMAP column ( $5 \mu\text{m}$ ,  $5 \text{ mm} \times 300$

$\mu\text{m}$ ; Thermo Scientific) using solvent A (0.1% formic acid) before being separated on an analytical column (Agilent Poroshell EC-C18, 2.7  $\mu\text{m}$ , 50 cm  $\times$  75  $\mu\text{m}$ ). The extracellular proteins were eluted during a 46 min run using the following gradient: 9–13% solvent B (0.1 formic acid in 80% acetonitrile) in 1 min, 13–44% solvent B in 37 min, 44–99% solvent B in 3 min, 99% solvent B for 4 min and back to 9% solvent B in 1 min. Similarly, the cellular proteins were eluted using a 104 min run with the following gradient: 9–13% solvent B in 1 min, 13–44% solvent B in 95 min, 44–99% solvent B in 3 min, 99% solvent B for 4 min and back to 9% solvent B in 1 min. The mass spectrometer was operated in data-dependent mode. Full-scan MS spectra from  $m/z$  375–1600 were acquired at a resolution of 60 000 at  $m/z$  200 after accumulation to the standard target value. Cycle time of 1 sec for the 46 min and 2 sec for the 104 min gradient with standard AGC targets, respectively. HCD fragmentation was performed at normalized collision energy of 28.

#### *Proteomics data analysis*

Raw data was analyzed with MaxQuant software (version 1.6.8.0) using label-free quantification (Cox et al., 2011). A false discovery rate (FDR) of 0.01 for proteins and peptides and a minimum peptide length of 7 amino acids were required. MS/MS spectra were searched against the database using the Andromeda search engine. Trypsin allowing N-terminal cleavage to proline was selected for enzyme specificity. Cysteine carbamidomethylation was selected as fixed modification, while protein N-terminal acetylation and methionine oxidation were selected as variable modifications. Up to two missing cleavages were allowed. Initial mass deviation of precursor ion was up to 7 ppm, mass deviation for fragment ions was 0.05 Da. Protein identification required one unique peptide to the protein group and match between run was enabled. In all cases, 4 biological replicates and at least 2 technical replicates were used. All correction analyses were carried out with Perseus software Version 1.6.10.0. All biological replicates had an  $R^2 > 0.97$ . Proteins were considered as present when they had been identified in at least 3 out of 4 biological replicates. Pfam and GO over-representation and signal peptide analysis were done as described (El-Gebali et al., 2019; Petersen et al., 2011).

#### *Cellulase activity assay*

Cellulase activity was quantified using the filter paper activity assay (FPase) (Xiao et al., 2004). To this end, 7-mm diameter round Whatman No. 1 filter paper was incubated with 60  $\mu\text{l}$  culture medium for 24 h at 50  $^{\circ}\text{C}$ . This was followed by a 5 min incubation at 95  $^{\circ}\text{C}$  to stop reaction after adding 120  $\mu\text{l}$  DNS (10 g  $\text{L}^{-1}$  3,5-dinitrosalicylic acid, 400 g  $\text{l}^{-1}$  KNa-tartrate and 16 g

NaOH l<sup>-1</sup>). Aliquots of the samples (100  $\mu$ l) were transferred to the wells of a flat-bottom plate and the A<sub>540</sub> was determined using a Synergy HTX Microplate Reader (BioTek, Winooski, VT, USA). Calibration curves were made using different concentrations of glucose. Units of cellulase activity were defined as 1  $\mu$ mol glucose being released in 1 min, respectively. Cellulase activity within the culture media of MA234.1 and  $\Delta$ *agsE* cultures and mixtures (1:1) thereof were analysed by one-way ANOVA, followed by a Dunnett's T3 test for multiple comparisons.

#### *Pathway and protein-protein interaction(PPI) analysis*

Protein expression were calculated by using R package “DESeq2” and KEGG enrichment analyses was performed using the “phyper” function from the R package stats (Kanehisa & Goto, 2000). The Benjamini-Hochberg was used to correct for significance p-value of 0.05. The PPI analysis was conducted by Cytoscape 3.90 (Shannon et al., 2003) by use string database (<http://string-db.org>).

## RESULTS

### *Impact of inactivation of *agsC* and *agsE* on morphology and biomass of *A. niger* and the pH of its culture medium*

Genes *agsC* (ATCC64974\_40950, AspGD) and *agsE* (ATCC64974\_10510, AspGD) were inactivated in strain MA234.1 to study the relationship between  $\alpha$ -(1,3)-glucan synthesis and biomass, micro-colony morphology, pH of the culture medium and the secretome. Spores of strains LZ04 ( $\Delta$ *agsC*) and LZ05 ( $\Delta$ *agsE*) and their parental strain MA234.1 were pre-cultured in transformation medium with 25 mM xylose (TM-X) for 16 h and transferred to minimal medium with 25 mM xylose (MM-X) for a total culturing time of 48 h. Biomass of wild-type strain MA234.1 and the  $\Delta$ *agsC* and  $\Delta$ *agsE* strains were similar with  $1.94 \pm 0.24$  g l<sup>-1</sup>,  $1.91 \pm 0.6$  g l<sup>-1</sup>, and  $2.15 \pm 0.5$  g l<sup>-1</sup>, respectively (Figure 2C). Diameter of micro-colonies of MA234.1 ( $3304 \pm 338$   $\mu$ m) and  $\Delta$ *agsC* ( $3302 \pm 252$   $\mu$ m) was also similar (Figure 2A, B). In contrast,  $\Delta$ *agsE* developed smaller pellets with a diameter of  $1229 \pm 113$   $\mu$ m. The pH of the culture media of MA234.1 (pH 5.2),  $\Delta$ *agsC* (pH 4.6) and  $\Delta$ *agsE* (pH 6.4) was different (initial MM pH 6.0) (Figure 2D), implying that inactivation of  $\alpha$ -(1,3)-glucan synthases impacts the secretion of organic acids. In addition, SDS PAGE indicated that the secretomes of  $\Delta$ *agsC* and MA234.1 were similar but that the secretome of  $\Delta$ *agsE* was different (Figure 2E). Taken together,  $\alpha$ -(1,3)-glucan synthase gene *agsE* is involved in colony morphology, in impacting culture medium pH and in protein secretion, while *agsC* only affects pH of the culture medium.

We aimed to complement the  $\Delta agsE$  strain to confirm that its phenotypes are caused by the inactivation of the  $\alpha$ -(1,3)-glucan synthase gene. However, the size of this gene (7533 bp) hampered complementation and therefore we used a different strategy by replacing the *agsE* promoter in the wild-type strain for the Tet-on promoter that is induced by doxycycline. This strategy enables to monitor the deletion phenotype (no doxycycline in the medium), the normal phenotype ( $x$  amount of doxycycline in the medium), as well as the over-expression phenotype ( $x + y$  amount of doxycycline in the medium). Strain LZ06 (*Tet-on:agsE*) was cultured in the presence of different concentrations of doxycycline both during the 16 h pre-culturing in TM-X and the 32 h culturing in MM-X. Morphology of the parental strain MA234.1 was not affected by the presence of  $2.5 \mu\text{g ml}^{-1}$  doxycycline ( $3156 \pm 725 \mu\text{m}$  versus  $3784 \pm 397 \mu\text{m}$  in absence and presence of the inducer, respectively). In contrast, micro-colony size of the *Tet-on:agsE* strain ranged from  $1206 \pm 113 \mu\text{m}$  (no doxycycline) to  $1923 \pm 224 \mu\text{m}$  ( $2 \mu\text{g ml}^{-1}$  doxycycline), and to  $3500 \pm 224 \mu\text{m}$  ( $2.5 \mu\text{g l}^{-1}$  doxycycline) (Figure 3A, B). Biomass of MA234.1 and *Tet-on:agsE* cultures were not statistically different, while pH was significantly higher in the *Tet-on:agsE* cultures compared to MA234.1 in the absence or presence of the inducer (Figure 3C, D). Next, the secretion profile was evaluated by SDS-PAGE. Presence of doxycycline did not affect the protein profile of the wild-type (Figure 3E). Notably, the protein profile of strain LZ06 was very similar to the wild-type in the presence of  $2.5 \mu\text{g l}^{-1}$  doxycycline, while it was highly different at  $\leq 2 \mu\text{g l}^{-1}$  inducer. These results show a relation between morphology and the protein profiles in the culture medium.

Cellulase activity of cultures MA234.1 and the *Tet-on:agsE* strain was evaluated in the absence and presence of doxycycline and in the mixture of the culture media of the two strains grown in the same concentration of the inducer. No statistical differences were observed in cellulase activity between the strains at the different concentrations of the inducer and also between the pure and mixed culture media. Yet, a trend towards higher cellulase activity was observed in the absence of inducer or in the presence of  $0.5 \mu\text{g l}^{-1}$  inducer, suggesting that large wild-type and small LZ06 micro-colonies show synergistic cellulase activity (Figure 3F). Similarly, cellulase activity of the  $\Delta agsE$  cultures was 41.6% higher than that of the wild type cultures (Figure 4D) and the 1:1 mixed cultures of MA234.1 and  $\Delta agsE$  exhibited 2.4- and 1.7-fold higher activity compared to the cultures of MA234.1 and  $\Delta agsE$ , respectively. Taken together, *agsE* influences the pH, micro-colony morphology and cellulase of *A.niger* and the protein profiles in the culture medium.

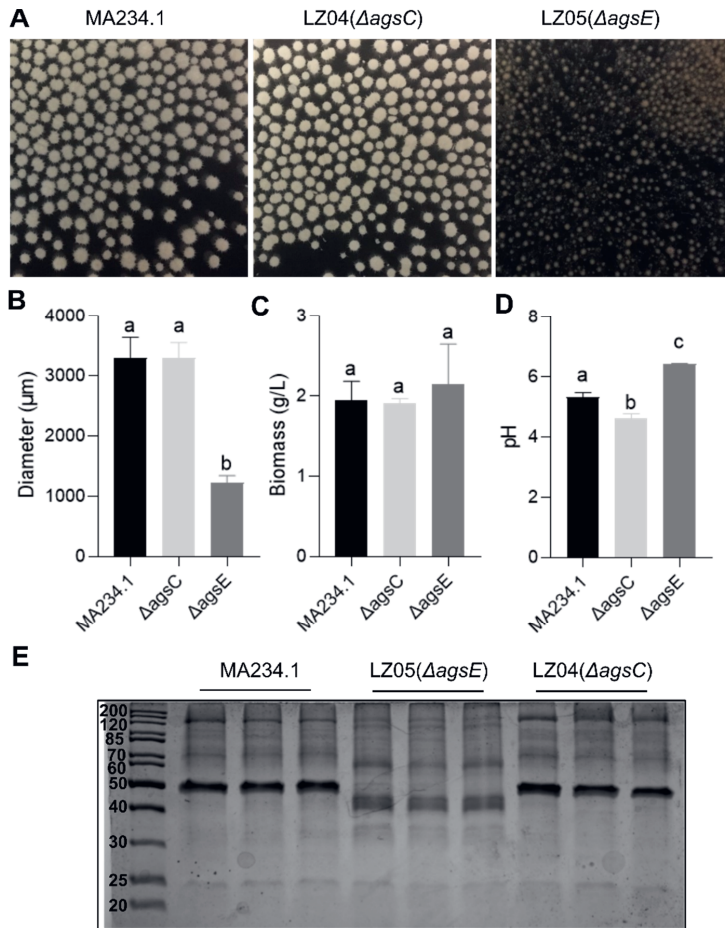


**Figure 2.** Morphology (A), diameter (B), biomass (C), pH (D) and SDS PAGE of proteins in the culture medium (E) of strains MA234.1,  $\Delta$ *agsC* and  $\Delta$ *agsE*. Different letters indicate statistical differences (B-D) as determined by a one-way ANOVA combined with Dunnet's T3 post-hoc test for diameter and Games-Howell post-hoc test for biomass and pH. Error bars indicate standard deviation.

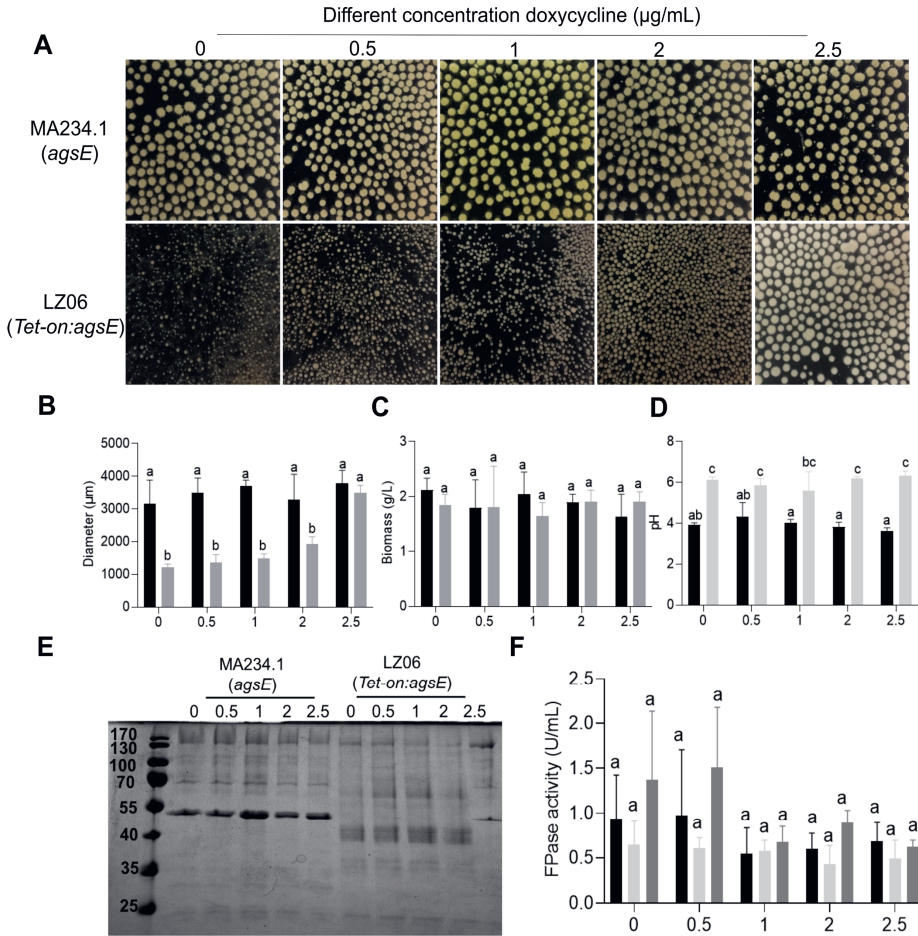


**Figure 3.** Morphology (A), diameter (B), biomass (C), pH (D), SDS PAGE of the proteins in the culture medium (E) and cellulase activity (F) of strains MA234.1 and LZ06 (*Tet-on:agsE*) at different concentrations of doxycycline in the culture medium. Letters indicate statistical significance (B-D,F) as determined by a one-way ANOVA combined with a Dunnet's T3 post-hoc test for diameter and cellulase activity (B, D) and Games-Howell post-hoc test for biomass and pH (C, F).

#### Secretome of MA234.1 and $\Delta$ agsE

Secretome analysis was performed of MA234.1 and  $\Delta$ agsE revealing a total number of 304 and 439 proteins, respectively, of which 219 and 201 are predicted to have a signal peptide for secretion (Figure 4C; Supplemental Tables 1 and 2). Thus, strain  $\Delta$ agsE releases more proteins

without signal peptides when compared to MA234.1. A total of 241 proteins was identified in the culture media of both MA234.1 and  $\Delta$ *agsE*, while 63 and 198 proteins were unique for these strains, respectively (Figure 4C; Supplemental Tables 3-5). Within the set of 241 shared proteins, 165 and 76 were predicted to have or lack a signal peptide for secretion (Figure 4C; Supplemental Table 3), respectively, while 45 and 59 proteins within the set of 241 shared proteins were significantly  $>2$  fold down- and up-regulated in  $\Delta$ *agsE* when compared to MA234.1 (Figure 4B; Supplemental Table 6). Of the 63 unique proteins of the wild-type strain,

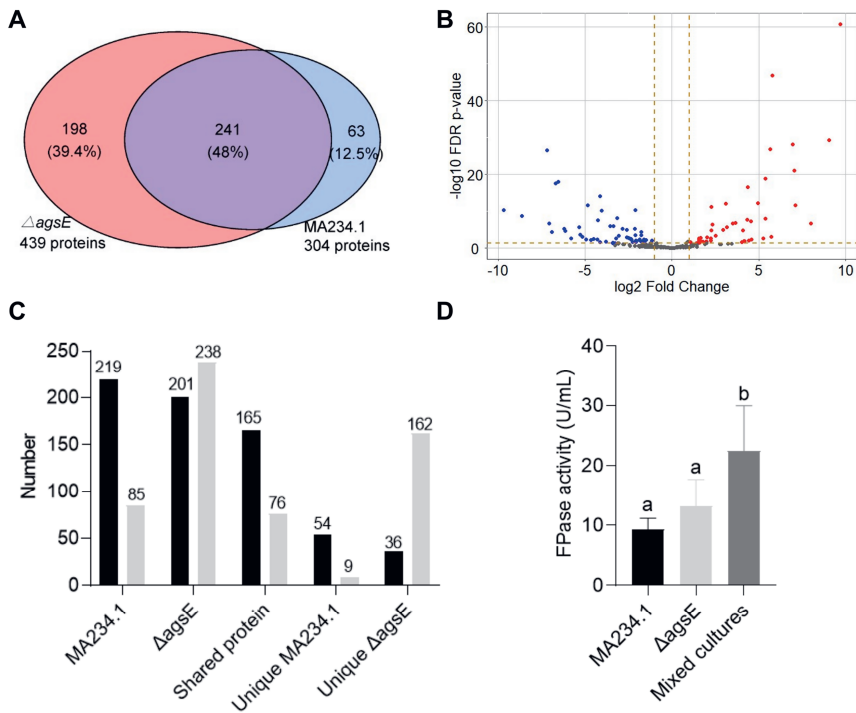


**Figure 4.** Venn diagram (A) and up- and down-regulated (B) proteins in the culture medium of strains MA234.1 and  $\Delta$ *agsE*. Red and blue dots in panel B indicate proteins that were  $\geq 2$  fold up- or down-regulated in  $\Delta$ *agsE* cultures when compared to MA234.1 cultures, respectively. (A) and (B) comprise proteins with and without signal sequence, while (C) distinguishes between proteins with (black shaded bars) and without (light shaded bars) a signal sequence. (D) Cellulase activity from liquid shaken cultures of MA234.1 and  $\Delta$ *agsE*. Proteins were analyzed after a total culturing time of 48 h. Statistical differences was determined by a one-way ANOVA combined with a Dunnett's T3 test for multiple comparisons. Letters indicate statistical differences, while error bars indicate standard deviation.



54 had a predicted signal sequence for secretion (Figure 4C; Supplemental Table 4). In contrast, only 36 proteins contain a signal sequence for secretion within the set of 198 unique proteins released by strain  $\Delta$ *agsE* (Figure 4C; Supplemental Table 5). Together, these data show that the  $\Delta$ *agsE* strain releases less proteins with a signal sequence when compared to the wild-type and that the set of unique proteins with a signal sequence is also smaller.

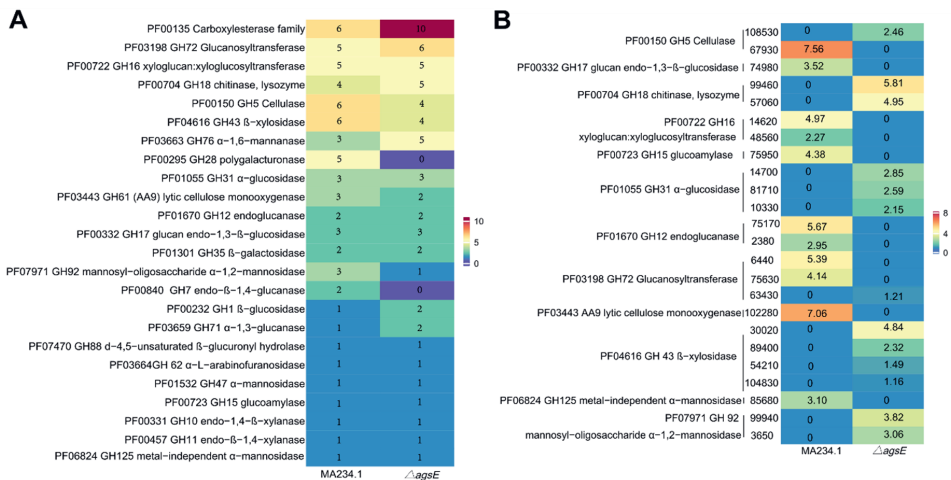


**Figure 5.** Protein family (Pfam) analysis of Cazyme proteins in the secretomes of strains MA234.1 and LZ05 ( $\Delta$ *agsE*) (A) and the significantly up- or down-regulated Cazymes of LZ05 ( $\Delta$ *agsE*) compared to MA234.1 (proteins present in cultures of both MA234.1 and  $\Delta$ *agsE*) (B). The number in (A) is the number of proteins identified in the cultures; the number in (B) represent the log fold change ( $\log_2(x)=y$ , x represent expression fold change, y is the number shown in panel B. 0 in blue is when  $x=1$ ; set as control). The number in B annotation represents X in the proteinID ATCC64974\_X of N402.

The 219 proteins with a signal peptide identified in the secretome of MA234.1 belong to 103 protein families (Supplemental Table 7). This set included 6 carboxylesterases (PF00135), 5 GH5 cellulases (PF00150), 5 GH28 polygalacturonases (PF00295), 5 GH16 glucanases / galactanases (PF00722) and 5 GH43 hemicellulases (PF04616) (Figure 5A). The 85 proteins that are released into the culture medium of MA234.1 and that lack a predicted signal peptide belong to 67 protein families (Supplemental Table 7). Eukaryotic aspartyl protease (PF00026) and pectate lyase superfamily protein (PF12708) were represented by 2 proteins each. The 201 proteins with a signal peptide for secretion that were released by strain  $\Delta$ *agsE* represent 100 protein families (Supplemental Table 8). This included 10

carboxylesterases (PF00135), 5 GH16 glucanases / galactanases (PF00722), 4 GH76  $\alpha$ -mannanases (PF03663), 3  $\alpha$ -amylases (PF00128) and 3 GH5 cellulases (PF00150) (Figure 5A). The 238 proteins without a predicted signal sequence that were identified in the culture medium of  $\Delta$ *agsE* belonged to 179 protein families (Supplemental Table 8). PF00083 sugar (and other) transporter (7 proteins), PF00248 aldo/keto reductase family (4 proteins), PF00326 prolyl oligopeptidase family (3 proteins) and PF01557 fumarylacetoacetate (FAA) hydrolase family (3 proteins) were the families with most representatives.

The set of 165 proteins with a predicted signal peptide that are shared between wild-type strain MA234.1 and strain  $\Delta$ *agsE* represents 88 protein families with PF00722 GH16 glucanases / galactanases (5 proteins), PF00150 GH5 cellulase (3 proteins), PF00704 GH18 chitinases / endo- $\beta$ -N-acetylglucosaminidases / carbohydrate binding modules / xylanase inhibitors (3 proteins), PF01055 GH31  $\alpha$ -glucosidases /  $\alpha$ -xylosidases / isomaltosyltransferases / glucoamylases (3 proteins), and PF04616 GH43 hemicellulases (3 proteins) having most representatives (Supplemental Table 9). The shared set of 76 proteins without a signal peptide belonged to 64 protein families with PF01042 endoribonuclease L-PSP and PF12708 pectate lyase superfamily being most represented with 2 proteins each (Supplemental Table 9). The 54 unique proteins with a predicted signal peptide in the culture medium of MA234.1 belonged to 31 protein families including 5 GH28 polygalacturonases (PF00295), 2 GH5 cellulases (PF00150), 2 GH7 cellulases/ $\beta$ -1,4-glucanases (PF00840) and 2 pectinesterases (PF01095) (Supplemental Table 10). No GH family was identified when we analyzed the 9 unique proteins without a signal peptide in the secretome of MA234.1 (Supplemental Table 10). The 36 unique proteins of  $\Delta$ *agsE* with a predicted signal peptide were classified into 24 protein families. The PF00135 carboxylesterase family (4 proteins), and the PF03663 GH76  $\alpha$ -mannanases (2 proteins) were among the most prominent protein families (Supplemental Table 11). Strain  $\Delta$ *agsE* secreted 162 unique proteins without predicted signal peptides that belong to 129 protein families (Supplemental Table 11). PF00083 sugar (and other) transporters (7 proteins) is the most represented family. Notably, strain  $\Delta$ *agsE* did not release a unique cellulase (GH5, GH8, GH9, GH44) when compared to MA234.1, implying we would not expect a synergistic cellulase activity. Yet, MA234.1 and  $\Delta$ *agsE* secreted members of 3 (GH28, GH5, GH7) and 3 (GH76, GH1, GH18) unique GH families, respectively. Thus, MA234.1 and LZ05 may have complementary activity on plant substrates.

A set of 57 proteins was significantly >2 fold up-regulated in  $\Delta$ *agsE* compared to MA234.1. This set included 4 GH43 hemicellulases (PF04616), 3 GH31  $\alpha$ -glucosidases /  $\alpha$ -

xylosidases / isomaltosyltransferases / glucoamylases (PF01055), 2 GH18 chitinases / endo- $\beta$ -N-acetylglucosaminidases / carbohydrate binding modules / xylanase inhibitors (PF00704), 2 GH92 PF07971  $\alpha$ -mannosidases, 1 GH 72 PF03198 glucanosyltransferase and 1 PF00150 cellulase (Figure 5B, Supplemental Table 12). In contrast, 46 shared proteins were  $> 2$  fold down-regulated in  $\Delta$ agsE, including 2 GH16 glucanase / galactanase (PF00722), 2 GH12  $\beta$ -glucanases (PF01670), 1 GH17  $\beta$ -glucan endohydrolases (PF00332), 1 GH15  $\alpha$ -glucosidase (PF00723), 2 GH 72 glucanosyltransferase (PF03198), 1 AA9 lytic cellulose monooxygenase (PF03443), 1 GH 125 exo- $\alpha$ -1,6-mannosidase (PF06824) and 1 cellulase (PF00150) (Figure 5B, Supplemental Table 12). Together, these data support that MA234.1 and LZ05 may have complementary activity on cellulose and plant substrates.

#### *Cellular proteomics of MA234.1 and $\Delta$ agsE during early germination*

Clusters of  $\Delta$ agsE spores that had formed after 4 h of incubation in liquid shaken medium were smaller in size and more loosely packed when compared to those of strain MA234.1 (Figure 6A). These differences became more pronounced in time. Therefore, cellular proteomics was performed of MA234.1 and  $\Delta$ agsE samples 6-10 hours after inoculation. A total of 344 and 220 proteins were detected that were significantly  $>2$ -fold up- and down-regulated in the  $\Delta$ agsE strain in at least one of the time points 6, 8 and 10 h post-inoculation when compared with MA234.1 (Supplemental Tables 13,14). Among these proteins, only 3 out of 344 and 6 out of 220 were up- and down-regulated at all time points, respectively (Figure 6B, C; Supplemental Table 14). The three up-regulated proteins (3-methyl-2-oxobutanoate hydroxymethyltransferase (ATCC64974\_92400), archaeal ribosomal protein S17P (ATCC64974\_49360) and ATP\_transf domain-containing protein (ATCC64974\_49360) cannot be clearly related to the smaller spore / germling aggregates of  $\Delta$ agsE. As expected,  $\alpha$ -1,3-glucan synthase was identified as one of the 6 significant downregulated proteins at all timepoints. This set also included carbonic anhydrase, which catalyzes the reversible conversion of CO<sub>2</sub> to HCO<sub>3</sub><sup>-</sup> and as such is involved in the formation of the second messenger cAMP (Klengel et al., 2005). In addition, this set consisted of the proteins FHA domain family protein (ATCC64974\_74820), lactamase\_B domain-containing protein (ATCC64974\_59840), B-block binding subunit of TFIIC family protein (ATCC64974\_27500) and a mitochondrial thiamine pyrophosphate carrier 1 (ATCC64974\_85730) that is related to rRNA processing and transmembrane transport. When compared with wild type, 61, 203 and 121 proteins were

significantly upregulated in  $\Delta$ *agsE* after 6, 8 and 10h of culturing, respectively, while 79, 129 and 37 were downregulated (Figure 6B, C; Supplemental Table 13).

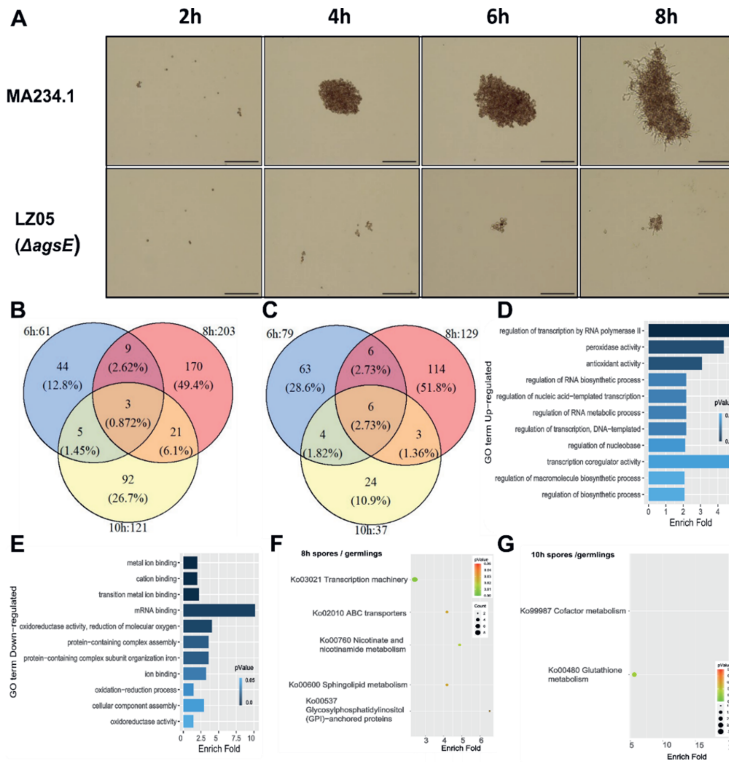


**Figure 6.** Light microscopy of individual spores/germlings of MA234.1 and  $\Delta$ *agsE* as well as their aggregates at different time points (Bar represents 100  $\mu$ m) (A) and cellular proteomics of germlings of MA234.1 and LZ05 ( $\Delta$ *agsE*) (B-G). Venn diagrams showing the shared (i.e. at more than 1 time point) and unique (i.e. at 1 time point) up- (B) and down- regulated (C) proteins in LZ05 compared with MA234.1. GO analysis of proteins up- (D) and down- (E) regulated in strain  $\Delta$ *agsE* in at least one of the time points 6, 8 and 10 h post-inoculation when compared with MA234.1 and KEGG analysis of proteins up- (F) and down- (G) regulated at a single time point post-inoculation.

The 344 proteins that were significantly up-regulated in the  $\Delta$ *agsE* strain in at least one of the time points 6, 8 and 10 h post-inoculation when compared with MA234.1 showed an over-representation of GO-terms especially related to transcription; regulation of transcription by RNA polymerase II, regulation of RNA biosynthetic process, regulation of nucleic acid

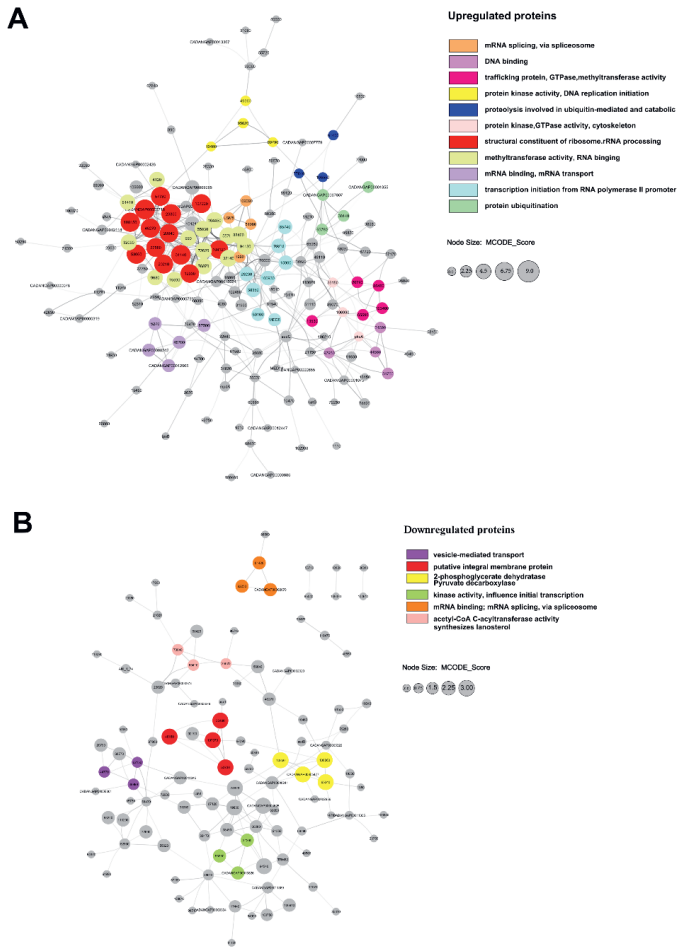


**Figure 7.** Network analysis of the proteins that were up- (A) and down-regulated (B) in at least 1 time point (6, 8, and / or 10 h post-inoculation) of LZ05 ( $\Delta$ *agsE*) compared to MA234.1. The numbers represent X in the proteinID ATCC64974\_X. of N402.

templated transcription, regulation of biosynthetic process, regulation of transcription DNA templated, regulation of nucleobase, and transcription co-regulator activity (Figure 6D, E). At the same time the GO term mRNA binding was over-represented in the 220 down-regulated proteins. KEGG analysis revealed no significantly changed pathway at 6h when MA234.1 and  $\Delta$ *agsE* were compared, while transcription machinery, ABC transporters and GPI anchored proteins pathways were changed at 8 h. Glutathione metabolism is significantly changed at 10 h (Figure 6F, G). A protein interaction network analysis illustrates the impact of deletion of

*agsE* on transcription, putative integral membrane protein and kinase activity clusters 6-10 hours post-inoculation (Figure 7).

The set of 344 up- and 220 down-regulated proteins that were significantly >2-fold up- and down-regulated in the  $\Delta$ *agsE* strain in at least one of the time points 6, 8 and 10 h post-inoculation when compared with MA234.1 included 6 transcription factors (TFs) (Supplemental Table 15). The up-regulated proteins included a MADS Box TF classified as a positive regulator of transcription by RNA polymerase II, a TF implicated in splicing of introns and a transcription factor predicted to be involved in the SREBP signaling pathway (Supplemental Table 15). The latter pathway has a role in sterol biosynthesis and hyphal development (Cao et al., 2018; Chang et al., 2009). The downregulated TFs included a homeodomain TF, a histon-like TF and a SART1 TF, the latter being implicated in splicing of mRNA (Supplemental Table 15). Overall, analysis indicated that the main part of the up- and down-regulated TFs are involved in general transcriptional regulation.

## DISCUSSION

Deletion of  $\alpha$ -1-3 glucan synthase genes impacts aggregation of germlings and, as a consequence, results in smaller *A. oryzae* micro-colonies in liquid cultures (He et al., 2014; Yoshimi et al., 2013). Here it is shown that inactivation of the  $\alpha$ -1-3 glucan synthase gene *agsE*, but not *agsC*, of *A. niger* also results in smaller micro-colonies. This is associated with changes in extracellular pH and protein profiles in the culture medium. In fact, data suggest that the wild-type strain and the  $\Delta$ *agsE* strain have complementary activity on plant substrates.

Recently, evidence has been provided that  $\alpha$ -1-3 glucan plays an important role as a structural polysaccharide in the cell wall of filamentous fungi (Kang et al. 2018, Ehren et al., 2020). Therefore, inactivation of  $\alpha$ -1-3 glucan synthase genes may impact cell wall integrity and therefore growth of the fungus. Yet, inactivation of *agsC* and *agsE* did not impact biomass formation in cultures of *A. niger*. Apparently, compensatory mechanisms such as the *crh* gene family that encodes putative glucan-chitin crosslinking enzymes are available to provide a functional cell wall. Deleting the entire *crh* gene family in a strain of *A. niger* that is deficient in  $\alpha$ -1,3-glucan results in a growth defect and an increased sensitivity towards a cell wall perturbing agent (van Leeuwe et al., 2020). In contrast, this effect was not observed in the wild-type.

The pH of the culture medium changed from 5.2 in the case of the wild-type to 4.6 and 6.4 for  $\Delta$ *agsC* and  $\Delta$ *agsE*, respectively. It is not clear why the deletion strains have a different effect on pH but they may differ in secretion of organic acids. The *agsC* gene had no apparent

impact on the secretome. This suggests that the lower pH in the culture medium of the *ΔagsC* strain has no effect on protein secretion. Inactivation of *agsE* did impact protein release into the medium. Secretome analysis showed a total number of 304 and 439 proteins that had been released into the culture medium of MA234.1 and strain *ΔagsE*, respectively, of which 219 and 201 have a signal peptide for secretion. Thus, *ΔagsE* releases more proteins without signal peptides when compared to MA234.1. It is not yet clear what the reason is of the increased release of proteins without signal sequence within the culture medium. Possibly, part of these proteins are released via a non-classical secretion pathway. Yet, they may also be released due to hyphal damage or lysis. Smaller micro-colonies may be more sensitive to mechanical damage due to shear stress in liquid shaken cultures. This would also explain why small wild-type colonies show more release of proteins without signal sequence in the culture medium when compared to large wild-type micro-colonies (**Chapter 2**). Moreover, reduced presence or even absence of  $\alpha$ -1-3 glucan may impact the cell wall integrity and thereby induces hyphal lysis. Yet, biomass of the cultures was shown not to be affected and there is evidence of mechanisms to compensate for the absence of  $\alpha$ -1-3 glucan in *A. niger* (see above).

A total of 219 and 201 proteins with a signal peptide for secretion were identified in the culture media of MA234.1 and the *ΔagsE* strain, of which 165 were shared between the two strains. Of the total number of proteins with a signal sequence for secretion, 5 have never been reported to be part of the secretome before (Supplemental Table 16). Part of the proteins that were found in the secretomes of both MA234.1 and *ΔagsE* were differentially expressed when compared to the other strain. The 45 proteins that were down-regulated in *ΔagsE* included GH16 glucanases / galactanases, GH12  $\beta$ -glucanases, a GH17  $\beta$ -glucan endohydrolases and a GH15  $\alpha$ -glucosidase (Figure 5). On the other hand, the 59 proteins that were up-regulated in *ΔagsE* when compared to MA234.1 included GH43 hemicellulases, GH31  $\alpha$ -glucosidases /  $\alpha$ -xylosidases / isomaltosyltransferases / glucoamylases, GH18 chitinases / endo- $\beta$ -N-acetylglucosaminidases / carbohydrate binding modules / xylanase inhibitors and GH92  $\alpha$ -mannosidases. The 54 unique proteins with a predicted signal peptide in the culture medium of MA234.1 included GH28 polygalacturonases, GH5 cellulases, GH7 cellulases/ $\beta$ -1,4-glucanases and 2 pectinesterases. On the other hand, the 36 unique proteins with a predicted signal peptide of strain *ΔagsE* included carboxylesterases, GH76  $\alpha$ -mannanases, GH1  $\beta$ -glucosidase, GH61 lytic polysaccharide monoxygenases and GH71  $\alpha$ -1,3-glucanase. The finding that a *ΔagsE* strain can secrete increased levels of a protein was also found for a heterologous cutinase in *A. oryzae* (Miyazawa et al., 2016). Together, these data suggest that the wild-type and the *ΔagsE* strains have complementary activity on plant substrates. In

addition, 6 cellulase proteins (GH5) are identified in the cultures of MA234.1 and 4 out of them were identified in  $\Delta$ *agsE* cultures as well (Supplemental Table 1-2), 2 of those 4 proteins without expression changes in statistic analysis. However, ATCC64974\_108530 is log fold change 2.46 times higher expression in cultures  $\Delta$ *agsE*, while ATCC64974\_67930 is log fold change 7.56 times higher in MA234.1 cultures compared to  $\Delta$ *agsE* (Figure 5). These data suggest that the wild-type and the  $\Delta$ *agsE* strains have complementary activity on cellulase.

Cellular proteomics analysis indicated that transcription is significantly upregulated in  $\Delta$ *agsE* compared to wild type MA234.1. This may be explained by the observation that conidia of the wild-type seem to germinate less when they are part of the spore clusters. Increased transcription is an important hall mark of germinating spores when compared to dormant spores (Leeuwen et al., 2013). A lower germination percentage of spores in the culture will reduce the overall increase in expression of transcription related genes but does not imply that individual germinating spores of  $\Delta$ *agsE* have a different expression of these genes compared to wild type MA234.1.

It has been reported that small micro-colonies release more protein than large micro-colonies (Tegelaar et al., 2020; **Chapter 2**). This may be explained by the fact that expression of genes of secreted proteins mainly occurs in a peripheral shell of the pellet and that, therefore, pellets with a radius  $\leq$  of the width of the expression shell would be more productive in terms of protein secretion (Tegelaar et al., 2020). However, the results of this study do not support the finding that smaller micro-colonies secrete more protein in the culture medium. The increased amounts of protein as observed on SDS PAGE is mainly explained by release of proteins without a signal sequence. Thus, it may be that inactivation of *agsE* stimulates protein secretion due to smaller micro-colonies formation but at the same time inhibits protein secretion due for instance to changes in cell wall composition, pH of the culture medium, cell lysis, or changes in activity of signalling pathways. Carbonic anhydrase was found to be upregulated in  $\Delta$ *agsE* germlings (this Chapter) and in small wild-type micro-colonies (**Chapter 2**). This enzyme catalyzes the reversible hydration of CO<sub>2</sub> to HCO<sub>3</sub><sup>-</sup> which can activate adenylyl cyclase forming cAMP (Klengel et al., 2005). This second messenger is involved in release of specific enzymes in the culture medium of fungal pathogens (Choi et al., 2015; Fuller & Rhodes, 2012). The inhibiting effects may be quite strong because only 49 out of 88 proteins with a signal peptide that were unique to small wild-type micro-colonies (i.e. present in B16 absent in F16) were also found in the small  $\Delta$ *agsE* micro-colonies (**Chapter 2**).



**REFERENCES**

- Cao, H., Huang, P., Yan, Y., Shi, Y., Dong, B., Liu, X., Ye, L., Lin, F., Lu, J. 2018. The basic helix-loop-helix transcription factor Crfl is required for development and pathogenicity of the rice blast fungus by regulating carbohydrate and lipid metabolism. *Environ Microbiol*, **20**, 3427-3441.
- Carlsen, M., Spohr, A.B., Nielsen, J., Villadsen, J. 1996. Morphology and physiology of an  $\alpha$ -amylase producing strain of *Aspergillus oryzae* during batch cultivations. *Biotechnol Bioeng*, **49**, 266-276.
- Chang, Y.C., Ingavale, S.S., Bien, C., Espenshade, P., Kwon-Chung, K.J. 2009. Conservation of the sterol regulatory element-binding protein pathway and its pathobiological importance in *Cryptococcus neoformans*. *Eukaryot Cell*, **8**, 1770-1779.
- Choi, J., Jung, W.H., Kronstad, J.W. 2015. The cAMP/protein kinase A signaling pathway in pathogenic basidiomycete fungi: Connections with iron homeostasis. *J Microbiol*, **53**, 579-587.
- Cox, J., Neuhauser, N., Michalski, A., Scheltema, R.A., Olsen, J.V., Mann, M. 2011. Andromeda: a peptide search engine integrated into the MaxQuant environment. *J Proteome Res*, **10**, 1794-805.
- de Bekker, C., Wiebenga, A., Aguilar, G., Wösten, H.A. 2009. An enzyme cocktail for efficient protoplast formation in *Aspergillus niger*. *J Microbiol Methods*, **76**, 305-306.
- de Bekker, C., van Veluw, G.J., Vinck, A., Wiebenga, L.A., Wösten, H.A.B. 2011. Heterogeneity of *Aspergillus niger* microcolonies in liquid shaken cultures. *Appl Environ Microbiol*, **77**, 1263-1267.
- de Vries, R.P., Burgers, K., van de Vondervoort, P.J., Frisvad, J.C., Samson, R.A., Visser, J. 2004. A new black *Aspergillus* species, *A. vadensis*, is a promising host for homologous and heterologous protein production. *Appl Environ Microbiol*, **70**, 3954-3959.
- Dynesen, J., Nielsen, J. 2003. Surface hydrophobicity of *Aspergillus nidulans* conidiospores and its role in pellet formation. *Biotechnol Prog*, **19**, 1049-1052.
- Ehren, H.L., Appels, F.V.W., Houben, K., Renault, M.A.M., Wösten, H.A.B., Baldus, M. 2020. Characterization of the cell wall of a mushroom forming fungus at atomic resolution using solid-state NMR spectroscopy. *Cell Surf*, **6**, 100046.
- El-Gebali, S., Mistry, J., Bateman, A., Eddy, S.R., Luciani, A., Potter, S.C., Qureshi, M., Richardson, L.J., Salazar, G.A., Smart, A., Sonnhammer, E.L.L., Hirsh, L., Paladin, L., Piovesan, D., Tosatto, S.C.E., Finn, R.D. 2019. The Pfam protein families database in 2019. *Nucleic Acids Res.*, **47**, D427-D432.

- Fontaine, T., Beauvais, A., Loussert, C., Thevenard, B., Fulgsang, C.C., Ohno, N., Clavaud, C., Prevost, M.C., Latge, J.P. 2010. Cell wall  $\alpha$ 1-3glucans induce the aggregation of germinating conidia of *Aspergillus fumigatus*. *Fungal Genet Biol*, **47**, 707-712.
- Fuller, K.K., Rhodes, J.C. 2012. Protein kinase A and fungal virulence: a sinister side to a conserved nutrient sensing pathway. *Virulence*, **3**, 109-121.
- Grimm, L.H., Kelly, S., Hengstler, J., Gobel, A., Krull, R., Hempel, D.C. 2004. Kinetic studies on the aggregation of *Aspergillus niger* conidia. *Biotechnol Bioeng*, **87**, 213-218.
- He, X., Li, S., Kaminskyj, S.G. 2014. Characterization of *Aspergillus nidulans*  $\alpha$ -glucan synthesis: roles for two synthases and two amylases. *Mol Microbiol*, **91**, 579-595.
- Kanehisa, M., Goto, S. 2000. KEGG kyoto encyclopedia of genes and genomes. *Nucl Acids Res*, **28**, 27-30.
- Kang, X., Kirui, A., Muszynski, A., Widanage, M.C.D., Chen, A., Azadi, P., Wang, P., Mentink-Vigier, F., Wang, T. 2018. Molecular architecture of fungal cell walls revealed by solid-state NMR. *Nat Commun*, **9**, 2747.
- Klengel, T., Liang, W.J., Chaloupka, J., Ruoff, C., Schroppel, K., Naglik, J.R., Eckert, S.E., Mogensen, E.G., Haynes, K., Tuite, M.F., Levin, L.R., Buck, J., Muhlschlegel, F.A. 2005. Fungal adenyl cyclase integrates CO<sub>2</sub> sensing with cAMP signaling and virulence. *Curr Biol*, **15**, 2021-2026.
- Krijghsheld, P., Altelaar, A.F., Post, H., Ringrose, J.H., Muller, W.H., Heck, A.J., Wösten, H.A.B. 2012. Spatially resolving the secretome within the mycelium of the cell factory *Aspergillus niger*. *J Proteome Res*, **11**, 2807-2818.
- Krijghsheld, P., Bleichrodt, R., van Veluw, G.J., Wang, F., Muller, W.H., Dijksterhuis, J., Wösten, H.A.B. 2013. Development in *Aspergillus*. *Stud Mycol*, **74**, 1-29.
- Leeuwen, M.R.V., Krijghsheld, P., Bleichrodt, R., Menke, H., Stam, H., Stark, J., Wösten, H.A.B., Dijksterhuis, J. 2013. Germination of conidia of *Aspergillus niger* is accompanied by major changes in RNA profiles. *Stud Mycol*, **74**, 59-70.
- Liu, D., Coloe, S., Baird, R., Pederson, J. 2000. Rapid mini-preparation of fungal DNA for PCR. *J Clin Microbiol*, **38**, 471.
- Marion, C.L., Rappleye, C.A., Engle, J.T., Goldman, W.E. 2006. An  $\alpha$ -(1,4)-amylase is essential for  $\alpha$ -(1,3)-glucan production and virulence in *Histoplasma capsulatum*. *Mol Microbiol*, **62**, 970-983.
- Metz, B., Kossen, N.W.F. 1977. The growth of molds in the form of pellets - a literature review. *Biotechnol Bioeng*, **19**, 781-799.

- Meyer, V., Ram, A.F., Punt, P.J. 2010. Genetics, genetic manipulation, and approaches to strain improvement of filamentous fungi. *Manual of Industrial Microbiology and Biotechnology, Third Edition*, 318-329.
- Meyer, V., Wu, B., Ram, A.F. 2011. *Aspergillus* as a multi-purpose cell factory: current status and perspectives. *Biotechnol Lett*, **33**, 469-476.
- Miyazawa, K., Yoshimi, A., Zhang, S., Sano, M., Nakayama, M., Gomi, K., Abe, K. 2016. Increased enzyme production under liquid culture conditions in the industrial fungus *Aspergillus oryzae* by disruption of the genes encoding cell wall  $\alpha$ -1,3-glucan synthase. *Biosci Biotechnol Biochem*, **80**, 1853-1863.
- Nodvig, C.S., Hoof, J.B., Kogle, M.E., Jarczynska, Z.D., Lehmbeck, J., Klitgaard, D.K., Mortensen, U.H. 2018. Efficient oligo nucleotide mediated CRISPR-Cas9 gene editing in *Aspergilli*. *Fungal Genet Biol*, **115**, 78-89.
- Park, J., Hulsman, M., Arentshorst, M., Breeman, M., Alazi, E., Lagendijk, E.L., Rocha, M.C., Malavazi, I., Nitsche, B.M., van den Hondel, C.A., Meyer, V., Ram, A.F. 2016. Transcriptomic and molecular genetic analysis of the cell wall salvage response of *Aspergillus niger* to the absence of galactofuranose synthesis. *Cell Microbiol*, **18**, 1268-1284.
- Petersen, T.N., Brunak, S., von Heijne, G., Nielsen, H. 2011. SignalP 4.0: discriminating signal peptides from transmembrane regions. *Nat Methods*, **8**, 785-786.
- Seekles, S.J., Teunisse, P.P.P., Punt, M., van den Brule, T., Dijksterhuis, J., Houbraeken, J., Wösten, H.A.B., Ram, A.F.J. 2021. Preservation stress resistance of melanin deficient conidia from *Paecilomyces variotii* and *Penicillium roqueforti* mutants generated via CRISPR/Cas9 genome editing. *Fungal Biol Biotechnol*, **8**, 4.
- Shannon, P., Markiel, A., Ozier, O., Baliga, N.S., Wang, J.T., Ramage, D., Amin, N., Schwikowski, B., Ideker, T. 2003. Cytoscape: a software environment for integrated models of biomolecular interaction networks. *Genome Res*, **13**, 2498-2504.
- Tegelaar, M., Aerts, D., Teertstra, W.R., Wösten, H.A.B. 2020. Spatial induction of genes encoding secreted proteins in micro-colonies of *Aspergillus niger*. *Sci Rep*, **10**, 1536.
- van Leeuwe, T.M., Arentshorst, M., Ernst, T., Alazi, E., Punt, P.J., Ram, A.F.J. 2019. Efficient marker free CRISPR/Cas9 genome editing for functional analysis of gene families in filamentous fungi. *Fungal Biol Biotechnol*, **6**, 13.
- van Leeuwe, T.M., Wattjes, J., Niehues, A., Forn-Cuní, G., Geoffrion, N., Mérida, H., Arentshorst, M., Molina, A., Tsang, A., Meijer, A.H., Moerschbacher, B.M., Punt, P.J., Ram, A.F.J. 2020. A seven-membered cell wall related transglycosylase gene family in

- Aspergillus niger* is relevant for cell wall integrity in cell wall mutants with reduced  $\alpha$ -glucan or galactomannan. *Cell Surf*, **6**, 100039.
- van Veluw, G.J., Teertstra, W.R., de Bekker, C., Vinck, A., van Beek, N., Muller, W.H., Arentshorst, M., van der Mei, H.C., Ram, A.F., Dijksterhuis, J., Wösten, H.A.B. 2013. Heterogeneity in liquid shaken cultures of *Aspergillus niger* inoculated with melanised conidia or conidia of pigmentation mutants. *Stud Mycol*, **74**, 47-57.
- Wanka, F., Arentshorst, M., Cairns, T.C., Jorgensen, T., Ram, A.F., Meyer, V. 2016. Highly active promoters and native secretion signals for protein production during extremely low growth rates in *Aspergillus niger*. *Microb Cell Fact*, **15**, 145.
- Wösten, H.A.B., van Veluw, G.J., de Bekker, C., Krijgsheld, P. 2013. Heterogeneity in the mycelium: implications for the use of fungi as cell factories. *Biotechnol Lett*, **35**, 1155-1164.
- Wösten, H.A.B. 2019. Filamentous fungi for the production of enzymes, chemicals and materials. *Curr Opin Biotechnol*, **59**, 65-70.
- Xiao, Z., Storms, R., Tsang, A. 2004. Microplate-based filter paper assay to measure total cellulase activity. *Biotechnol Bioeng*, **88**, 832-837.
- Yoshimi, A., Sano, M., Inaba, A., Kokubun, Y., Fujioka, T., Mizutani, O., Hagiwara, D., Fujikawa, T., Nishimura, M., Yano, S., Kasahara, S., Shimizu, K., Yamaguchi, M., Kawakami, K., Abe, K. 2013. Functional analysis of the  $\alpha$ -1,3-glucan synthase genes *agsA* and *agsB* in *Aspergillus nidulans*: *agsB* is the major  $\alpha$ -1,3-glucan synthase in this fungus. *PLoS One*, **8**, e54893.
- Yuan, X.L., van der Kaaij, R.M., van den Hondel, C.A., Punt, P.J., van der Maarel, M.J., Dijkhuizen, L., Ram, A.F. 2008. *Aspergillus niger* genome-wide analysis reveals a large number of novel alpha-glucan acting enzymes with unexpected expression profiles. *Mol Genet Genomics*, **279**, 545-561.

**SUPPLEMENTAL MATERIAL**

**Supplemental Table 1.** Proteins with and without a predicted signal sequence for secretion in the secretome of MA234.1. [https://docs.google.com/spreadsheets/d/1bJZetK4FamFjg-BT6\\_shZRrB43QEMsRd/edit?usp=sharing&ouid=100415537618493008153&rtpof=true&sd=true](https://docs.google.com/spreadsheets/d/1bJZetK4FamFjg-BT6_shZRrB43QEMsRd/edit?usp=sharing&ouid=100415537618493008153&rtpof=true&sd=true).

**Supplemental Table 2.** Proteins with and without a predicted signal sequence for secretion in the secretome of LZ05 (*ΔagsE*). [https://docs.google.com/spreadsheets/d/1bJZetK4FamFjg-BT6\\_shZRrB43QEMsRd/edit?usp=sharing&ouid=100415537618493008153&rtpof=true&sd=true](https://docs.google.com/spreadsheets/d/1bJZetK4FamFjg-BT6_shZRrB43QEMsRd/edit?usp=sharing&ouid=100415537618493008153&rtpof=true&sd=true).

**Supplemental Table 3.** Proteins that are shared in the secretomes of MA234.1 and LZ05 (*ΔagsE*). [https://docs.google.com/spreadsheets/d/1bJZetK4FamFjg-BT6\\_shZRrB43QEMsRd/edit?usp=sharing&ouid=100415537618493008153&rtpof=true&sd=true](https://docs.google.com/spreadsheets/d/1bJZetK4FamFjg-BT6_shZRrB43QEMsRd/edit?usp=sharing&ouid=100415537618493008153&rtpof=true&sd=true).

**Supplemental Table 4.** Proteins that are unique in the secretome of MA234.1. [https://docs.google.com/spreadsheets/d/1bJZetK4FamFjg-BT6\\_shZRrB43QEMsRd/edit?usp=sharing&ouid=100415537618493008153&rtpof=true&sd=true](https://docs.google.com/spreadsheets/d/1bJZetK4FamFjg-BT6_shZRrB43QEMsRd/edit?usp=sharing&ouid=100415537618493008153&rtpof=true&sd=true).

**Supplemental Table 5.** Proteins that are unique in the secretome of LZ05 (*ΔagsE*). [https://docs.google.com/spreadsheets/d/1bJZetK4FamFjg-BT6\\_shZRrB43QEMsRd/edit?usp=sharing&ouid=100415537618493008153&rtpof=true&sd=true](https://docs.google.com/spreadsheets/d/1bJZetK4FamFjg-BT6_shZRrB43QEMsRd/edit?usp=sharing&ouid=100415537618493008153&rtpof=true&sd=true).

**Supplemental Table 6.** Up and down-regulated proteins (> 2-fold) within the protein set that is shared in the secretomes of MA234.1 and LZ05 (*ΔagsE*). [https://docs.google.com/spreadsheets/d/1bJZetK4FamFjg-BT6\\_shZRrB43QEMsRd/edit?usp=sharing&ouid=100415537618493008153&rtpof=true&sd=true](https://docs.google.com/spreadsheets/d/1bJZetK4FamFjg-BT6_shZRrB43QEMsRd/edit?usp=sharing&ouid=100415537618493008153&rtpof=true&sd=true).

**Supplemental Table 7.** Protein family analysis of the secretome of MA234.1. <https://docs.google.com/spreadsheets/d/1JMt9vdRbnbKDeWzbu5BBRT2m6VM4ErY0/edit?usp=sharing&ouid=100415537618493008153&rtpof=true&sd=true>.

**Supplemental Table 8.** Protein family analysis of secretome of LZ05 (*ΔagsE*). <https://docs.google.com/spreadsheets/d/1JMt9vdRbnbKDeWzbu5BBRT2m6VM4ErY0/edit?usp=sharing&ouid=100415537618493008153&rtpof=true&sd=true>.

**Supplemental Table 9.** Protein family analysis of proteins identified in the culture medium of both LZ05 (*ΔagsE*) and MA234.1.

The  $\alpha$ -(1,3)-glucan synthase gene *agsE* impacts the secretome of liquid shaken cultures of *Aspergillus niger* by reducing micro-colony size  
<https://docs.google.com/spreadsheets/d/1JMt9vdRbnbKDcWzbu5BBRT2m6VM4ErY0/edit?usp=sharing&ouid=100415537618493008153&rtpof=true&sd=true>.

**Supplemental Table 10.** Protein family analysis of unique proteins in the secretome of MA234.1.

<https://docs.google.com/spreadsheets/d/1JMt9vdRbnbKDcWzbu5BBRT2m6VM4ErY0/edit?usp=sharing&ouid=100415537618493008153&rtpof=true&sd=true>.

**Supplemental Table 11.** Protein family analysis of unique proteins in the secretome of LZ05 ( $\Delta$ *agsE*).

<https://docs.google.com/spreadsheets/d/1JMt9vdRbnbKDcWzbu5BBRT2m6VM4ErY0/edit?usp=sharing&ouid=100415537618493008153&rtpof=true&sd=true>.

**Supplemental Table 12.** Protein family analysis of significant >2-fold up- or down-regulated proteins in LZ05 ( $\Delta$ *agsE*) in the set of shared proteins in the secretomes of LZ05 and MA234.1.

<https://docs.google.com/spreadsheets/d/1JMt9vdRbnbKDcWzbu5BBRT2m6VM4ErY0/edit?usp=sharing&ouid=100415537618493008153&rtpof=true&sd=true>.

**Supplemental Table 13.** Expression of cellular proteins in LZ05 ( $\Delta$ *agsE*) compared with MA234.1.

[https://docs.google.com/spreadsheets/d/1\\_CDEwe71xL9bvWUXKDDI7t9QuKbb9Vr7/edit?usp=sharing&ouid=100415537618493008153&rtpof=true&sd=true](https://docs.google.com/spreadsheets/d/1_CDEwe71xL9bvWUXKDDI7t9QuKbb9Vr7/edit?usp=sharing&ouid=100415537618493008153&rtpof=true&sd=true).

**Supplemental Table 14.** Proteins up- or down-regulated in common in LZ05 ( $\Delta$ *agsE*) compare with MA234.1 at 6, 8, and 10h.

[https://docs.google.com/spreadsheets/d/1\\_CDEwe71xL9bvWUXKDDI7t9QuKbb9Vr7/edit?usp=sharing&ouid=100415537618493008153&rtpof=true&sd=true](https://docs.google.com/spreadsheets/d/1_CDEwe71xL9bvWUXKDDI7t9QuKbb9Vr7/edit?usp=sharing&ouid=100415537618493008153&rtpof=true&sd=true).

**Supplemental Table 15.** Transcription factors identified in the set of up- and down-regulated proteins in LZ05 ( $\Delta$ *agsE*) compare to MA234.1 at 6, 8 and 10h.

[https://docs.google.com/spreadsheets/d/1\\_CDEwe71xL9bvWUXKDDI7t9QuKbb9Vr7/edit?usp=sharing&ouid=100415537618493008153&rtpof=true&sd=true](https://docs.google.com/spreadsheets/d/1_CDEwe71xL9bvWUXKDDI7t9QuKbb9Vr7/edit?usp=sharing&ouid=100415537618493008153&rtpof=true&sd=true).

**Supplemental Table 16.** Proteins with a predicted signal sequence that had not been reported before to be part of the *A. niger* secretome.

[https://docs.google.com/spreadsheets/d/1\\_CDEwe71xL9bvWUXKDDI7t9QuKbb9Vr7/edit?usp=sharing&ouid=100415537618493008153&rtpof=true&sd=true](https://docs.google.com/spreadsheets/d/1_CDEwe71xL9bvWUXKDDI7t9QuKbb9Vr7/edit?usp=sharing&ouid=100415537618493008153&rtpof=true&sd=true).



# **Chapter 6**

## **Summary and General Discussion**



## **Background and aim of the Thesis**

Fungi are widely used in biotechnology to produce enzymes and small molecular weight chemicals (Wösten, 2019). For instance, *Aspergillus niger* has been used for a century to produce citric acid at an industrial scale for use as a food and beverage ingredient. This filamentous fungus is also widely used for the production of enzymes such as glucoamylase that converts starch into glucose syrup. *A. niger* is grown in large scale bioreactors to produce the small molecular weight molecules and enzymes. In such liquid dynamic cultures, but also in lab-scale liquid shaken cultures, *A. niger* forms (sub-)millimeter sized micro-colonies. Micro-colonies with a distinguishable center and outer periphery are called pellets, while such a distinction cannot be made in the case of dispersed mycelium. Experimental evidence indicates that these differences in morphology impact productivity. For instance, micro-colonies of *A. niger* produce more citric acid when compared to dispersed mycelium (Clark, 1962; Clark et al., 1966), while dispersed mycelium and small micro-colonies more highly express genes encoding secreted proteins (Tegelaar et al., 2020). Yet, the relation between micro-colony morphology and production of chemicals and enzymes is still poorly understood. Morphology in bioreactors is controlled by changing growth conditions such as the amount and formulation of inoculum and medium composition (Krijgsheld et al., 2013; Wösten et al., 2013). Therefore, it is not possible to conclude whether the changes in productivity are the result of the changes in mycelium morphology, the culture conditions, or both. Moreover, the fact that micro-colony morphology can be heterogeneous in liquid cultures (de Bekker et al., 2011) complicates to establish the relation between micro-colony morphology and productivity.

Liquid shaken cultures of *A. niger* are routinely inoculated with conidia. Germination of these spores results in germlings that develop into branching hyphae that in turn form a micro-colony. Dormant spores and germlings can aggregate in liquid shaken cultures, known as primary and secondary aggregation, respectively (Grimm et al., 2004). These aggregation events result in large micro-colonies, while non-aggregated spores and germlings give rise to dispersed mycelium.

The aim of this thesis was to reveal the relation between micro-colony morphology, stress resistance and protein secretion and to reveal molecular mechanisms underlying this relation.

## **Relation between micro-colony morphology, stress resistance, and protein secretion**

As was described above, by controlling micro-colony morphology by changing culture conditions one cannot conclude whether the changes in productivity are the result of the

changes in mycelium morphology, the culture conditions, or both. **Chapter 2** describes a method to control micro-colony morphology without changing the culture conditions during the production phase. To this end, spores were encapsulated in alginate beads for different time periods during germination, after which the beads were dissolved, followed by transferring the fungal cells / hyphae to fresh medium to monitor protein secretion and stress resistance. This method yielded micro-colonies ranging in size between  $\leq 300 \mu\text{m}$  and  $\geq 3000 \mu\text{m}$ . By using this encapsulation method evidence was obtained that heterogeneity in micro-colony size can be functional. In fact, it is proposed that partial aggregation of spores and germlings has evolved in nature to form different sized micro-colonies that together produce a meta-secretome optimally suited to degrade complex substrates and to promote survival when exposed to stress (Figure 1).

Small and large micro-colonies had released 556 and 208 different proteins in the culture medium (**Chapter 2**). The small micro-colonies did not only release a more diverse palette of proteins, they also secreted higher amounts of a set of proteins that were also released by the large micro-colonies. From this it was concluded that smaller pellets are more productive than large micro-colonies with respect to protein secretion. This may be explained by the fact that expression of genes encoding secreted protein mainly occurs at the periphery of micro-colonies (Tegelaar et al., 2020). Cultures with small micro-colonies will have relatively more mycelium in this outer shell when compared to cultures with the same biomass that form large micro-colonies, thus explaining why small micro-colonies secrete relatively more protein. Of significance, although the large micro-colonies were less effective in protein production, they did release their own unique set of proteins. In fact, cellulase activity of large and small colonies showed synergy when the culture media were combined.

I tried to identify regulatory proteins involved in differential protein secretion in large versus small micro-colonies. To this end, cellular proteomics was performed. This revealed that, among other proteins, the carbonic anhydrase protein AacA and the transcription factor ZtfA were both higher expressed in large micro-colonies when compared to small micro-colonies. Inactivation of their encoding genes did, however, not result in changed biomass, micro-colony morphology, or secretome (unpublished data). For the carbonic anhydrase this was somewhat surprising because it was also down-regulated in the  $\Delta\text{agsE}$  micro-colonies when compared to the large wild-type micro-colonies (**Chapter 5**), again suggesting a relation between micro-colony size and carbonic anhydrase abundance.

About half of the proteins that were released in the culture medium by small micro-colonies did not have a signal sequence for secretion, while this was only  $\leq 15\%$  in the case of

large micro-colonies. These proteins may be released in the medium by lysis as indicated by the presence of biomarkers of early stages of autolysis in the culture medium (White et al., 2002; McIntyre et al., 2002). It should be noted that microscopy did not reveal autolysing hyphae in the cultures. Therefore, proteins without signal sequence may also be released into the medium by non-classical secretion (Duran et al., 2010; Manjithaya et al., 2010). Hsp70 is involved in this type of non-classical secretion (Rabouille, 2017). Notably, this protein was found in the culture medium of small micro-colonies. Recently, 51 proteins have been suggested to be secreted via the non-classical pathway in *A. niger* (Vivek-Ananth et al., 2018), 31 of them were identified in our secretomes. Of these 31 proteins, 8 proteins had a signal sequence for secretion. Of the remaining 23 proteins, a total of 13 and 23 were released by large and small micro-colonies, respectively. Together, these data suggest that at least some proteins are released by non-classical secretion.

Data described in **Chapter 2** are of interest for biotech companies. If one is interested to highly produce a single protein, one would generally opt to grow small micro-colonies of uniform size, most preferably with a radius  $\leq$  the width of the peripheral expression zone of this particular gene (Tegelaar et al., 2020). Yet, if one is interested in a blend of enzymes, for instance to convert agricultural waste into simple sugars for biofuel or bioplastic production, one would use micro-colonies with heterogeneous size. Such heterogeneity can be obtained by making blends of pre-cultures with micro-colonies of different size. Alternatively, one can use conditions that result in cultures with variable micro-colony size.

The synergy in enzyme activity between small and large micro-colonies as was observed in liquid shaken cultures raises the question whether this phenomenon also occurs in nature. The surfaces of spores and germlings of *A. niger* may have evolved to allow that part, but not all, spores and germlings aggregate (Figure 1). As a result, micro-colonies of different size would be formed for instance in a water droplet on a leaf surface. In such a case, these micro-colonies would help each other to degrade the plant polymers. Notably, while the small micro-colonies are the main enzyme secretors, the large micro-colonies are more resistant to heat and H<sub>2</sub>O<sub>2</sub> (**Chapter 3**). Conidia were found in the core of large pellets (but not in small micro-colonies) that were shown to originate from the inoculum of the liquid culture. As far as we know, this is the first report of resting conidia in the core of a micro-colony. Of interest, the resistance of large micro-colonies to heat and H<sub>2</sub>O<sub>2</sub> was shown to partly result from these spores and partly from the hyphae at the micro-colony periphery that form a protective shield for the micro-colony center. Spores are more stress resistant than vegetative hyphae (Dijksterhuis, 2019), explained by the high levels of compatible solutes like trehalose, mannitol and glycerol

that ensure dormancy and protect the cellular membrane and proteins (Baltussen et al., 2020). The reason why part of the spores in the centre of large micro-colonies do not germinate is consistent with spore germination studies (Ijadpanahsaravi, 2021; Punt et al., 2022). Conidia of *A. niger* (Ijadpanahsaravi, 2021) and *Penicillium roqueforti* (Punt et al., 2022) have a very heterogeneous germination response. For instance, only 20% of the *A. niger* spores germinate within 14 h in a defined medium with glucose as a carbon source and similar responses were observed when amino acids were used as a carbon source. This heterogeneity was proposed to be a bet hedging strategy to prevent that the whole population would die when exposed to stress (Ijadpanahsaravi, 2021). For instance, when temperature would increase above the cardinal temperature during daytime, the germlings would be killed but not the stress resistant conidia. It is tempting to speculate that heterogeneity in spore germination also has evolved to protect stress survival of micro-colonies.

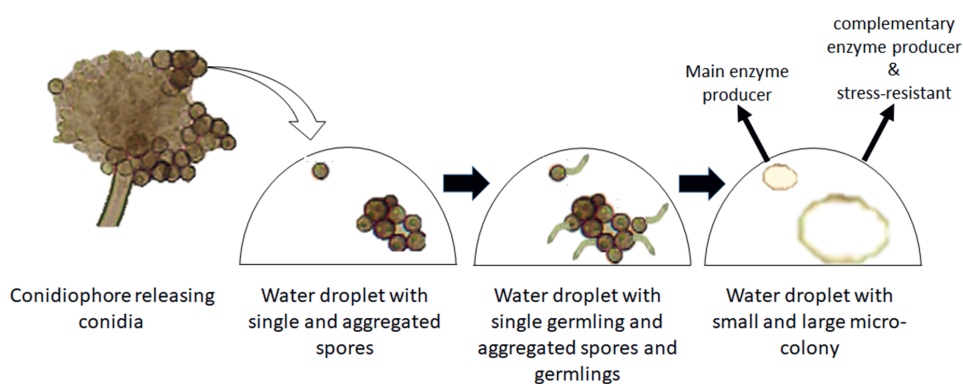


**Figure 1.** Formation of small and large micro-colonies and their role in an aqueous environment. Germination is triggered by inducing compounds in the water droplet.

### Genes related to pellet forming

The  $\alpha$ -1-3 glucan synthase *AgsE* has been reported to be involved in secondary aggregation of spores of aspergilli (Fontaine et al., 2010; He et al., 2014; Yoshimi et al., 2013). Indeed, deletion of *agsE* in *A. niger* resulted in a reduction of micro-colony diameter from 3304 to 1229 (Chapter 5). This reduction of micro-colony size was accompanied by changes in the secretome. Micro-colonies of  $\Delta$ *agsE* secreted 439 proteins, while the parent strain released 304 proteins. A total of 198 and 63 proteins were unique for these strains, respectively. Among the 241 proteins that were found in the secretomes of both strains, 46 and 57 proteins were significantly >2 fold down- and up-regulated in  $\Delta$ *agsE*. These data are consistent with the

finding that the  $\Delta$ agsE strain of *A. oryzae* secretes increased levels of a cutinase (Miyazawa et al., 2016) and confirm the findings of **Chapter 2** that small micro-colonies release more protein in the culture medium. Like small wild-type micro-colonies,  $\Delta$ agsE released many proteins without a signal sequence. As discussed above, this could be due to non-classical secretion and / or cell lysis. Indeed, levels of Hsp70, indicative of non-classical secretion, were higher in the secretome of  $\Delta$ agsE micro-colonies when compared to the large wild-type micro-colonies. In addition, aspartyl proteases, indicative of early stage autolysis of hyphae (White et al., 2002), were found in the secretomes of  $\Delta$ agsE micro-colonies and of large wild-type micro-colonies, indicative of a basic level of hyphal lysis (McIntyre et al., 2000). Notably, prolyl oligopeptidase was found in  $\Delta$ agsE but not wild-type, which suggests that lysis incidence is higher in the deletion strain. Together, **Chapter 2** and **Chapter 5** suggest that large micro-colonies are not only more resistant to heat and oxidative stress when compared to small micro-colonies (**Chapter 3**) but also to shear forces.

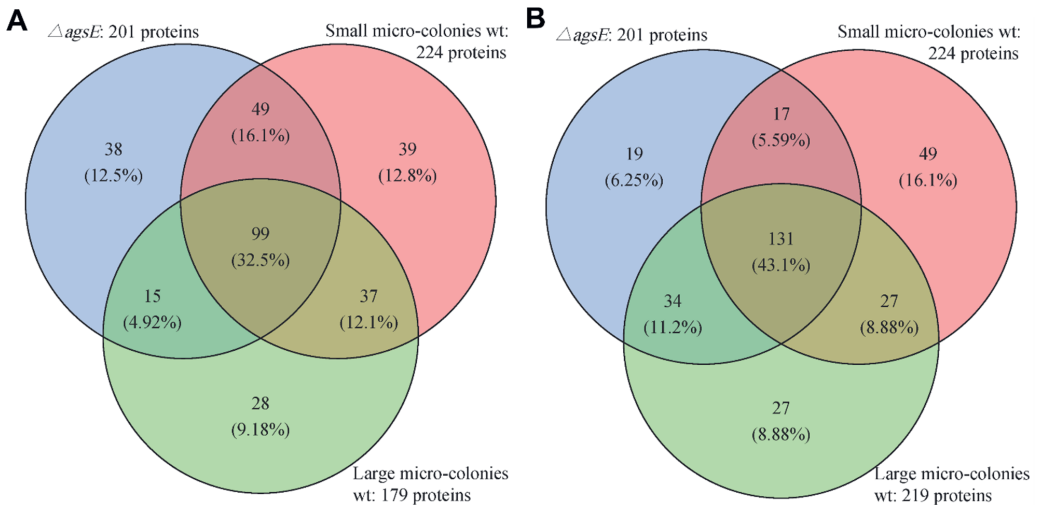


**Figure 2.** Venn diagram of proteins with a predicted signal peptide in the secretomes of large and small micro-colonies of MA234.1 and  $\Delta$ agsE. The secretomes of the small wild-type and  $\Delta$ agsE micro-colonies are described in **Chapter 2** and **Chapter 5**, respectively, while those of the large micro-colonies are from **Chapter 2 (A)** and **Chapter 5 (B)**.

Venn diagrams of proteins with a signal sequence that were released by small (**Chapter 2**) and large (**Chapter 2** and **5**) wild-type micro-colonies and by the small  $\Delta$ agsE micro-colonies (**Chapter 5**) are compared in Figure 2. This shows that the majority of the secreted

proteins are shared by these three types of micro-colonies. It also shows that the small wild-type and  $\Delta agsE$  micro-colonies share a set of proteins but also have their own unique set of proteins. Thus, deleting  $\Delta agsE$  not only impacts protein secretion by its effect on micro-colony size but also by some other unknown mechanisms. For instance, the absence of  $\alpha$ -1-3-glucan may activate some compensatory mechanisms that includes a set of secreted proteins.

Notably, synergy in cellulase activity (see above) was also shown when  $\Delta agsE$  micro-colonies were mixed with the large wild-type micro-colonies. The fact that the large micro-colonies of the wild-type strain secreted two unique GH5 cellulases and over-express one additional GH5 cellulase, while  $\Delta agsE$  over-expressed another GH5 cellulase may explain the synergistic effect of mixing the culture media of these strains (**Chapter 5**; Supplemental Tables 1, 2). Possibly, synergy can also be observed when mixing small wild-type and  $\Delta agsE$  micro-colonies since each type of mycelium secretes a different GH5 cellulase. Future experiments should reveal whether there is indeed such a synergy.

As described above, the small micro-colony phenotype of  $\Delta agsE$  of *A. niger* did not come to a surprise. In contrast, this phenotype was not expected for low *pyrG* expressing strains of this fungus. Gene *pyr4* from *N. crassa* is a homologue of *pyrG* of *A. niger* that is widely used for complementation of uridine and uracil auxotrophy (Diez et al., 1987). However, complementation of a *pyrG* strain of *A. niger* with *pyr4* resulted in small micro-colonies (diameter  $\leq 1000 \mu\text{m}$ ), while large micro-colonies were obtained when this strain was complemented with *pyrG* (diameter  $\geq 3000 \mu\text{m}$ ). Small micro-colonies were also obtained when *pyrG* and *pyr4* were lowly expressed from the inducible *Tet-on* promoter system, while high induction of this promoter resulted in large micro-colonies. From these results it was concluded that the small micro-colony phenotype is explained from a relatively low activity of the *pyr4* promoter when compared to that of *pyrG*. The impact of low *pyrG* or *pyr4* expression on micro-colony morphology was explained by a reduced primary aggregation of conidia and possibly also that of germlings (**Chapter 4**). Cellular proteomics of spores complemented with *pyr4* or *pyrG* revealed differences in cell wall related proteins. In particular, glucanases, glucan synthases and the hydrophobins HypB, HypC and HypE were differentially expressed. Single knockouts of the encoding hydrophobin genes did not reveal a spore aggregation phenotype. This may be explained by redundancy and therefore a triple hydrophobin knockout is currently being constructed.

## REFERENCES

- Baltussen, T.J.H., Zoll, J., Verweij, P.E., Melchers, W.J.G. 2020. Molecular mechanisms of conidial germination in *Aspergillus* spp. *Microbiol Mol Biol Rev*, **84**, e00049-19.
- Clark, D.S. 1962. Submerged citric acid fermentation of ferrocyanide-treated beet molasses: morphology of pellets of *Aspergillus niger*. *Can J Microbiol*, **8**, 133-136.
- Clark, D.S., Ito, K., Horitsu, H. 1966. Effect of manganese and other heavy metals on submerged citric acid fermentation of molasses. *Biotechnol Bioeng*, **8**, 465-471.
- de Bekker, C., van Veluw, G.J., Vinck, A., Wiebenga, L.A., Wösten, H.A.B. 2011. Heterogeneity of *Aspergillus niger* microcolonies in liquid shaken cultures. *Appl Environ Microbiol*, **77**, 1263-1267.
- Diez, B., Alvarez, E., Cantoral, J.M., Barredo, J.L., Martin, J.F. 1987. Selection and characterization of *pyrG* mutants of *Penicillium chrysogenum* lacking orotidine-5'-phosphate decarboxylase and complementation by the *pyr4* gene of *Neurospora crassa*. *Curr Genet*, **12**, 277-282.
- Dijksterhuis, J. 2019. Fungal spores: Highly variable and stress-resistant vehicles for distribution and spoilage. *Food Microbiol*, **81**, 2-11.
- Duran, J.M., Anjard, C., Stefan, C., Loomis, W.F., Malhotra, V. 2010. Unconventional secretion of Acb1 is mediated by autophagosomes. *J Cell Biol*, **188**, 527-536.
- Fontaine, T., Beauvais, A., Loussert, C., Thevenard, B., Fulgsang, C.C., Ohno, N., Clavaud, C., Prevost, M.C., Latge, J.P. 2010. Cell wall  $\alpha$ 1-3glucans induce the aggregation of germinating conidia of *Aspergillus fumigatus*. *Fungal Genet Biol*, **47**, 707-712.
- Grimm, L.H., Kelly, S., Hengstler, J., Gobel, A., Krull, R., Hempel, D.C. 2004. Kinetic studies on the aggregation of *Aspergillus niger* conidia. *Biotechnol Bioeng*, **87**, 213-218.
- He, X., Li, S., Kaminskyj, S.G. 2014. Characterization of *Aspergillus nidulans*  $\alpha$ -glucan synthesis: roles for two synthases and two amylases. *Mol Microbiol*, **91**, 579-595.
- Ijadpanahsaravi, M., Punt, M., Wösten, H.A.B., Teertstra, W.R. 2021. Minimal nutrient requirements for induction of germination of *Aspergillus niger* conidia. *Fungal Biol*, **125**, 231-238.
- Krijgsheld, P., Bleichrodt, R., van Veluw, G.J., Wang, F., Muller, W.H., Dijksterhuis, J., Wösten, H.A.B. 2013. Development in *Aspergillus*. *Stud Mycol*, **74**, 1-29.
- Manjithaya, R., Anjard, C., Loomis, W.F., Subramani, S. 2010. Unconventional secretion of *Pichia pastoris* Acb1 is dependent on GRASP protein, peroxisomal functions, and autophagosome formation. *J Cell Biol*, **188**, 537-546.

- McIntyre, M., Berry, D.R., McNeil, B. 2000. Role of proteases in autolysis of *Penicillium chrysogenum* chemostat cultures in response to nutrient depletion. *Appl Microbiol Biotechnol*, **53**, 235-242.
- Miyazawa, K., Yoshimi, A., Zhang, S., Sano, M., Nakayama, M., Gomi, K., Abe, K. 2016. Increased enzyme production under liquid culture conditions in the industrial fungus *Aspergillus oryzae* by disruption of the genes encoding cell wall  $\alpha$ -1,3-glucan synthase. *Biosci Biotechnol Biochem*, **80**, 1853-1863.
- Punt, M., Teertstra, W.R., Wösten, H.A.B. 2022. *Penicillium roqueforti* conidia induced by L-amino acids can germinate without detectable swelling. *Antonie van Leeuwenhoek*, **115**, 103-110.
- Rabouille, C. 2017. Pathways of unconventional protein secretion. *Trends Cell Biol*, **27**, 230-240.
- Tegelaar, M., Aerts, D., Teertstra, W.R., Wösten, H.A.B. 2020. Spatial induction of genes encoding secreted proteins in micro-colonies of *Aspergillus niger*. *Sci Rep*, **10**, 1536.
- Vivek-Ananth, R.P., Mohanraj, K., Vandanashree, M., Jhingran, A., Craig, J.P., Samal, A. 2018. Comparative systems analysis of the secretome of the opportunistic pathogen *Aspergillus fumigatus* and other *Aspergillus* species. *Sci Rep*, **8**, 6617.
- White, S., McIntyre, M., Berry, D.R., McNeil, B. 2002. The autolysis of industrial filamentous fungi. *Crit Rev Biotechnol*, **22**, 1-14.
- Wösten, H.A.B. 2019. Filamentous fungi for the production of enzymes, chemicals and materials. *Curr Opin Biotechnol*, **59**, 65-70.
- Wösten, H.A.B., van Veluw, G.J., de Bekker, C., Krijgsheld, P. 2013. Heterogeneity in the mycelium: implications for the use of fungi as cell factories. *Biotechnol Lett*, **35**, 1155-1164.
- Yoshimi, A., Sano, M., Inaba, A., Kokubun, Y., Fujioka, T., Mizutani, O., Hagiwara, D., Fujikawa, T., Nishimura, M., Yano, S., Kasahara, S., Shimizu, K., Yamaguchi, M., Kawakami, K., Abe, K. 2013. Functional analysis of the  $\alpha$ -1,3-glucan synthase genes *agsA* and *agsB* in *Aspergillus nidulans*: AgsB is the major  $\alpha$ -1,3-glucan synthase in this fungus. *PLoS One*, **8**, e54893.





# **Nederlandse Samenvatting**

## **Achtergrond en doel van het proefschrift**

Schimmels worden grootschalig door de industrie gebruikt om enzymen en chemicaliën te produceren. Zo wordt *Aspergillus niger* al een eeuw gebruikt om citroenzuur op industriële schaal te produceren voor het gebruik in voedsel en dranken. Deze schimmel wordt ook veel toegepast voor de productie van enzymen, zoals glucoamylase dat zetmeel omzet in glucosestroop. *A. niger* wordt gekweekt in industriële bioreactoren. In dergelijke bioreactoren, maar ook in vloeibare schudculturen op laboratoriumschaal, kan *A. niger* micro-kolonies van verschillende grootte vormen. Experimenteel bewijs geeft aan dat grootte van micro-kolonies de productiviteit kan beïnvloeden. Toch is de relatie tussen de morfologie van micro-kolonies en de productiviteit nog steeds slecht begrepen. Morfologie in bioreactoren wordt namelijk gestuurd door het veranderen van de groeiomstandigheden zoals de samenstelling van het groeimedium. Daarom is het niet mogelijk om te concluderen of de veranderingen in productiviteit het gevolg zijn van de veranderingen in de myceliummorfologie en / of de groeiomstandigheden. Bovendien wordt het vaststellen van de relatie tussen micro-kolonie morfologie en productiviteit bemoeilijkt doordat micro-kolonie grootte heterogeen kan zijn in vloeibare schudculturen. Het doel van dit proefschrift was dan ook om moleculaire mechanismen op te helderen die ten grondslag liggen aan de morfologie van micro-kolonies en de functionaliteit ervan te bepalen in relatie tot stress resistentie en eiwitproductie.

## **Relatie tussen micro-kolonie morfologie, stress resistentie en eiwitproductie**

**Hoofdstuk 2** beschrijft een methode om de morfologie van micro-kolonies te controleren zonder de kweekomstandigheden tijdens de productiviteitsfase te veranderen. Hiertoe werden sporen gedurende het ontkiemen ingekapseld in alginaatkorrels, waarna de korrels werden opgelost, het schimmelmateriaal werd overgebracht naar vers medium, en eiwit productie en stress resistentie werden bepaald. Door de inkapselingstijd te variëren werden micro-kolonies verkregen variërend in grootte tussen respectievelijk  $\leq 300 \mu\text{m}$  en  $\geq 3000 \mu\text{m}$ . Door gebruik te maken van deze inkapselingsmethode werd bewijs verkregen dat het verschil in grootte van een micro-kolonie functioneel kan zijn. Gedeeltelijke aggregatie van sporen en kiemlingen zou zelfs geëvolueerd kunnen zijn om micro-kolonies van verschillende grootte te vormen, zodat overleving bevorderd wordt bij blootstelling aan stress en een meta-secretoom geproduceerd wordt dat optimaal geschikt is om complexe substraten af te breken. De resultaten van **Hoofdstuk 2** zijn interessant voor biotechnologie bedrijven. Als men geïnteresseerd is in het produceren van een enkel eiwit dan zou men over het algemeen kiezen om kleine micro-kolonies van uniforme grootte te kweken. Als men echter geïnteresseerd is in een mengsel van

enzymen, bijvoorbeeld om landbouwafval om te zetten in eenvoudige suikers voor de productie van biobrandstof of bioplastic, dan zou men micro-kolonies met heterogene grootte moeten kweken.

Kleine en grote micro-kolonies scheidde 556 en 208 verschillende eiwitten in hun medium uit (**Hoofdstuk 2**). De kleine micro-kolonies scheidde niet alleen een diverser pallet aan eiwitten uit, ze secreteerden ook grotere hoeveelheden van een set aan eiwitten die ook door de grote micro-kolonies werden uitgescheiden. Hieruit werd geconcludeerd dat kleinere micro-kolonies productiever zijn dan grote micro-kolonies met betrekking tot eiwitproductie. Dit kan worden verklaard door het feit dat expressie van genen die coderen voor uitgescheiden eiwitten voornamelijk plaatsvindt aan de buitenkant van micro-kolonies. Cultures met kleine micro-kolonies zullen relatief meer mycelium in deze buitenste schil bevatten en daarmee relatief meer eiwit uitscheiden. Van belang is dat, hoewel de grote micro-kolonies minder effectief waren in eiwitproductie, zij wel hun eigen unieke set aan eiwitten uitscheidde. Een interessante observatie was dat de cellulase-activiteit van grote en kleine kolonies synergie vertoonden wanneer de kweekmedia werden gemengd. Deze bevinding roept de vraag op of dit fenomeen ook in de natuur voorkomt. De oppervlakken van sporen en kiemlingen van *A. niger* kunnen zo zijn geëvolueerd dat een slechts een deel aggregereert. Als gevolg hiervan zouden micro-kolonies van verschillende grootte worden gevormd, bijvoorbeeld in een waterdruppel op een bladoppervlak, waarbij zij elkaar helpen om de plantaardige polymeren af te breken.

Terwijl de kleine micro-kolonies de belangrijkste eiwit producenten zijn, zijn de grote micro-kolonies beter bestand tegen hitte en H<sub>2</sub>O<sub>2</sub> (**Hoofdstuk 3**). Sporen bleken aanwezig in de kern van de grote micro-kolonies (maar niet in kleine micro-kolonies). Experimenteel bewijs toonde aan dat deze sporen afkomstig zijn van de oorspronkelijke ent van de vloeibare cultuur. De resistentie van de grote micro-kolonies tegen hitte en H<sub>2</sub>O<sub>2</sub> wordt gedeeltelijk bepaald door deze sporen maar ook door de schimmeldraden aan de buitenkant van de micro-kolonie die een beschermend schild vormen voor de hyfen en sporen in het centrum van de micro-kolonie. Het is verleidelijk om te speculeren dat de heterogeniteit in ontkieming van sporen in het centrum van de micro-kolonie is geëvolueerd om de overleving van micro-kolonies tijdens stress te bevorderen.

### Genen gerelateerd aan micro-kolonie vorming

Het  $\alpha$ -1-3-glucansynthase *AgsE* is betrokken bij de aggregatie van kiemlingen van aspergilli, wat leidt tot grote micro-kolonies. Inderdaad bleek dat deletie van *agsE* in *A. niger* resulteerde



in een reductie van de diameter van de micro-kolonies van 3304 tot 1229  $\mu\text{m}$  (**Hoofdstuk 5**). Deze vermindering in grootte ging gepaard met veranderingen in het secretoom. Micro-kolonies van  $\Delta\text{agsE}$  scheidde 439 eiwitten uit, terwijl de ouderstam 304 eiwitten uitscheidde. In totaal waren respectievelijk 198 en 63 eiwitten uniek voor deze stammen. Van de 241 eiwitten die werden gevonden in beide secretomen bleken 46 en 57 eiwitten  $> 2$ -voudig neerwaarts en opwaarts gereguleerd te zijn in  $\Delta\text{agsE}$ . Deze bevindingen bevestigen de resultaten van **Hoofdstuk 2** waarin werd aangetoond dat kleine micro-kolonies meer eiwitten afgeven in het kweekmedium. Kleine wildtype en  $\Delta\text{agsE}$  micro-kolonies scheidde daarnaast meer eiwitten uit zonder signaalsequentie dan grote wildtype-microkolonies. Experimenten suggereren dat het uitscheiden van eiwitten zonder signaalsequentie wordt verklaard door niet-klasseke secretie en / of cellysis. Dit laatste impliceert dat grote microkolonies niet alleen beter bestand zijn tegen hitte en oxidatieve stress dan kleine micro-kolonies (**Hoofdstuk 3**), maar ook beter bestand zijn tegen mechanische krachten (**Hoofdstuk 5**). Synergie in cellulase-activiteit (zie hierboven) werd ook aangetoond wanneer het culture medium van  $\Delta\text{agsE}$  micro-kolonies werden gemengd met dat van grote wild-type micro-kolonies. Deze resultaten kunnen worden verklaard door een verschillende samenstelling van cellulasen in de kweekmedia van deze stammen. Verschillen in eiwitsamenstelling in het kweekmedium werden ook waargenomen tussen de kleine micro-kolonies van het wildtype en die van  $\Delta\text{agsE}$ . Het verwijderen van  $\text{agsE}$  heeft dus niet alleen invloed op de eiwitsecretie door het effect op de grootte van de micro-kolonie, maar ook door andere mechanismen. De afwezigheid van  $\alpha$ -1-3-glucaan kan bijvoorbeeld compenserende mechanismen activeren, bijvoorbeeld door het uitscheiden van bepaalde eiwitten.

Zoals hierboven werd beschreven kwam het kleine micro-kolonie fenotype van  $\Delta\text{agsE}$  van *A. niger* niet onverwacht omdat dit al was gevonden voor andere aspergilli. Daarentegen werd dit fenotype niet verwacht voor stammen die *pyrG* laag tot expressie brengen. Gen *pyr4* van *Neurospora crassa* is een homoloog van *pyrG* van *A. niger* dat veel wordt gebruikt voor complementatie van uridine en uracil auxotrofie. Complementatie van een  $\Delta\text{pyrG}$  stam van *A. niger* met *pyr4* resulteerde echter in kleine micro-kolonies (diameter  $\leq 1000 \mu\text{m}$ ), terwijl grote micro-kolonies werden verkregen wanneer deze stam werd gecomplementeerd met *pyrG* (diameter  $\geq 3000 \mu\text{m}$ ). Kleine micro-kolonies werden ook verkregen wanneer *pyrG* en *pyr4* laag tot expressie werden gebracht gebruikmakend van het induceerbare *Tet-on* systeem, terwijl hoge inductie van deze promotor resulteerde in grote micro-kolonies. Uit deze resultaten werd geconcludeerd dat het fenotype van een kleine micro-kolonie wordt verklaard door een relatief lage expressie van *pyrG* of *pyr4*. De impact van lage expressie van deze genen op de

morfologie van micro-kolonies werd verklaard door een verminderde aggregatie van sporen, en mogelijk ook die van kiemlingen, kort na het beënten van de culture (**Hoofdstuk 4**). Cellulaire proteomics van sporen liet verschillen in celwand-gerelateerde eiwitten zien wanneer lage *pyr4* en hoge *pyrG* expressie werd vergeleken. Zo werden glucanasen, glucaansynthasen en de hydrofobines HypB, HypC en HypE differentieel tot expressie gebracht. Het verwijderen van één van deze hydrofobinegenen liet geen sporenaggregatie fenotype zien. Dit zou verklaard kunnen worden door redundantie en daarom wordt momenteel een drievoudige hydrofobine-knock-out gemaakt.





# 中文总结



## 论文的背景和目的

一个世纪以来，真菌一直被广泛用于工业生产有机酸和化学产品。例如，黑曲霉一直被用于工业化大规模生产用于食品和饮料的柠檬酸。同时这种真菌还被广泛用于生产工业酶，其中最著名的是能够将淀粉转化为玉米糖浆的葡糖淀粉酶。为了大规模获得酶制剂以及次级代谢产物（有机酸等），一般会将黑曲霉培养在大型生物反应器中。在这样的生物反应器或者在用于研究的实验室规模的液体摇瓶培养中，黑曲霉都可以形成不同大小的菌丝球。实验表明，这些菌丝球的大小会影响其生产能力。然而，由于科学家们对菌丝球形态和生产效率之间的具体关系仍然知之甚少（不同产物可能有不同的对应关系），目前一般是通过改变生长条件（例如培养基的组成）来控制菌丝球的形态。因此，无法断定生产效率的改变是由于菌丝形态变化还是生长条件的变化。此外，菌丝球形态和生产效率之间的关系是复杂的，因为在同一液体摇瓶培养中可能同时出现形态不同的菌丝球。本论文的目的是阐明菌丝球形态对抗逆性和蛋白质分泌的影响，并确定菌丝球形成的分子机制。

## 菌丝球形态对抗逆性和蛋白分泌的影响

第 2 章描述了一种在发酵阶段无需改变培养条件即可控制菌丝球形态的新方法。通过在萌发期间将孢子包裹在海藻酸钙颗粒中，同时在培养一段时间后使用 1M 的柠檬酸溶液将海藻酸钙颗粒溶解，无菌水洗涤之后将萌发的菌丝转移到新鲜的液体培养基中继续培养。通过对海藻酸钙颗粒溶解时间的调控，我们将得到不同粒径的菌丝球。当在 8h 之前溶解时，可以得到直径大于 3000 微米的菌丝球；当溶解时间晚于 10h 时，菌丝球的粒径小于 300 微米。通过使用这种包埋的方法，我们得到了不同粒径的菌丝球并对其进行了抗性和胞外蛋白的检测。实验表明在液体培养中，不同大小的菌丝球可能具有协同作用，即粒径较小的菌丝球由于比表面积大，蛋白的分泌能力比较强；粒径较大的菌丝球由于其内部难以获得生长所需底物以及溶氧，一些孢子被贮藏其中停止萌发，因而具有更强的抗逆性。进一步推测，在液体培养中孢子和刚萌发的菌丝甚至可能会主动聚集形成粒径不同的菌丝球，这种粒径不同的菌丝球群落能够分泌种类更丰富的酶到液体培养基中用以降解复杂的底物，同时还有利于在生存环境变得不利时提高整体群落的适应性。当人类为了自身的利益将丝状菌培养在发酵罐中并优化最适条件时，可能对微生物而言并不是理想的生长环境，例如高密度培养和持续的剪切力。因此，它们选择形成大小不一的菌丝球来提高整体群落的适应性。从应用的角度说，一些生物技术公司可能会对这第二章的内容比较感兴趣。一般来说，如果一公司对生产单一品种的蛋白感兴趣，他们应该选择去诱导真菌形成粒径比较均匀的菌丝球。然而，如果人们对酶的混合物感兴趣，例如将农业废物转化为单糖或者降解生物塑料，那么人们应该偏向培养不同大小的菌丝球，因为理论上这种培养方式可以产生种类更丰富的酶系。

粒径较小和较大的菌丝球分别在其培养基中分泌了 556 和 208 种不同的蛋白质（第 2 章）。小菌丝球不仅分泌了种类更丰富的蛋白质，对于那些同时也能够由较大的菌丝球分泌的蛋白质，它们也有着更高的产量。由此得出结论，在蛋白质生产方面，较小的菌丝球比大的菌丝球更具生产力。这可以通过以下研究结果来解释：当对菌丝

球不同部位进行研究时，编码底物降解相关的蛋白仅仅表达在菌丝球的表面而非菌丝球内部，而粒径较小的菌丝球相对具有更大的比表面积，因此蛋白质分泌能力比较强。重要的是，尽管粒径较大的菌丝球在蛋白质生产方面效率较低，但它们确实分泌了自己特有的蛋白质（不能被小菌丝球生产）。有趣的是，当将来自于不同粒径菌丝球的培养液混合时，大小菌丝球的发酵液中纤维素酶活性显示出协同作用（对纤维素降解效果显著高于单一发酵液）。这一发现使我们思考这种现象是否也发生在自然界中：黑曲霉是否可能已经进化能自主选择部分聚集孢子和刚萌芽的菌丝，由此形成不同大小的微菌落（例如在叶子表面的水滴中），帮助彼此分解植物聚合物。

虽然小的菌丝球是主要的蛋白质生产者，但大的菌丝球对热和一些氧化剂的抵抗力更强（第 3 章）。同时在粒径较大的菌丝球中心发现了孢子（但在较小菌丝球中没有发现类似结构）。实验表明，这些孢子来自于初始接种而非后期产生。粒径较大的菌丝球对热和  $H_2O_2$  的抵抗力部分取决于这些孢子，但也取决于菌丝球的体积，外部菌丝为菌丝球中心的菌丝和孢子形成了保护屏障。我们推测，大菌丝球中心未萌芽的孢子具有更强的抗性，当生存环境变得恶劣时，这种延迟萌发能够提高整个群落的适应性与存活率。

### 与菌丝球形成相关的基因

$\alpha$ -1-3-葡聚糖酶 *AgsE* 被证明能够通过影响黑曲霉孢子和刚萌发的菌丝的聚集影响菌丝球的形态。事实上，黑曲霉中 *agsE* 基因的缺失导致菌丝球的粒径从 3304 微米减小到 1229 微米，同时培养基中有更多的蛋白被检测到（第 5 章）。*agsE* 缺失株分泌了 439 种蛋白质，而亲本菌株则共分泌了 304 种蛋白质，其中 241 种蛋白在两种发酵液中均被检测到，198 和 63 种蛋白质分别是这两株菌所独有的。在两株菌的发酵液中同时发现的 241 种蛋白质中，发现 46 和 57 种蛋白质在 *agsE* 敲除株中显著下调和上调大于 2 倍。这些发现证实了第 2 章的结果，即较小的菌丝球能够分泌更多（种类与产量）的蛋白到培养基中。此外，经海藻酸钙包埋形成的野生型较小菌丝球和 *agsE* 缺失株形成的小菌丝球比大粒径野生型菌丝球分泌了更多无信号肽的蛋白质。研究表明，没有信号肽的蛋白质在培养基中被检测到可以通过非经典途径分泌或者细胞裂解来解释。后者意味着大的菌丝球不仅比小的菌丝球有更强的抵抗热和氧化应激的能力（第 3 章），而且具有更强的抵抗机械力的能力（第 5 章）。当 *agsE* 缺失株的培养基与野生型形成较大菌丝球的培养基混合时，同样检测到了纤维素酶活性的协同作用（见上文）。这些结果可以通过能够在两种培养液中检测到的不同种类（以及浓度）的纤维素酶来解释。在同样形成较小菌丝球的野生型和 *agsE* 缺失株之间也观察到培养液中蛋白质组成（包括纤维素酶）的差异。因此证明敲除 *agsE* 不仅通过调控菌丝球大小来影响蛋白质分泌，而且还通过其他机制影响蛋白质分泌。例如，缺乏  $\alpha$ -1-3-葡聚糖可以激活补偿机制去分泌某些特定蛋白质。

如上所述，来自黑曲霉的 *agsE* 缺失株形成较小菌丝球的表型并不出人意料，因为它已经在其他曲霉中被发现。相反，弱表达 *pyrG* 的菌株同样能够形成较小的菌丝球是意外发现。粗糙脉孢菌基因 *pyr4* 是来自黑曲霉的基因 *pyrG* 的同源物，广泛用于尿苷/尿嘧啶营养缺陷型的回补。然而，黑曲霉的 *pyrG* 缺失菌株与 *pyr4* 的回补导致小的



菌丝球（直径小于 1000 微米）的形成，而当该菌株使用 *pyrG* 回补时获得较大的菌丝球（直径大于 3000 微米）。当 *pyrG* 和 *pyr4* 使用诱导型启动子 Tet-on 系统时，未添加或者添加低剂量诱导剂时形成粒径较小的菌丝球，而对该启动子的高表达则诱导大粒径菌丝球的形成。从这些结果可以得出结论，菌丝球粒径较小的表型与 *pyrG/pyr4* 的表达水平相关。*pyrG/pyr4* 低表达对菌丝球形态的影响可以通过在显微镜下孢子（或者刚萌发的菌丝）显著地减少了聚集来解释（第 4 章）。当 *pyrG/pyr4* 表达量不同时，孢子的细胞蛋白质组学显示细胞壁相关蛋白存在差异，葡聚糖酶、葡聚糖合酶和疏水蛋白 HypB、HypC 和 HypE 等蛋白的表达具有显著差异。这些疏水蛋白基因的单敲除并未得到明显的表型，我们推测可能是这些蛋白之间会形成一个动态网络，当编码某一个蛋白的基因被敲除或者被诱导弱表达时，其他一些特定基因可能会过表达来补偿其生物学功能，因此目前正在对这三个疏水蛋白同时进行敲除。

---

## Curriculum vitae

Jun Lyu was born on Feb 14th, 1992 in Anqing, China. He followed his secondary education at the Susong middle school at Anqing and enrolled the Bachelor Biotechnology at Jilin Institute of Chemical Technology September 2010. After receiving his bachelor's degree in 2014, he continued his master study at Jiangnan University, Wuxi, China. Under the supervisor of Prof Ganrong Xu and Prof Bobo Zhang, he established a bi-phase fermentation and purification technology for yellow pigment production in *Monascus*. Jun obtained his MSc diploma in June 2017. He worked on wastewater treatment for one year resulting in a patent application of a slow release carrier in the treatment reactor. In October 2018, with the support of China Scholarship Council (CSC), he got the opportunity to start his PhD within the Molecular Microbiology group of the Department of Biology at Utrecht University under the supervision of Prof dr HAB Wösten and Dr H de Cock. His research focused on the relation between fungal morphology, stress resistance and protein secretion, and the results of his work are described in this thesis.



## List of publications

Ruan, W.Q., Lyu, J., Deng, J.X., Zhong, H.C., Zhang, P.H., Zhang, Y. CN108018280A a method of slow released microbiology carrier.

Zhang, B.B., Shi, B.M., Lyu, J., Xu, G.R., Zheng, Y.P. CN106967082A a method of purification of yellow pigment from biphasic fermentation system.

Lyu, J., Tegelaar, M., Post, H., Altelaar, A. F. M., Bleichrodt, R. J., de Cock, H., Lugones, L. G., Wösten, H. A. B. Different sized micro-colonies of the fungus *Aspergillus niger* help each other to digest food. In preparation.

Lyu, J., Torres, J.P.M., Post, H., Punt, M., Altelaar, A.F.M, de Cock, H., Wösten, H. A. B. The orotidine 5'-phosphate decarboxylase gene *pyrG* influences *Aspergillus niger* pellet formation and secretome in liquid shaken cultures. In preparation.

Lyu, J., Torchia, C., Post, H., Torres, J.P.M., Altelaar, A.F.M, de Cock, H., Wösten, H. A. B. Han A. B. Wösten. The  $\alpha$ -(1,3)-glucan synthase gene *agsE* impacts the secretome of liquid shaken cultures of *Aspergillus niger* by reducing micro-colony size. In preparation.

# Acknowledgements

The passage of time is just like the flow of water, which goes on day and night. I have stayed in Utrecht university for the past 4 years. Although I can't fulfill the initial promise publishing in Nature, it's no change for this fantastic journey, for the amazing people I have met.

Han, when I am writing to this stage, I realized I couldn't find any words to express my respect and appreciation. I admire your passion to research and your wise to science questions. You are the most patient people I have ever met, I always heard you say "interesting" and I believe everyone get encouragement from your positive feedback. In the past 4 years, every night you spend your time reading and revising the manuscript, while you never set restriction to us, which make me understand the old saying "strict with yourself and be lenient with others". I also enjoy the discussion about the religion and politics with you, these interesting topics further my understanding of different cultures.

Hans, as my co-supervisor. without you spend some weekends reading and revising my manuscript, I couldn't image how many time I still need to finish it. I can always see you passion when we discuss. During group meeting, when everyone thought one direction and balance the difficulties, you sometimes suddenly suggest a new direction and shed the light to opposite. Also, I am very impressed about your critical, sometimes when the manuscript already proceed to the 20th version, you still can find some mistake numbers in some tables, I am afraid you are the only one who indeed counting and calculating the numbers (shame of me).

Luis, you spend a lot time in the lab and still doing experiment personally. I see your affection from the developing mushroom on a wood in your office. We meet each other quite often on weekends, I go to the lab because I have nothing else to do on weekends while you go for the attractive mushroom. I sometimes have a short talk with colleagues when waiting for coffee, we all admire your life style and we hope we can also keep the curiosity after long period career. Wieke, you are always so thoughtful. I always get a long email including every details if I asked some questions, this bring me a lot confidence into some new projects,



---

especially when I start working with *niger* for the first year, enjoy the family time after retirement.

Robert-Jan, you showed us every cool stuff. In my first year, we are in the same office, and you build an auto-water plant system by assembling some sensors, later you organized a workshop show us how to use Arduino to make an alarming system in your house, follows we see your mushroom pressure system, all these cool things display how you combined your hobby and work, I wish someday I can get fun and establish some novel things in my work as well. Robin, as the professor of bioinformatics, thanks for the help for Omics analysis, finally I can make simple coding to fungi, it's really cool. Pauline, it was great to meet you during my first year phd, you always very kind and helped me a lot especially when I work into proteomics initially.

Harm, we have an awesome collaboration, effective and achievement. Thanks for the help of MS, I couldn't image how difficult to go through my project without your support, hope you will have a fantastic journey in new company as well!

Hi *Aspergillus* people, Juan, Xiaoyi and Maryam. We are the small group who doing experiment and meeting together, you are the people I feel most relax to talk with. Juan, you always start working from setting sun, sometimes I work late then we start gossip, topics include but are not limited to our project, relationship, friends and families... sometimes we make very mean joke to each other and sometimes we try to support, too bad I need to leave and I will cherish this period work together with you, wish you can keep your pure pursuit to science and become an influential researcher in future. Xiaoyi, you always very happy and it bring me a lot positive attitude, you have a super good reputation among my friends, we always saying go to Dimsun together since 3 years ago, while it haven't come true until I write to here, thanks for the relax talk especially when I feel pressure from personal life . Maryam, you move your office in the halfway, you are a very nice person always considering other people, and you are ambitious to research, probably you will become the most successful people among *Aspergillus* group, don't forget me when it come true. And thanks again for all of you made the lovely videos to my wedding, I will keep it forever!

Freek, you always thought about international people during Christmas, I spend 2 Christmas with your family, everyone is so kind and warm, transfer my best wishes to Elissa, Sam and your son. Maarten (family man), we had some good talk in the lab, some serious conversion and a lot mean jokes, I will remember you kill me at least 3 times when we playing

chess in the new year eve (at your place!), please contact me if you by any chance will go to China, let me revenge. Peter Jan, as the expert of cloning, bioinformatics, western blot..., I think I have asked you so many questions including all mentioned topics, you always very kind and give the answers, hope you still enjoy the lab without my bothering. Jesus, you are super easy going and always with a good humor, we are the most pathetic party committee, I am pretty sure now you already get a lot friends in the new company, enjoy! Jordi, initially I am a bit scared to talk with you because you looks muscular man ( I hope it not offend you), while it turns out you are a so thoughtful and careful person, thanks for helping me ordered so many stuff in the past years. Koen, we have been to some bar watching footballs and playing a lot pinpong last winter, thanks for bring me into these activities which enriched my life in the lab.

Pellet research group, Costanza, Pim, Sindy en Paco. Costanza, I finish 2 chapters of my thesis and you finish other 2, when you working in the lab, you always laughing (Italian blood), it's too bad corona run through your whole internship year, hope you will have a more colorful life in new working environment. Pim, you are one of the most friendly people I have meet, you always with a positive attitude and very patient, it's very relax to work with you, pretty sure you already made a lot friends in new working environments. Sindy, you are a very funny person (sometimes sensitive), we chat a lot when doing experiment, you bring a lot interesting "facts" and jokes, you should proud of doing so many work in the lab (just need some luck). Paco, you are always very serious towards your experiment and easily got panic (forgive me sometimes I mocked about it), I think that's the reason you get good results in the end, I think your patient and time investment will bring you a success career.

David, Martin, Esther, Eline, Ivan, Fleur, Natalia, Marieke, Ria, Marian, Jacq, Stephanie, Nienke, Brigit, Maaike, Eric, Antonio, Inge, Emmeline, Guus...It's very lucky having a very good time to work with such nice people as you!

行文至此，博士生涯已接近尾声，首先应该感谢 CSC 提供给我出国留学的机会，使我学习了知识，开阔了视野，获得了选择的机会！在乌特这四年了，认识了很多有趣的小伙伴。毅队，感谢将前 26 年只看过世界杯的我带进了足球队，平时更是组织许多有趣的活动，这极大得丰富了我的生活，缓解了我的思乡之情，我会记住你说的“有朋友的地方就是家”。桃子，球场上的亲密战友，生活中的快乐玩伴，这四年蹭你的车去了很多地方玩耍，以及许多次在你家的聚餐，麻将，十分期待将来我在国内做东道的那一天。曦晨，球场上是指挥葫芦娃（7人制）的中后卫指挥，职业上是带我入行的





老大哥，希望你的事业更上十层楼。泽光，我加入球队的时候你已经快毕业，江湖上只剩下哥的传说，十分感谢在瑞士带我玩了一圈，祝你早日青千；还有志雄、瑞学、李洋、娄博、刘超、杨超（向单总、安东和艾琳问好）、杨翰、阿秋、小韦、Gray、王豪、庆一、宇浩、嘉诚、正越以及足球队其他的兄弟，感谢大家在足球上的指点以及每周五的聊天，都让我感受到生活的丰富多彩，希望我们的队伍不断壮大！

接下来是饭友圈。杜杰，墨水和小乐知，十分羡慕你们家其乐融融的氛围，还有精致的伙食，让我对未来生活充满憧憬，希望留在科研界的阿杰早日发出大 paper。鹏总，我们的奢华生活（小炒加喝茶）皆由你而起，这四年来在你家吃了太多次饭，聊了太多人生，吐槽了太多事情，你的幽默每次都让我觉得之前的烦恼都不是事，一直相信你会拥有远大的前程（钱程），争取早日回国，刘备出曹营的时候说过一句“此一去如鱼入大海，鸟入山林，再也不受羁绊了”，这句话送给临近毕业的你！吃辣无敌的逸哥，敏感善良又十分仗义，每次在你家吃饭都是说不出的放松，每次与你聊天都会带来不一样的视角，祝你早日实现愿望，拿到宇宙尽头的编制。无微不至的莉姐，每一次聚餐都是你准备所有事情，操持所有，希望你早日找到理想工作，在荷兰过上幸福安逸的生活。人生赢家老叶，你对人生的规划，对科研严谨、执著的态度，以及努力与自律都十分影响我，让我意识到其实我可以做的更好，你跟王梦即将迎来你们的 Baby，祝科研顺利，家庭幸福！乌村社交天王庆午，有幸被纳入你的朋友圈，多少次我们在阳台聊科研，聊人生，对未来迷茫又好奇，对人生忧虑又憧憬，你对朋友的仗义与对生活的洒脱都是非常值得学习的地方，祝早日脱单！气氛担当振国，每次饭局焦点人物，自己从你找到女朋友退出江湖，我们的酒饭再不如从前香了，希望你早日重出江湖，因为有你地方，最快乐！乌特瓜王相洁，作为我们与娱乐圈之间的唯一桥梁，你贡献了大部分的聚餐瓜，希望你新的公司成为技术大咖的同时也不要抛弃娱乐致死的精神，有大瓜记得通知我，我会搬好小板凳。

另外，感谢中国科学技术大学博士生刘晓东和南京大学博士生钱高飞，我们的友谊始于 6 年前的大创，6 年来我们仍在不断地交流科研与技术，与你们的 meeting 总会给我带来新的思考，新的动力，真挚地希望两位早发 CNS，在自己的领域都将有所建树，期待将来你们带我一起打天下的那一天。还有徐晟，同为一个独自在荷兰求学的老父亲，每次感到孤独的时候回头看一看，嗯，老哥也还在；如今我早一步回去，

祝你实验顺利，文章多多，早日带着PRL回去团聚；还有张浩、徐彤、解敏、老邱、李爽、王俊杰、张柱、李林格、王蕾、邹杨、吴建君、沈梓盈、胡洋、李新，真诚地祝福各位工作顺利，生活顺利！

最重要的，要感谢我的家庭。生我养我把我培养大的父母，这么多年他们对我的选择无条件支持，一直嘴上说的都是在哪里舒适就在哪里生活，只有很偶尔说漏嘴的时候说在帮我数着日子还有多久回去，我想应该没有语言可以表达我的感激之情，希望你们和奶奶身体健康，吃嘛嘛香。我的岳父岳母，也给了我十分有利的支持，我不在国内的日子里，你们承担了大部分照顾林希和品品的工作，对我说的永远都是不要省钱，照顾好自己，希望两位老人和外婆身体健康，幸福快乐！

感谢我的妻子周林希，从研究生我去工厂时你给的安慰，到你陪我备战雅思，夏天骑电动车出去吹头发，后来送我来荷兰来以及再后来中间辞掉工作来荷兰，后来一个人在家照顾品品...这些年你付出了很多，甚至品品出生的那一刻我还在隔离；你的操持给了我极大的支持；让我没有后顾之忧，可以专心完成我的学业。我们稳定、简单而且幸福的生活就在眼前了，十分期待！ Lastly, I want to say something to Pin (PumpKin, 胖品品), you are the priceless gift from the god, I can't express how happy every time I see you. I leave you when you are 2 month-old, backing and forthing between lab and my small room in Europe for finishing my study. Now I almost finished the thesis, however, you mom forbid me travelling to any place (I haven't been to Italy, Spin, Portugal, Greece...), I am convinced by her because we don't want to lost any page with you. I am really expect decades later, you accidently find this dusty thesis from the shelf, and find the best wishes from father (hope you can read English), you will know father loves you, family loves you...you should have courage to face any challenges in life!

Jun

Aug 2022

Zeist, The Netherlands









